The Influence of Isoprostanes on Angiogenesis *In Vitro*

Doctoral thesis

Submitted by
Apothekerin Anke Gnann

Institute of Experimental and Clinical Pharmacology and Toxicology
Clinical Pharmacology
Faculty of Mathematics, Computer Sciences and Natural Sciences
Department of Chemistry
University Hamburg

Hamburg, 2009

1. Referee: Prof. Dr. H. J. Duchstein

2. Referee: Prof. Dr. R. H. Böger

Day of the disputation: 06.03.2009

Contents

List of Figures

1 Introduction

1.1 Oxidative Stress

Molecular oxygen is essential for the survival of higher aerobic organisms. Paradoxically it is also associated with the damage of biomolecules and cell structures. Aerobic metabolism uses energy released by the oxidation of nutrients via oxygen consumption. O_2 serves as the final electron acceptor for cytochrome-*c*-oxidase, the terminal enzymatic component of the mitochondrial enzymatic complex that catalyzes the four-electron reduction of O_2 to H_2O. The intermediate steps of oxygen reduction are the formation of the superoxide anion radical ($O_2^{\bullet -}$), hydrogen peroxide (H_2O_2), and the hydroxyl radical ($OH^{\bullet}$) corresponding to the steps of reduction by one, two, and three electrons, respectively. These intermediates are referred to as reactive oxygen species (ROS). The aerobic organism has developed an efficient and sophisticated antioxidant system to prevent itself from damage caused by ROS. An imbalance between increased exposure to ROS (which occurs under pathophysiological conditions) and antioxidant defences in favor of free ROS is designated as oxidative stress. Monitoring of free radicals directly in biological systems is difficult due to their extreme reactivity and due to the lack of sensitive technologies [1]. However, the appliance of appropriate biomarkers is required to assess the oxidative status *in vivo* and to explore the role of oxidative stress in the pathogenesis of human disorders.

1.1.1 Reactive Oxygen Species

ROS include oxygen free radicals and non-radical oxygen derivatives that are involved in oxygen radical production. Oxygen radicals, in combination with other atoms or larger molecules, can occur as alkyl or peroxyl radicals, in e.g. lipids. The most important

source of ROS is their leakage from the mitochondria during normal respiration. Neutrophils and macrophages also produce ROS to kill bacteria within immune defence, a process known as oxidative burst. ROS can also derive from exogenous sources such as environmental toxins, cigarette smoke, and different types of irradiation. ROS are highly reactive due to the presence of unpaired valence shell electrons. They are able to cause damage to lipids, proteins, and DNA. Molecular oxygen, in its triplet state, has two unpaired electrons with parallel spins. ROS generation is initiated with the formation of $O_2^{\bullet -}$ via a monovalent electron transfer. Superoxide, present in almost all aerobic cells, is generated beneath respiratory chain by several enzymes such as xanthine-, NADPH-dependent-, cytochrome-c- and aldehyde-oxidases [2]. At physiologic pH superoxide rapidly dismutates to H_2O_2 and O_2. This reaction is catalysed by the enzyme superoxide dismutase. A further possibility of H_2O_2 generation is given by a divalent reduction of O_2 through oxidases like uric acid- and glycolat-oxidases. H_2O_2 is apolar, able to permeate cell membranes and can directly attack cell structures [3]. Its toxicity is based on its ability to oxidize thiol-groups as well as to generate $OH^{\bullet}$. H_2O_2 can be decomposed to O_2 and H_2O by the enzyme catalase. In the presence of transition metal ions like iron and copper H_2O_2 can be reduced to $OH^{\bullet}$ and hydroxide anion (OH^-) via the Fenton reaction. $OH^{\bullet}$ is the most reactive oxygen free radical. It reacts rapidly with almost all biomolecules and its reactions are diffusion-limited, i.e. they take place at the site of generation. If $O_2^{\bullet -}$ is present, it can reduce ferric iron (III) to ferrous iron (II), which catalyses the reduction of H_2O_2 to $O_2^{\bullet -}$ via the Fenton reaction. The nett reaction of H_2O_2 with $O_2^{\bullet -}$ is also called the Haber-Weiss reaction.

Besides their pathophysiological effects free radicals play an important role in a wide range of physiological processes. Oxygen radicals function as regulator molecules. They control several enzyme reactions e.g. cytochrome P_{450} and cyclooxygenases [4]. Additionally it is postulated that they influence the proliferation of fibroblasts and take part in platelet aggregation and adhesion. Transcription factors like nuclear factor kB (NF-kB) and activating protein-1 (AP-1) are activated through H_2O_2 and even the initiation of apoptosis is influenced by oxygen radicals [5].

1.1.2 Antioxidants

A balance between oxidant and intracellular antioxidant systems is vital for cell functions. Under normal circumstances ROS are detoxified from the cell via antioxidants. The term antioxidant is defined by Halliwell and Gutteridge as a substance that, when present at low concentrations compared with that of an oxidizable substrate, significantly delays or inhibits oxidation of that substrate [6]. Antioxidant defences can be classified in three categories: prevention of ROS generation, interception with ROS and repair processes, which remove damaged biomolecules before they can accumulate and alter cell functions or viability. Antioxidants exist in aqueous and membrane compartments [7]. Transition metal binding proteins like ferritin, transferrin, and lactoferrin sequester iron and copper thus decreasing the formation of hydroxyl radicals. Antioxidant enzymes like superoxide dismutase and catalase catalyze the degradation of superoxide anion and hydrogen peroxide. Additionally the glutathione peroxidase catalyzes the reduction of hydrogen- or lipid hydroperoxide to water and their corresponding alcohol. Within cell membranes and lipoproteins α-tocopherol, a member of the vitamin E family, traps peroxyl radicals and forms a relatively stable tocopheroxyl radical, which can be regenerated by other, hydrophilic, antioxidants in the aqueous interface [8]. A tocopheroxyl radical can also be completely oxidised to tocopherol quinone or two tocopheroxyl radicals form a stable dimer. α-Tocopherol provides an effective inhibitor of the propagation of lipidperoxidation and is also referred to as a chain breaking antioxidant. Other chain breaking antioxidants are ubiquinol and carotenoids as well as ascorbate, urate and thiols.

1.1.3 Modifications of Biomolecules

As mentioned above increased levels of ROS result in damage of DNA, proteins, and lipids (Figure 1.1). Stable primary and secondary products of radical damage can be used as biomarkers for oxidative stress, given that appropriate analytic methods are available. Damage to DNA leads to single-strand breaks, DNA-protein cross-links and base oxidations. One example of a well known oxidized base is 8-hydroxy-2-deoxyguanosine. This mutagenic DNA mispairs with adenine during DNA replication and transcription and is associated with neurologic disorders [9]. Urinary 8-hydroxy-2-deoxyguanosine can

be measured by HPLC and is accepted as biological marker of oxidative DNA damage [10].

Protein carbonyl groups represent the most studied marker of oxidative damage to proteins. They are formed by oxidation of their side chains containing lysine, proline, arginine, and threonine residues. The measurement of protein carbonyls following their reaction with 2,4-dinitrophenylhydrazine has become the most widely utilized measure of protein oxidation [11]. An increase in protein carbonyl content is associated with a number of pathological disorders including Alzheimer's and Parkinson's disease [12, 13].

Lipids are a major target of free radical attack. The oxidative destruction of polyunsaturated fatty acids (PUFAs) is a radical chain process involving three sequences: initiation, propagation and termination [14]. Cell membranes and lipoproteins are rich sources of PUFAs, e.g. linoleic acid, arachidonic acid and docosahexaenoic acid. Their susceptibility to free radical attack increases with their number of double bounds. Free radical-induced peroxidation of membrane lipids leads to alteration in the properties of the cell membrane, such as the degree of fluidity, and to inactivation of membrane-bound receptors and enzymes. The initiation starts with an abstraction of a hydrogen atom from a methylene group in the side chain of a fatty acid by an attack of a ROS. The presence of a double bond in the fatty acid weakens the C-H bonds on the carbon atom adjacent to the double bond and makes H-removal easier. The carbon radical tends to be stabilized by a molecular rearrangement to form a conjugated diene, which combines with molecular oxygen to form a peroxyl radical. Peroxyl radicals are able to abstract hydrogens from other lipid molecules thus causing autocatalytic chain reactions. Furthermore peroxyl radicals can combine with hydrogen, yielding a hydroperoxide. This reaction characterizes the propagation stage. Peroxyl radicals can also be transformed into cyclic peroxides or even cyclic endoperoxides. Termination is achieved by the reaction of a peroxyl radical with chain breaking molecules like α-tocopherol. Peroxyl radicals can also react with any kind of alkyl radicals to give non-initiating and non-propagating dimers or hydroxylated derivatives. Secondary peroxidation products which can be formed are hydrocarbons and aldehydes. Riely first reported in 1974 that hydrocarbon gases were released by mice upon treatment with CCl_4 [15]. Several reports demonstrated that measurement of volatile hydrocarbons like ethane and pentane can be used as an index of lipid oxidation. They are generated by oxidation of ω-3 (linolenic acid) and ω-6 PUFAs (arachidonic- and linoleic acid), the most abundant PUFAs in cell membranes.

The most widely used index of lipid peroxidation is malondialdehyde (MDA) formation, often assayed with the 2-thiobarbituric acid (TBA) assay. MDA represents another secondary product resulting from the oxidation of ω-3 and ω-6 PUFAs. However, beside MDA, several other compounds are also reactive towards TBA and are referred to as thiobarbituric acid reactive substances (TBARS) [16].

A new and reliable marker for oxidative stress is the measurement of F_2-isoprostanes. They are prostaglandin F_2 (PGF_2)-like compounds generated via free radical-induced lipid oxidation of arachidonic acid (AA) and will be described in detail in the next section.

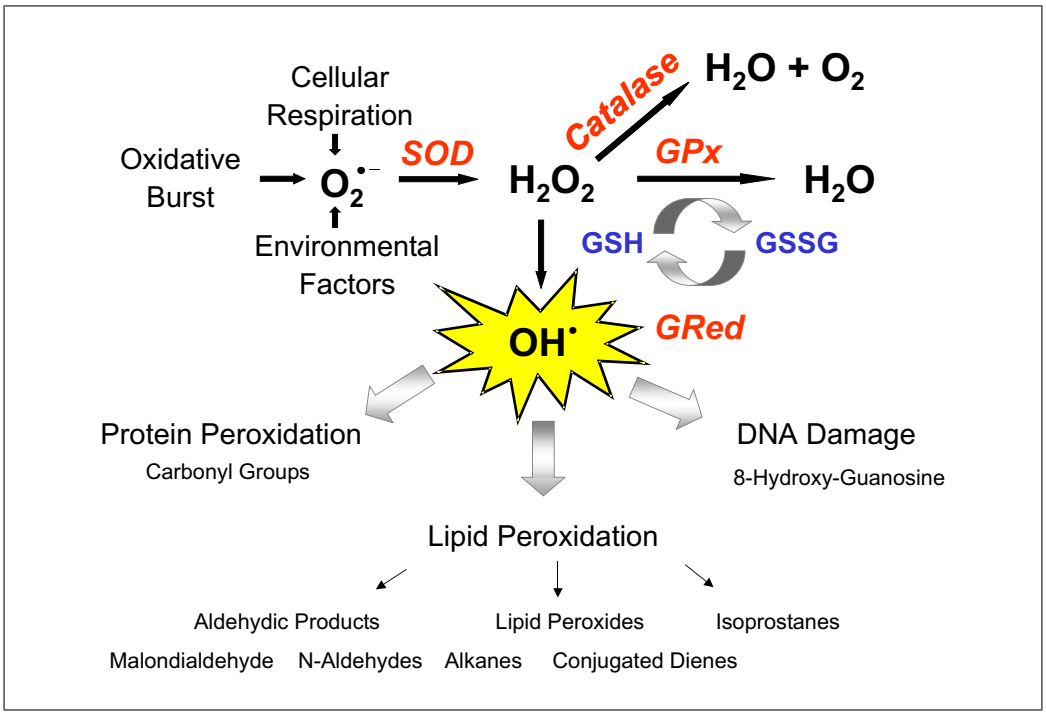

Figure 1.1: Oxidative stress. Abbreviations: DNA, deoxyribonucleic acid; SOD, superoxide dismutase; GPX, Glutathionperoxidase; GSH, Glutathion; GSSG, Glutathiondisulfid; GPx, glutathione peroxidase; GRed, glutathione reductase.

1.2 Isoprostanes

The formation of PG-like compounds via a nonenzymatical, autooxidized pathway was first reported 1966 by Nugteren [17] and confirmed by Pryor and Porter [18, 19]. However, the relevance of PG-isomers was not recognized until 1990, when Morrow et al. reported the formation of PGF_2-like compounds by a non-cyclooxygenase (COX), free radical-induced mechanism *in vivo* [20]. Because these compounds contain the F-type prostane ring like $PGF_{2\alpha}$, they were referred to as F_2-isoprostanes.

1.2.1 Molecular Mechanisms of Isoprostane Formation

F_2-Isoprostanes formation starts with an abstraction of a bisallylic hydrogen atom from AA by a free radical, leading to the formation of three, resonance-stabilized, arachidonyl radicals (Figure 1.2). In the presence of molecular oxygen, they give rise to six different peroxyl radicals. Four of them, i.e. the 9-, 8-, 12-, and 11-peroxyeicosatetraenoic acid (HPETE, peroxyl radical), can undergo cyclization to form isomeric bicyclic endoperoxides (1a-4a). 5- and 15-HPETE peroxyl radicals can not cyclize and generate isoprostanes. Molecular oxygen and hydrogen is added to the endoperoxides, generating the corresponding hydroperoxides (1b-4b), which in turn can be reduced to hydroxides (1c-4c, Figure 1.2). The reaction demonstrated for group 4 (Figure 1.2) is consistent with the PGH_2 synthase-catalyzed transformation of PGG_2 to PGH_2 during PG formation. PGH_2 synthase catalyzes only the transformation of one specific isomer (8R,9S,11R,12S,15S). A subsequent reduction of (8R,9S,11R,12S,15S) PGH_2 by e.g. prostaglandin-F synthase yields the solely endproduct $PGF_{2\alpha}$. Therefore the hydroperoxides and hydroxides shown in Figure 1.2 are also referred to as G_2- and H_2-isoprostanes, respectively. A further reduction leads to the formation of four regioisomeric F_2-isoprostanes (1-4). Each of this regioisomers can comprise of eight racemic diastereoisomers. Thus there is theoretically the possibility of generating 64 F_2-isoprostanes [21].

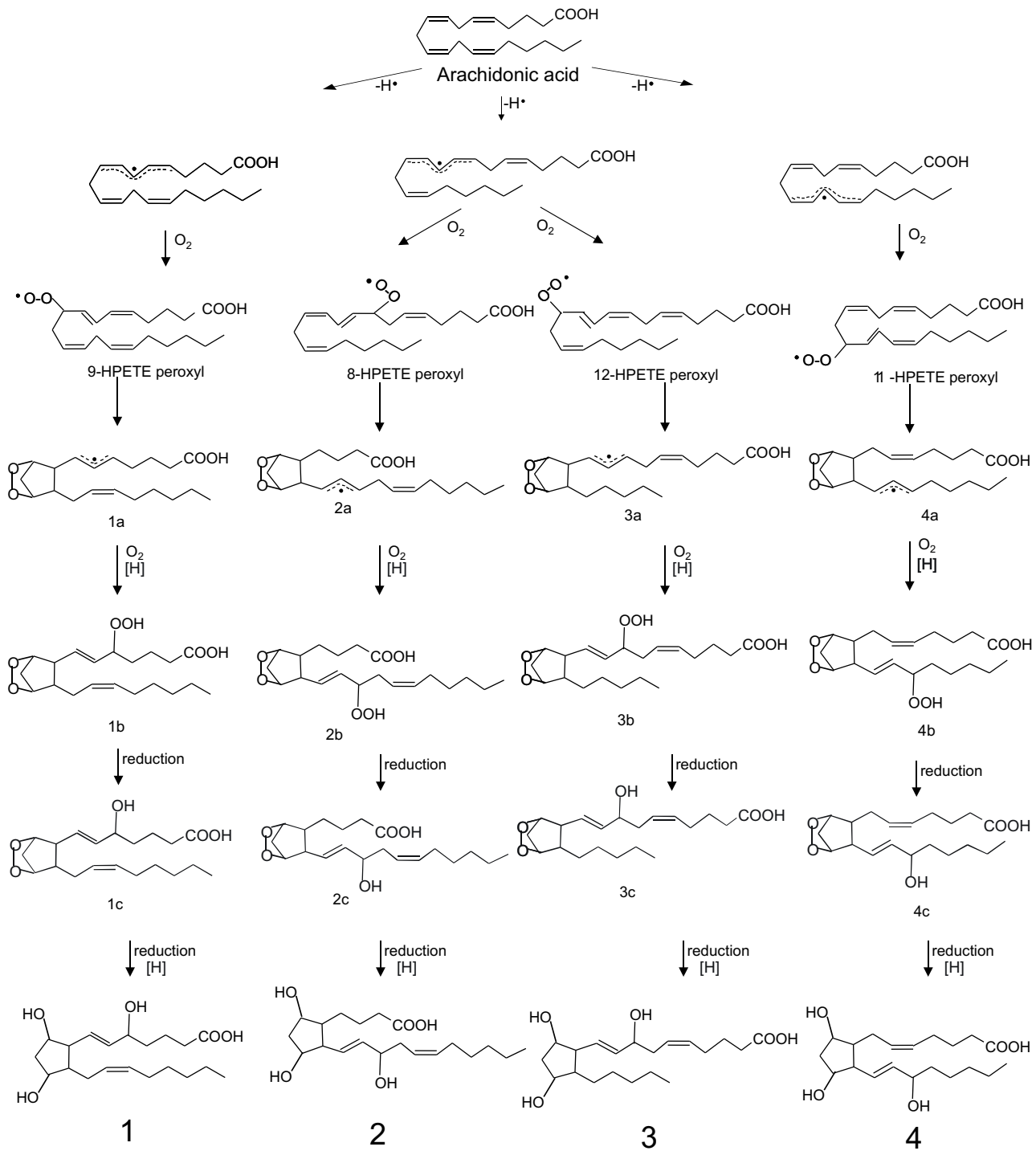

Figure 1.2: Mechanism of the formation of the F_2-isoprostanes.

D- and E-ring isoprostanes can be generated *in vivo* via rearrangement of H_2-isoprostanes [22]. D_2/E_2-isoprostanes are formed competitively with F_2-isoprostanes, and studies have demonstrated that the depletion of cellular reducing agents, such as GSH or α-tocopherol, favors the formation of D_2/E_2-isoprostanes over that of reduced F_2-isoprostanes [23]. D- and E-ring isoprostanes are not terminal products of the isoprostane pathway. They readily dehydrate *in vivo* to yileld A_2- and J_2-isoprostanes, which are also known as cyclopentenone isoprostanes. They contain an α,β-unsaturated cyclopentenone ring structure. Figure 1.3 shows exemplary transformation possibilities for one H_2-isoprostane. Same applies for the other three regioisomers [24].

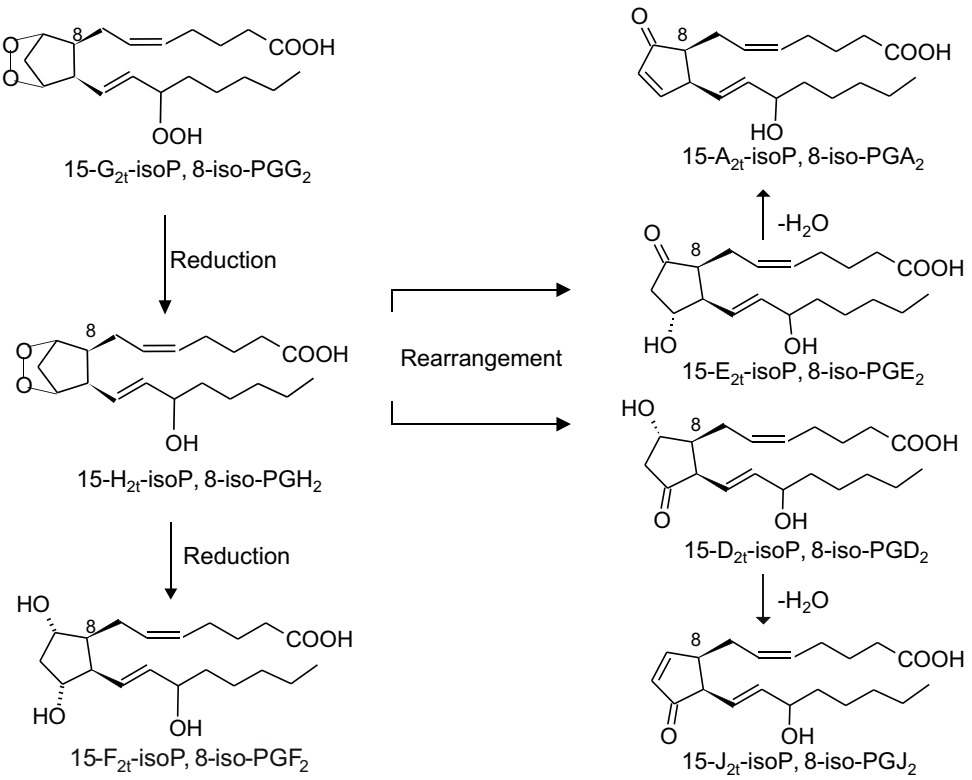

Figure 1.3: Transformation of 8-iso-PGH$_2$ to metabolites with different ring substitutions.

1.2.2 Nomenclature of Isoprostanes

Currently two nomenclature systems are used [25, 26]. The IUPAC and Eicosanoid Nomenclature Committee have approved the Taber/Roberts nomenclature, which follows the normal PG convention. Isoprostane is abbreviated as IsoP. The carboxyl carbon is designated as C_1 and different regioisomer classes are designated by the carbon number of the side chain, where the hydroxyl-group is positioned. The four regioisomer classes derived from AA are designated as 5-, 12-, 8-, or 15-series according to 1, 2, 3, and 4 shown in Figure 1.2, respectively. The best known isoprostane is 15-F_{2t}-IsoP. The subscript 2t refers to the number of double bounds, i.e. two, and the orientation of the side chains and alcohol at the five-membered ring, i.e. trans. 15-F_{2t}-IsoP is also referred to as 8-iso-$PGF_{2\alpha}$, because its structure solely differs from $PGF_{2\alpha}$ in the orientation of the bound of C8. The same applies for 15-E_{2t}-IsoP and 15-A_{2t}-IsoP (Figure 1.3). The trivial names are used in this work.

The second nomenclature from Rokach designates the regioisomer classes based on the ω-carbon, which is attacked to form the arachidonyl radical. The ω indicates the number of carbon atoms from the methyl end of the acyl chain. Free radical attack at carbon ω-8 leads to the formation of regioisomer Type III, attack at ω-11 leads to Type IV and V and attack at ω-14 leads to Type VI formation. The designation of regioisomer classes derived from AA starts with Type III, because AA is a ω-6 PUFA. ω-6 Fatty acids have a double bound six carbons from the methyl carbon. The four classes of F_2-isoprostanes are designated as Type III, IV, V, and VI according to pathway 4, 3, 2, and 1 shown in Figure 1.2, respectively. Other ω-PUFAs including ω-6 and ω-3 PUFAs are also able to generate PG-like compounds via the isoprostane pathway. The oxidation of ω-3 PUFAs leads to the formation of PG-like compounds starting with Type I. For example the oxidation of docosahexaenoic acid (DHA), a ω-3 PUFA which is abundant in the central nervous system, leads to the formation of isoprostane-like compounds, termed neuroprostanes (nP or iP_4) [27]. DHA contains six double bounds and free radical attack to Cω 5, 8, 11, 14, and 17 leads to the formation of eight regioisomers, each.

1.2.3 Isoprostane Formation *in Vivo*

The *in vivo* formation of each four classes of F_2-isoprostanes has been demonstrated in an animal model where rats were treated with CCL_4 to induce oxidative stress [28]. Further experiments have shown that the 12- and 8-series isoprostanes formed *in vivo* are less abundant than the 5- and 15-series [29]. One reason for that could be that 12- and 8-series isoprostanes derive from the same arachidonyl radical precursor. Furthermore the bicyclic peroxyl radicals, which can generate 12- and 8-series isoprostanes can also undergo a kinetically preferred 5-exo-cyclization, that ultimately leads to the formation of dioxolane-isoprostanes (Figure 1.4) [30]. The prefix exo indicates that the breaking bond during ring closure is outside the ring which is formed. In contrast to COX-derived PG formation, non-enzymatic isoprostane formation preferentially leads to compounds in which the two side chains are cis orientated in relation to the prostane ring [31]. Particular attention has focused on 8-iso-$PGF_{2\alpha}$, which is the best investigated F_2-isoprostane. Although 8-iso-$PGF_{2\alpha}$ is produced via free radical peroxidation of AA, it is also a minor product of platelet COX-1 and monocyte COX-2 dependent metabolism of AA *in vitro* [32]. However, urinary excretion of 8-iso-$PGF_{2\alpha}$ is unaffected by COX-inhibition [33]. Another F_2-isoprostane, which could be detected in the human urine is 5-F_{2t}-IsoP [34]. The urinary excretion of 5-F_{2t}-IsoP (737±20.6 pg/mg creatinine) is eight-fold higher compared to those of 8-iso-$PGF_{2\alpha}$ (15-F_{2t}-IsoP) [33]. The stereoisomers 5-F_{2c}-IsoP and 5-epi-5-F_{2c}-IsoP could also be detected [35].

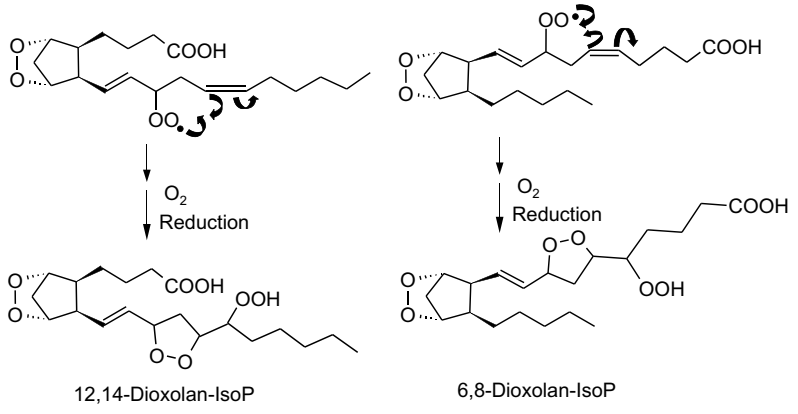

Figure 1.4: Formation of dioxolane-isoprostanes.

1.2.4 Fate of Isoprostanes

Isoprostanes are formed predominantly *in situ* on phospholipids of cell membranes. Subsequently they are released in the plasma via hydrolysis, presumably by phospholipase A_2, filtered by the kidneys and excreted in urine [36]. Isoprostanes occur in plasma free or esterified to phospholipids and only free in urine. The metabolism of isoprostanes should be analog as for PGs. Various combination of β-oxidation, double bound reduction, alcohol group oxidation, ω-hydroxylation and ω-oxidation should yield plenty of metabolites. Two major metabolites of 8-iso-$PGF_{2\alpha}$ have been identified in human urine: 2,3-dinor-8-iso-$PGF_{2\alpha}$ and 2,3-dinor-5,6-dihydro-8-iso-$PGF_{2\alpha}$, (Figure 1.5) [37, 38]. Thereby the latter is the most abundant. Like 8-iso-$PGF_{2\alpha}$ the urinary excretion of both increases in cigarette smokers and is not reduced by COX-inhibition.

Because metabolism of isoprostanes differ between species, different metabolites have been found in animals. In rabbits intravenous administration of 8-iso-$PGF_{2\alpha}$ leads to the formation of 15-keto-8-iso-$PGF_{2\alpha}$ and its β-oxidised products, whereas 2,3,4,5-tetranor-15-keto-13,14-dihydro-8-iso-$PGF_{2\alpha}$ has been identified as the major urinary metabolite [38, 39]. Another β-oxidation product 2,3,4,5-tetranor-8-iso-$PGF_{2\alpha}$ has been found to be a major product of rat hepatocyte metabolism.

8-iso-PGE_2 can degrade spontaneously to 8-iso-PGA_2. In rats the major metabolite of 8-iso-PGA_2 was identified as a mercapturic acid sulfoxide conjugate in which the carbonyl at C-9 was reduced to an alcohol [40]. The major urinary metabolite of 8-iso-PGA_2 in humans has not been identified yet.

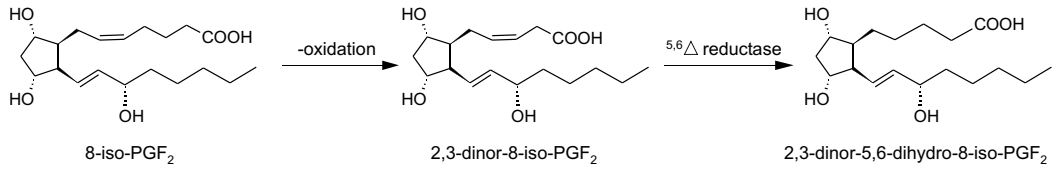

Figure 1.5: Chemical structure of 8-iso-$PGF_{2\alpha}$ and its major metabolites 2,3-dinor-8-iso-$PGF_{2\alpha}$ and 2,3-dinor-5,6-dihydro-8-iso-$PGF_{2\alpha}$.

1.2.5 Phytoprostanes

Higher plants are not able to synthesize AA, so that neither PGs nor isoprostanes can be formed. α-Linolenic acid (18:3, ω-3) is the predominant PUFA in plants. On the one hand it is utilized for the synthesis of PG-like compounds from the jasmonate type via an enzymatic pathway. Jasmonates are known to be important signaling compounds in plants, e.g. they mediate defense responses by accumulation of antimicrobial secondary metabolites (phytoalexin). On the other hand α-linolenate can undergo autoxidation via a nonenzymatic, free radical catalyzed pathway, analogous to the isoprostane pathway in animals, yielding dinor isoprostanes, which are referred to as phytoprostanes (PhytoPs, PPs). The sequence of hydrogen abstraction, peroxidation, bicyclization and second peroxidation of α-linolenic acid leads to the formation of two series of regioisomeric G_1-PhytoPs. They are designated as 16-G_1- and 9-G_1-PhytoPs according to the Taber/Roberts nomenclature or as G_1-PP type I and II according to the Rokach nomenclature, respectively. A reduction of G_1-PhytoPs leads to the formation of F_1-PhytoPs (Figure 1.6, A). Additionally, in the presence of water, G_1-PhytoPs can also rearrange to E_1- and D_1-PhytoPs [41, 42]. E_1-PhytoPs are prone to undergo dehydration and isomerization to yield A_1- and B_1-PhytoPs. Also D_1-PhytoPs can dehydrate yielding J_1- and desoxy-J_1-PhytoPs (Figure 1.6, B,C). In contrast to desoxy-J_1-PhytoPs, which are known to be major metabolites of the phytoprostane pathway, desoxy-B_1-PhytoPs have not been detected yet.

All above mentioned classes of phytoprostanes (A_1-, B_1-, D_1-, E_1, F_1- and desoxy-J_1-PhytoPs) have been detected in over 20, taxonomically different plant species [43]. Phytoprostanes are thought to be generated from esterified linolenate in plant membranes *in situ*, from which they are released by lipases similar to isoprostanes in mammals [44]. 90% of F_1-PhytoPs were found to be esterified in most plant parts [45]. Plants accumulate higher levels of F_1-PhytoPs than E_1-PhytoPs, because phytoprostane formation preferentially occurs in hydrophobic cell membrane, which stabilizes the endoperoxide intermediates and favors F_1-PhytoPs, rather than E_1-PhytoPs formation [42]. Additionally the reduction of endoperoxide intermediates to F-ring prostanoids by glutathione appears to be faster than rearrangement to E-ring prostanoids, at least in mammals [46]. Phytoprostanes are suggested to display similar biological activities like jasmonates with respect to antibiotics (phytoalexin) biosynthesis in plants [47]. Whether phytoprostanes

exert any biological activity in humans remains to be investigated.

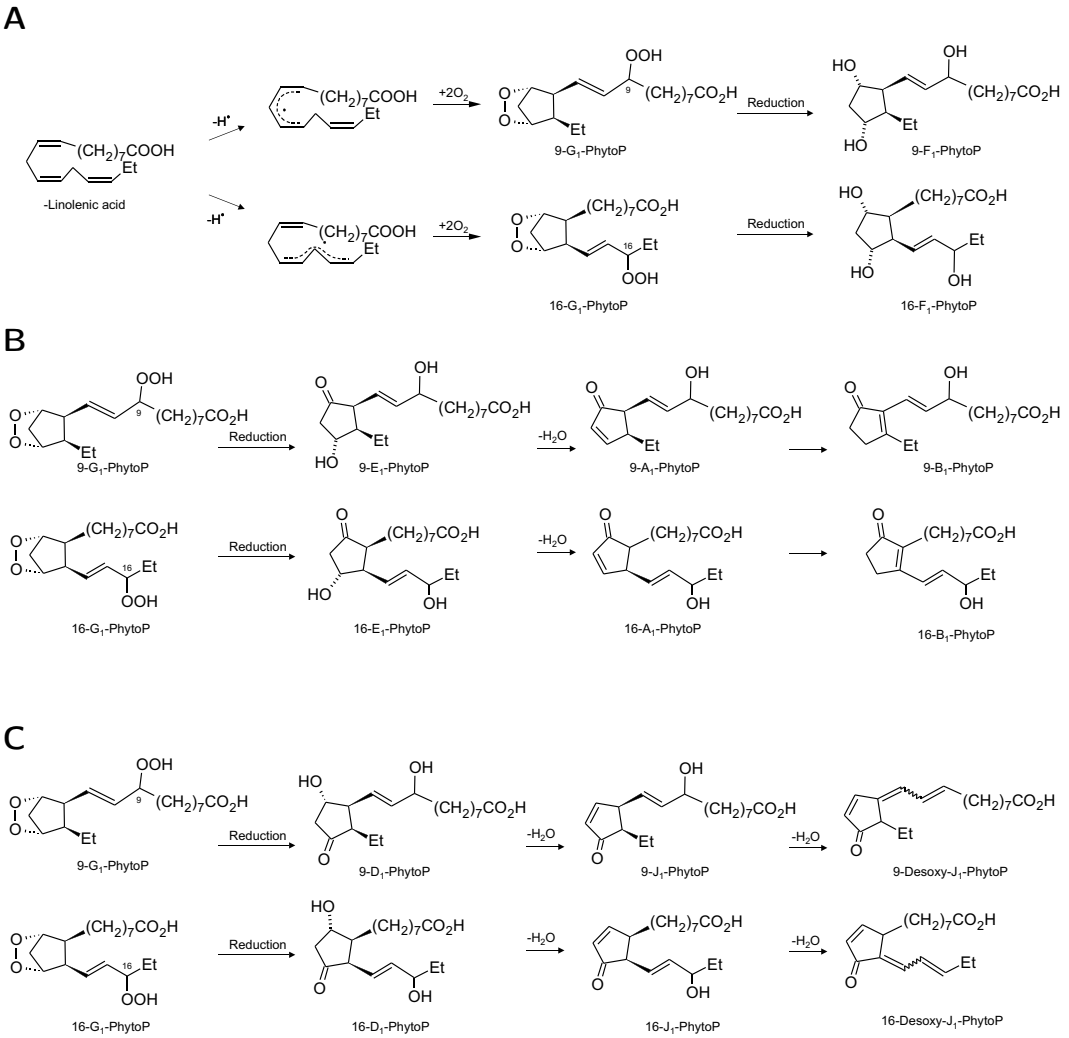

Figure 1.6: Formation of Phytoprostanes. **A**: Autoxidation and cyclization of α-linolenic acid yields two structurally different G_1-PhytoPs. Subsequent reduction leads to chemically stable F_1-PhytoPs. **B**: Rearrangement and reduction of G_1-PhytoPs yields E_1-PhytoPs, which can dehydrate and isomerize to A_1- and B_1-PhytoPs. **C**: Rearrangement of G_1-PhytoPs can also lead to the formation of D_1-PhytoPs, which can dehydrate to J_1- and desoxy J_1-PhytoPs.

1.2.6 Markers and Mediators of Oxidative Stress

Most assays previously developed to measure oxidative stress *in vivo* have several shortcomings, namely the lack of specificity and sufficient sensitivity. For example the most commonly used method, the measurement of MDA by the TBARS assay, is problematic because MDA is not only produced by lipid peroxidation and TBARS assays are not specific for MDA [48]. Also the measurement of exhaled volatile alkanes like ethane and pentane has not been referred as ideal [48]. F_2-isoprostanes are considered to be reliable biomarkers of oxidative stress status and lipid peroxidation *in vivo* [49]. There are a number of favorable attributes that make measurement of F_2-isoprostanes so conclusive: They are specific products of lipid peroxidation and chemically stable. Their levels are present in detectable quantities in all normal biological fluids and tissues, allowing the definition of a normal range and theiy are unaffected by lipid content of the diet [20]. Moreover, F_2-isoprostanes levels increase substantially in animal models of oxidant injury, e.g. administration of CCL_4, which can be modulated by administration of antioxidant agents [50]. Furthermore, the measurement of F_2-isoprostanes in urine is non-invasive. F_2-isoprostanes are very stable in urine and artifactual formation is avoided. The measurement of F_2-isoprostanes has revealed a role of free radicals and oxidant injury in a wide variety of human diseases (Table 1.1). Elevated levels of 8-iso-$PGF_{2\alpha}$ have been found in conditions of cardiovascular risk such as diabetes mellitus [51, 52], obesity [53], cigarette smoking [54, 55], hypertension [56] and hypercholesterolemia [57]. Furthermore, 8-iso-$PGF_{2\alpha}$ has also been shown to accumulate in coronary arteries in patients suffering from coronary heart disease (CHD) [58]. Our group showed in 2004 that urinary 8-iso-$PGF_{2\alpha}$ is an independent risk marker of CHD [59]. Moreover, isoprostanes are suggested to accumulate in the hypoxic myocardium [60] and levels of 8-iso-$PGF_{2\alpha}$ have been shown to increase in settings of myocardial reperfusion [61, 62].

Table 1.1: Conditions implicated with increased oxidative stress according to measurement of F_2-isoprostanes.

Pathophysiological condition	References
Cardiovascular Diseases	
Atherosclerosis	[63, 64]
Ischemia/reperfusion injury	[61, 62]
Coronary artery disease	[65, 66]
Heart failure	[67, 68]
Renovascular disease	[69]
Lung Diseases	
Asthma	[70, 71]
COPD	[72, 73]
Cystic fibrosis	[74, 75]
Interstitial lung diseases	[76]
Acute lung injury, adult respiratory distress syndrome	[77]
Risk Factors for Cardiovascular Diseases	
Smoking	[55, 54]
Hypercholesterolemia	[57, 78]
Diabetes	[52, 51]
Hyperhomocysteinemia	[79]
Male gender	[80]
Obestiy	[53]
Renal Diseases	
Hemodialysis	[81]
Rhabdomyolysis renal injury	[82]
Neurolingual Diseases	
Alzheimers‘disease	[83, 84, 85]
Huntington‘s disease	[86]
Multiple sclerosis	[87, 88]
Creutzfeld-Jacob‘s disease	[88]
Liver Diseases	
Alcoholic liver disease	[89, 90]
Hepatorenal syndrome	[91]
Primary biliary cirrhosis	[92]
Liver transplantation	[93]
Inflammatory Diseases	
Rheumatoid arthritis	[94]
Scleroderma	[95]
Other Diseases	
Osteoporosis	[96]
Crohn‘s disease	[97]

But isoprostanes are not only markers of oxidative stress. They have been shown to exert biological activities, suggesting that they may also function as pathophysiological mediators of oxidant injury. Due to the fact that biological responses to isoprostanes are compound, species, and tissue specific, each isoprostane has to be investigated separately. Unfortunately, most isoprostanes are not commercial available yet. 8-iso-$PGF_{2\alpha}$ is the best described F_2-isoprostane. Its biological activity can be observed in tissues as soon as its free, active form reaches levels in the micromolar range, which can occur in certain (physiological and) pathophysiological conditions (Figure 1.7). First it is able to affect the integrity and fluidity of cell membranes, subsequent the adjacent tissue, leading to the status of oxidative stress. 8-iso-$PGF_{2\alpha}$ is also known to exert concentration-dependent vasocontricion in a variety of vascular beds (Table 1.2). Interestingly, its major metabolite 2,3-dinor-5,6-dihydro-8-iso-$PGF_{2\alpha}$ has been reported to induce vasoconstriction in retinal and brain microvessels [98]. Allergen challenge has been shown to lead to an increase in F_2-isoprostanes formation in mouse lungs. Additionally, 8-iso-$PGF_{2\alpha}$ is able to induce airway hyperresponsiveness (AHR), an important feature of asthma. A causative link between these findings is evidenced in mice, but which findings have relevance for humans can only be suggested [99]. F_2-isoprostanes are suggested to play a role in the pathophysiology of atherosclerosis. Leitinger et al. demonstrated that 8-iso-$PGF_{2\alpha}$ stimulates monocytes to bind endothelial cells, an initiating event in the development of atherosclerotic leasions [100]. Furthermore, several *in vitro* assays have shown that F_2-isoprostanes promote platelet activation, induce mitogenesis in vascular smooth muscle cells and stimulate minimally oxidatively modified low-density lipoprotein (LDL) to bind neutrophils [99]. Moreover, F_2-isoprostanes formation is increased during LDL-oxidation *in vitro* and studies with two different mouse models (apoprotein E- and LDL receptor-deficient mice), have shown that 8-iso-$PGF_{2\alpha}$ directly promotes atherogenesis by activating the thromboxane A_2 receptor (TBXA2R) [101]. In addition, 8-iso-$PGF_{2\alpha}$ has shown to stimulate cell proliferation and endothelin-1 expression in endothelial cells (ECs) [102]. Similarly to 8-iso-$PGF_{2\alpha}$ 8-iso-PGE_2 is also known as potent vasoconstrictor in several vascular beds [22, 103, 104].

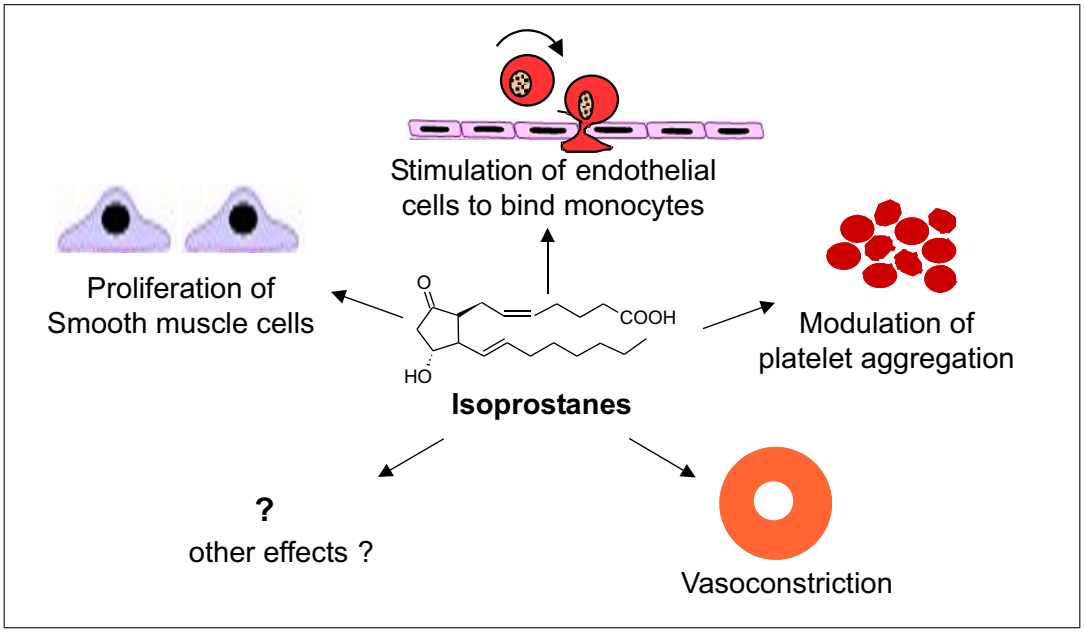

Figure 1.7: Biological effects of isoprostanes.

Table 1.2: Vasoconstrictive effects of 8-iso-PGF$_{2\alpha}$ according to vascular bed and species.

Tissue	Species	References
Aortig ring segments	rat	[105]
Cerebral arterioles	rat, pig	[106, 107]
Kidney	human, rat	[20, 108]
Pulmonary artery	rabbit, guinea pig, rat	[109, 110, 20]
Retinal vessel	piglet	[111]
Coronary artery	bovine, porcine	[112]
Portal vein	rat	[113]
Mammary artery	human	[114]

1.2.7 Analytical Methods

In a recent multi-investigator study, termed the Biomarkers of Oxidative Stress (BOSS) Study, it was found out that the quantification of plasma and urinary isoprostanes provides the "gold standard" to asses oxidative injury *in vivo* [49]. A number of techniques have been developed to quantify the isoprostanes. Gas chromatography with mass spectrometry (GC-MS) was the first technique to characterize the structures of isoprostanes and became the reference analytical method for their quantification [28, 27, 20]. GC-MS in the negative ion chemical ionization (NICI) mode reliably detects 8-iso-$PGF_{2\alpha}$ with a detection limit of 5 pg/mL [115]. Admittedly this method requires prior purification procedures, such as one solid phase extraction (SPE) and two thin layer chromatography (TLC) steps or one SPE, one TLC and one high-performance liquid chromatogratphy (HPLC) step successively. These time-consuming sample preparations can be reduced by means of GC-MS/MS, which requires only one SPE followed with one TLC step. Furthermore, immunoaffinity chromatography (IAC) provides a time saving possibility for 8-iso-$PGF_{2\alpha}$ extraction. In addition, a number of liquid chromatography (LC)-mass spectrometry for F_2-isoprostanes have been developed. Sample preparation for LC-MS is simpler than for GC-MS because no additional derivatization procedures converting isoprostanes into volatile derivatives are required [116, 117]. The advantages of MS over other approaches include its high sensitivity and specificity. On the other hand MS is a considerably expensive and labor intensive method. For this reason, other techniques such as radioimmunoassays (RIA), and enzyme immunoassays (EIA) have been developed to quantify isoprostanes. Immunoassays are widely used due to their low cost and relative ease use. However, a potential drawback of these methods is that limited information regarding their precision and accuracy are available. In addition, little data exist comparing isoprostanes levels determined by immunoassay to MS.

1.3 TBXA2R and Signal Transduction

The action mechanism of isoprostanes is still unclear, but experimental findings showed that many effects of 8-iso-$PGF_{2\alpha}$ were blocked by the TBXA2R antagonist SQ-29548, leading to the suggestion that isoprostanes may act as an alternative ligand for the TBXA2R [22, 101, 118, 109, 119]. TBXA2R activation mediated by thromboxane A_2

plays a key role in vascular haemostasis [120, 121]. Thromboxane A_2 stimulates platelet aggregation, causes vasoconstriction, and is able to mediate mitogenic responses in vascular smooth muscle cells (VSMCs). It also stimulates the release of prostacyclin, which acts as a physiological antagonist of thromboxane A_2. Alteration in TBXA2R signaling has been involved in a number of cardiovascular disorders, e.g. myocardial infarction [122], ischaemic heart disease [121], unstable angina [123], and pregnancy-induced hypertension [124]. In contrast to thromboxane A_2, which rapidly degrades into an inactive form *in vivo*, isoprostanes may represent stable TBXA2R agonists. A single gene on chromosome 19p13.3 leads to the expression of two separate TBXA2R isoforms: TBXA2R-α and a splice variant termed TBXA2R-β [125, 126, 127]. Comparison of the two sequences reveals that even though the first 328 amino acids are the same for both isoforms, the TBXA2R-β isoform exhibits an extended C-terminal cytoplasmatic domain. Expression and tissue distribution of the two isoforms were explored and it could be shown that TBXA2R-α is broadly expressed, whereas TBXA2R-β has a more limited tissue distribution [128]. Despite advances exploring their individual functional and regulatory characteristics, the distinction between TBXA2R-α and TBXA2R-β with respect to their ultimate physiological or pathophysiological roles remains unclear.

TBXA2R stimulation leads to the activation of different signaling cascades that regulate the cytoskeleton, cell adhesion, cell motility, nuclear transcription factors, proliferation, cell survival, and apoptosis. The TBXA2R couples with several G-proteins including $G_q/_{11}$, $G_{12}/_{13}$, G_i, G_s, G_h, which in turn control several effectors (Figure 1.8). G-protein coupling is tissue- or cell type-dependent and it is assumed that the major G-proteins that communicate with TBXA2R are G_q and G_{13}. G_q coupling leads to phospholipase C-δ (PLC-δ) activation, which induces inositol 1,4,5-triphosphate (IP_3) and diacylglycerol (DAG) accumulation, which in turn activate Ca^{2+} release from the endoplasmatic reticulum and protein kinase C (PKC), respectively. Stimulation of $G_{12}/_{13}$ leads to p115-RhoGEF activation and induces thereby Rho-mediating signaling. Rho is known to play a key role in the regulation of the actin cytoskeleton, cell motility, and cell proliferation. Stimulation of G$\beta\gamma$ causes activation of phosphatidylinositol 3-kinase (PI3K), phospholipase C-β2 (PLC-β2), and p44/42 mitogen-activated protein kinase (MAPK) also known as extra-regulated protein kinase-1/2 (ERK-1/2). G_h activates phospholipase C-δ (PLC-δ), resulting in similar response to that mediated by G_q. G_i inhibits adenylyl cyclase while G_s stimulates it, both inducing changes in cyclic AMP

(cAMP) levels. Pertussis toxin (PTX) has been widely used as a reagent to characterize the involvement of heterotrimeric G-proteins in signaling. This toxin catalyses the adenosindiphosphat (ADP)-ribosylation of specific G-protein α subunits of the G_i family, and this modification prevents the occurrence of the receptor G-protein interaction.

However, it was also suggested that 8-iso-$PGF_{2\alpha}$ may act as a partial TBXA2R agonist in human platelets [129]. Furthermore, some investigators reported that 8-iso-$PGF_{2\alpha}$ may act at receptor sites related to, but distinct from the TBXA2R in VSMCs [130, 131]. However, molecular evidence for the existence of a distinct receptor for isoprostanes has not been found, yet.

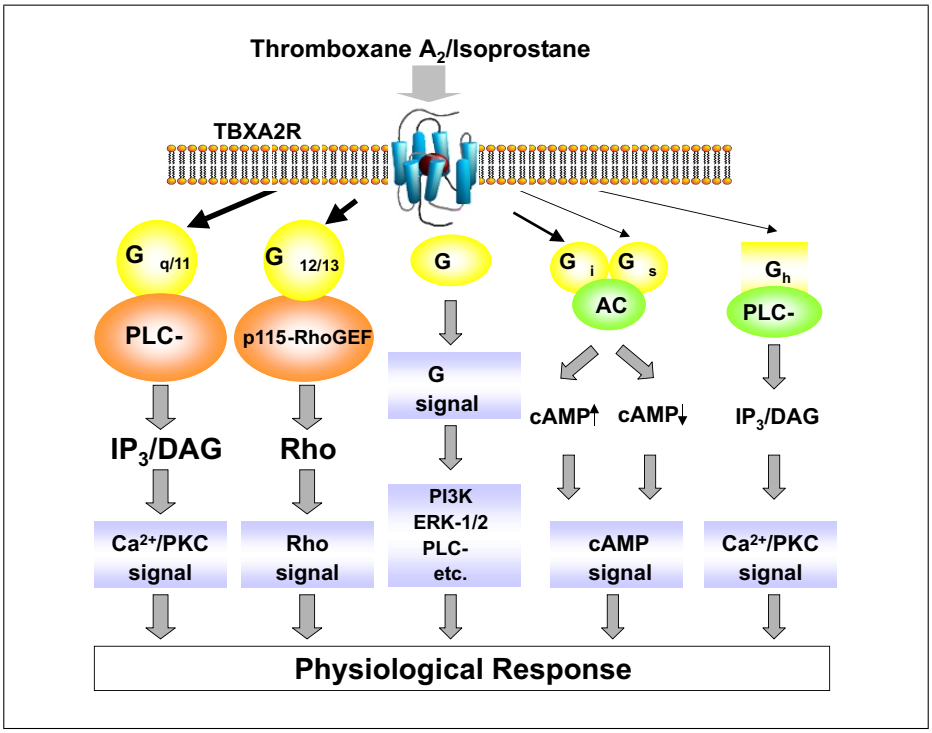

Figure 1.8: G-protein coupling of TBXA2R and signal trandsduction. Abbreviations: PLC-β, phospholipase C-β; p115-RhoGEF, p115 guanine nucleotide exchange factor for Rho; AC, adenylyl cyclase; PLC-δ, phospholipase C-δ; IP_3, inositol 1,4,5-triphosphate; DAG, diacylglycerol, cAMP: cyclic AMP, PI3K: phosphatidylinositol 3-kinase, ERK-1/2, extracellular regulated kinase, PKC: protein kinase C ([132], modified).

1.4 Mechanisms of Angiogenesis

Angiogenesis, the formation of new blood vessels from preexisting ones, plays an important role in physiological processes like wound healing and ovulation, but also in pathophysiological conditions, such as myocardial ischemia in patients with CHD. It is crucial for collateral vessel growth to maintain the blood supply. Angiogenesis is a tightly regulated process, requiring a controlled interplay between pro- and anti-angiogenic factors. Excessive angiogenesis contributes to numerous disorders e.g. cancer, psoriasis, arthritis, and blindless. On the other hand, insufficient vessel growth causes heart and brain ischemia as well as neurodegeneration, pre-eclampsia, osteoporosis and other disorders [133]. Angiogenesis requires different sequential steps starting with vasodilatation, a process involving nitric oxide (NO). Afterwards increased vascular permeability allows extravasation of plasma proteins that provides a temporary scaffold guiding migrating cells to their targets. Subsequent extracellular matrix (ECM) degradation induced by metalloproteases relieves pericyte-EC contacts and liberates ECM-sequestered growth factors. Finally, ECs proliferate and migrate to distant sites and assemble as cord that acquire a lumen (Figure 1.9) [134, 135].

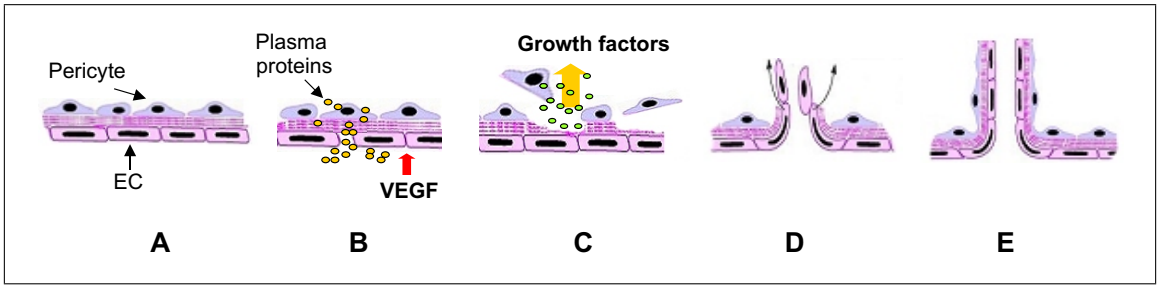

Figure 1.9: Steps in angiogenesis. **A**: Qiescent, stable monolayer of ECs. **B**: VEGF triggers vasodilataion and vascular permeability allowing extravasation of plasmaproteins. **C**: Degradation of the ECM relieves pericyte-EC contacts and liberates ECM-sequestered growth factors. **D**: ECs proliferate and migrate to their final destination. **E**: ECs assemble as tubes. Abbreviations: ECs, endothelial cells; VEGF, vascular endothelial growth factor; ECM, extracellular matrix.

Cell migration requires generation of membrane protrusions in the direction of movement as well as formation of transient adhesions at the leading edge to the substratum. Furthermore, a contractile force drives the cell body forward while the rear part of the cell is simultaneously detached from the substratum. These processes require the formation of adhesive structures and cellular contractions. All these steps are largely controlled by the major angiogenic factor vascular endothelial growth factor (VEGF), which stimulates angiogenesis in a strict dose-dependent manner. VEGF comprises a family of structurally related proteins including seven members. The prototype member, VEGF-A, can express five distinct isoforms, under which VEGF-A_{165} (generally referred to as VEGF) is the dominant subtype in terms of amount and biological activity [136]. VEGF expression can be induced by hypoxia [137]. The main receptors involved in VEGF signaling transduction belong to the platelate derived growth factor (PDGF) receptor superfamily of receptor tyrosine kinases (RTK). The VEGF-receptor 2 (VEGFR-2), also referred to as kinase insert domain-containing receptor (KDR) mediates almost all processes occurring during angiogenesis [138, 133]. The stimulation of VEGFR-2 leads to activation of a number of downstream signaling cascades (Figure 1.10). The activation of the phosphatidyl inositol 3 kinase (PI3K) /Akt pathway by VEGF leads to phosphorylation of several Akt targets, which contribute to EC survival, growth, and proliferation [139, 140]. Furthermore, Akt activates the endothelial nitric oxide synthase (eNOS) through direct phosphorylation, thus enhancing the eNOS-derived NO production, which can stimulate vasodilatation, vascular remodeling, and angiogenesis [141, 142, 143]. Moreover activation of PI3K/Akt can also stimulate VEGF expression by increasing the production of the transcription factors referred to as hypoxia inducible factor1/2α (HIF1α and HIF2α), which regulate hypoxia-mediated VEGF gene upregulation [137, 140]. Ultimately, Akt is required for proper EC migration, via an unknown mechanism [144].

The ERK-1/2 signaling pathway is also involved in cell morphogenesis and motility [145]. ERK-1/2 belongs to the family of MAPK and is activated via a cascade of specific phosphorylation events beginning with the activation of rat sarcoma (Ras), followed by activation of rat fibrosarcoma (Raf-1). Subsequently, Raf-1 phosphorylates and activates MAPK ERK Kinase-1/2 (MEK-1/2), which in turn phosphorylates and activates ERK-1/2 [145, 146]. When activated, ERK-1/2 can phosphorylate various downstream substrates involved in a multitude of cellular responses from cytoskeletal changes to

gene transcription. Identified substrates include several protein kinases, e.g. myosin light chain kinase (MCLK), which is involved in the formation of membrane protrusions and focal adhesion turnover. Phosphorylation of focal adhesion kinase (FAK) by ERK-1/2 may also contribute to the regulation of focal adhesion dynamics [147].

The Ras homologues (Rho) protein family of small GTPases is an essential downstream effector of VEGF signaling as well. The main representatives of the Rho protein family are RhoA, ras-related C3 botulinum substrate (Rac1) and cell division cycle (Cdc) 42, which are key regulators of filament (F)-actin cytoskeletal dynamics that control cell contraction, movement, and adhesion as well as organization of cell-to-matrix and cell-to-cell contacts [148, 149, 150]. Rho proteins can switch between an active guanosine triphosphate (GTP)- and an inactive guanosine diphosphate (GDP)-bound state. Three classes of regulatory proteins, working immediately upstream of these Rho proteins, control this cycling activation/inactivation process: GPTase-activating proteins (GAPs), guanine nucleotide dissociation inhibitors (GDIs) and guanine nucleotide exchange factors (GEFs). GAPs promote the inactive GDP-bound state, GDIs modulate Rho activity by sequestration of Rho proteins in the GDP-bound state and GEFs activate the Rho family by stimulating the exchange of GDP to GTP [134]. A coordinated spatiotemporal activity of Cdc42, Rac1, and RhoA enables the constant remodeling of the F-actin cytoskeleton into filopodia, lamellipodia, and stress fibers, respectively [151]. Filopodia, the thin, needle-like projections at the leading edge, are capable of sensing motile stimuli. Lamellipodia are broad, flat, sheet-like protrusions, which are able to form focal complexes, an important step in the attachment of migrating cells to the ECM. The formation of both lamellipodia and filopodia is coupled with actin polymerization [152]. RhoA stimulates cell contractility and adhesion by inducing the formation of stress fibers and focal adhesions, respectively. RhoA exerts these functions by activating its main effector the Rho-associated kinase (ROCK). ROCK increases myosin light chains (MLCs) phosphorylation not only by inhibiting MLC phosphatase activity but also by leading to direct phosphorylation of MLC [153]. Activated myosin in turn bundles F-actin, resulting in the formation of stress fibers, which are linked to the plasma membrane through focal adhesions. Focal adhesions are dynamic and multimolecular protein complexes connecting the cytoskeleton with the ECM. RhoA induced contractility is involved in tail detachment of migrating cells. [150].

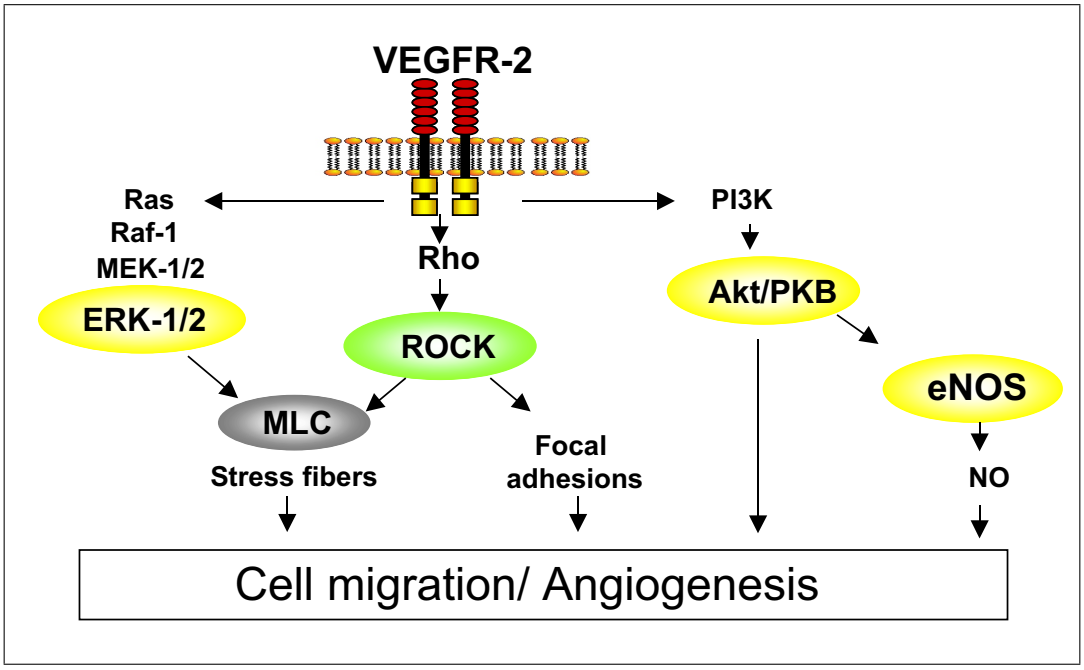

Figure 1.10: VEGF-induced signaling pathways involved in angiogenesis. Abbreviations: VEGFR-2, Vascular endothelial growthfactor receptor-2; Ras, rat sarcoma; Raf-1, rat fibrosarcoma; MEK-1/2, MAPK/ERK/Kinase-1/2; ERK-1/2, extracellular regulated protein kinase-1/2; PI3K, Phosphatidylinositol 3 kinase; Akt/PKB, Akt/protein kinase B; MLC, Myosin light chain; eNOS, endothelial nitric oxide synthase; NO, nitric oxide.

1.5 Objectives

1) The first objective was to investigate the influence of isoprostanes on angiogenesis. For this purpose the effects of the isoprostanes 8-iso-$PGF_{2\alpha}$, 8-iso-PGA_2, and 8-iso-PGE_2 on basal and VEGF-induced migration and tube formation of ECs were investigated.

2) The second objective was to find out via which signaling pathways isoprostanes mediate their effects. In this matter the PI3K/ Akt- and the ERK-1/2-pathway as well as the role of Rho kinase were elucidated.

2 Methods

2.1 Cell Culture

Two types of primary human endothelial cells were used for this work: human coronary artery endothelial cells (HCAECs) and human dermal microvascular endothelial cells (HDMECs), both from promoCell, Heidelberg, Germany. They were available as cryopreserved cells in serum-free medium and stored at -196 °C in liquid nitrogen. All procedures with cells were performed under a laminar airflow bench. Cells were thawed according to manufacturer's instructions. They were cultured in a special formulated medium for microvascular endothelial cells (Endothelium Cell Growth Medium MV, PromoCell, Heidelberg, Germany), containing 5 % fetal bovine serum (FCS), 10 ng/mL recombinant epidermal growth factor, 1 µg/mL hydrocortisone, 500 µg/mL gentamicin and 500 ng/mL amphotericin B. Cells were cultered in 25- or 75-cm^2 flasks under 5 % CO_2 and 36 °C.

HCAECs were proliferated and subcultured to passage 3, then aliquoted and stored again in liquid nitrogen. A new aliquot was thawed and passages 4-7 were used for experiments.

HDMECs were purchased anew from the manufacturers for every series of experiments. They were not refrozen after thawing in order to maintain their cellular response to growth factors. HDMECs in passages 2-5 were used for migration assays and Western blots. Medium was changed every other day and cells were subcultured until a confluence of 75 % was reached. Basal endothelial medium (without endothelial growth supplement) added with 0.1 % bovine serum albumin (BSA) was used for experiments.

2.2 Migration Assay

Migration assays were performed with a Boyden chamber from Neuroprobe, Gaithersburg, USA. The Boyden chamber assay is based on a chamber of two medium-filled compartments separated by a polycarbonate membrane. Cells are placed in the upper compartment and are allowed to migrate through the pores of the membrane into the lower compartment, in which chemotactic agents are present (Figure 2.1). A 96-well Boyden Chamber was used for this work. Test solutions were prepared in basal endothelial medium with 0.1 % BSA. Stock solution of the test substances were in ethanol, so that the final concentration of ethanol in all samples was 0.1 %. Therefore, a sample without any test substance in basal endothelial medium with 0.1 % BSA and 0.1 % ethanol was used as vehicle. VEGF, a potent growth and angiogenic cytokine was applied as positive control in a concentration of 50 ng/mL in basal endothelial medium containing 0.1 % BSA and ethanol, respectively. The bottom wells were filled with 30 µL chemotactic test solutions. A polycarbonate filter with 8 µm diameter pores was thin-coated overnight with 100 µg/mL type I collagene (Angiotech, Vencouver, Canada), diluted in 20 mmol/L acetic acid. Afterwards the filter was washed with phosphate buffered saline (PBS), dried and placed on the lower compartment of the Boyden Chamber, which already contained the chemotactic test solutions. Subsequently cells were washed twice with PBS and lifted with 0.05 % trypsin/0.53 mM EDTA. As soon as they had detached from the bottom of the bottle, 10 % fetal bovine serum (FBS) diluted in basal endothelial medium with 0.1 % BSA was pipetted in. Thereafter the cell suspension was centrifugated at 220 RCF and 30 °C for 4 min, the supernatant was sucked off and the cell pellet was solved in basal endothelial medium with 0.1 % BSA. The cell concentration was calculated via the Neubauer counting chamber and adjusted to 200.000-300.000 cells/mL. 50 µL of this cell suspension was pippeted into each top well on the upper compartiment of the Boyden chamber. The filled apparatus was incubated at 37 °C in humidified air with 5 % CO_2 to let the cell migrate. The incubation time lasted 4 h for HCAECs and 5 h for HDMECs. After incubation the filter was removed from the apparatus and cells were fixed with methanol and stained with a Giemsa solution. Non-migrated cells were removed from the upper surface of the insert with a cotton swab. The number of migrated cells was counted in four randomly chosen fields under 400x magnification and averaged. All experiments were performed at least in triplicate and each experiment was repeated at

least twice. The migration was expressed as percentage of basal cell migration.

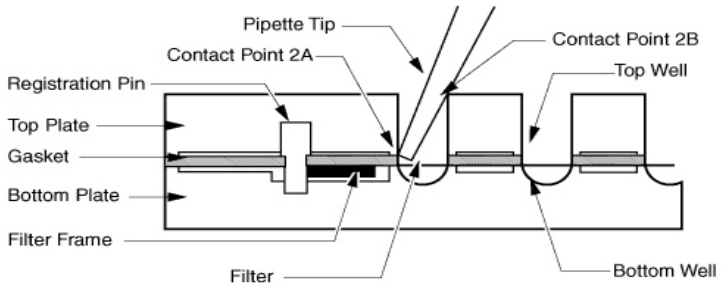

Figure 2.1: Boyden chamber.

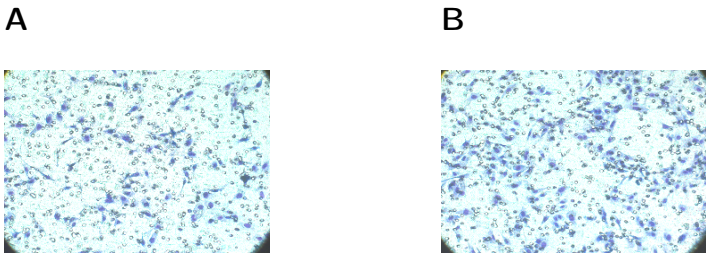

Figure 2.2: Migrationsassay performed with HDMECs. A: Vehicle (0.1 % EtOH). **B:** positive control (VEGF 50 ng/mL).

2.3 Tube Formation Assay

The tube formation assay is based on the differentiation of ECs on a basement membrane matrix. BD Matrigel Basement Membrane Matrix® (matrigel) is a solubilized basement membrane preparation extracted from the Engelbreth-Holm-Swarm (EHS) mouse sarcoma, a tumor rich in extracellular matrix proteins. It mainly contains laminin and collagen whose interaction provide a foundation for the assembly of other basement membrane components. ECs differentiate and form capillary-like structures on matrigel. Matrigel was thawed overnight on ice at 4 °C and used for thin-coating of a

48-well plate. Subsequently HCAECs were lifted as described before. Approximately 30.000 cells suspended in basal medium enriched with 0.1 % BSA und 5 % FCS were added in each well. After 1 h incubation time medium was removed and replaced with basal medium enriched with 0.1 % BSA and 5 % FCS with/without VEGF 20 ng/mL as well as with/without test substances. The cells were then let to incubate for 24 h, at 37 °C and 5 % CO_2.

Cells were incubated with a 1:5.000 dilution of 2',7'-bis'(carboxyethyl)-5-(6')- carboxyfluorescein/acetoxymethylester (BCECF/AM), a nonfluorescent lipophilic acetoxymethylester, that readily enters cells and is enzymatically hydrolyzed to fluorescent BCECF once inside. A confocal laser scanning microscope equipped with an argon laser at 488 nm was used and optical filters were set to visualize the emission fluorescence spectra over 500 nm. Two pictures of each well were taken in 10x magnification with AxioCam PRc5 camera, and analyzed with Zeiss LSM Image Browser v. 3.2.0. Tubes were measured in a 800.000 μm^2-area, only node-to-node continuous were measured and counted as tubes.

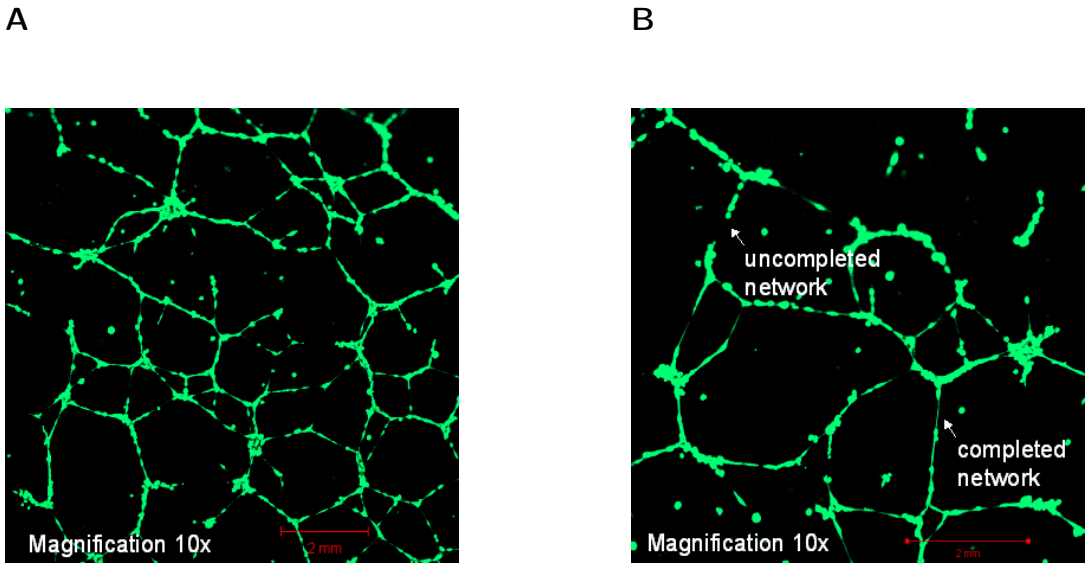

Figure 2.3: Tube formation performed with HCAECs. A: tube network. **B:** close-up on completed and uncompleted tube structures.

2.4 Protein Analysis

2.4.1 Protein Extraction

For protein extraction cultured cells were rinsed twice with PBS and lysed with 80 µL ice cold lysis buffer per 25 cm^2. They were mechanically harvested by means of a cell scraper and the obtained suspension was transferred in an aliquot set on ice. After homogenization by pipetting up and down the homogenate was centrifugated at 4 °C and 12.000 g for 5 min. The supernatant was aliquoted and frozen at -80 °C until further use.

2.4.2 Protein Quantification

The protein concentration was determined by the Bradford protein assay, which is a dye-binding assay in which a differential color change of a dye occurs in response to various concentrations of protein. For the protein concentration determination 10 µL of supernatant of protein samples were added to 790 µL *aqua ad injectabilia*. After addition of 200 µL Bradford reagent and incubation at room temperature for 15 min, the absorbance at 595 nm was measured with a spectrophotometer. Substraction of the blank value (800 µL *aqua ad injectabilia* plus 200 µL Bradford reagent) and comparison with a standard (immunoglobulin G) curve in the concentrations 3.45, 6.90, 10.35 and 13.8 µg/mL provided a relative measurement of protein concentration. Each protein determination was performed in duplicate.

2.4.3 Western Blot Analysis

Separation of the proteins was performed by gel electrophoresis under reducing and denaturing conditions. Therefore 30 µg protein were prepared with Laemmli buffer, adjusted to a volume of 50 µL with *aqua ad injectabilia* and denaturated by heating at 95 °C for 5 min. Subsequently the samples were loaded on a SDS-containing polyacrylamide gel, consisted of a collecting- and seperating gel. Electrophoresis was carried out at 150 V for 1.5 h in electrophoresis running buffer. The Precision Plus Protein Standard® was used as molecular weight marker. After separation, the proteins were transferred

Primary antibodies	Dilution	Secondary antibodies	Dilution
1.Phospho-Akt (Ser473) Antibody	1:1.000	Anti-rabbit IgG HRP	1:1.000
2.Phospho-p44/42 MAPK (Thr202/204) Antibody	1:1.000	Anti-rabbit IgG HRP	1:1.000
3.Phospho-eNOS (Ser1177)	1:1.000	Anti-rabbit IgG HRP	1:1.000

Table 2.1: Primary Antibodies used for Western blot analysis.

onto a nitrocellulose membrane with a constant current of 400 mA for 1 h. This transfer was performed in transfer buffer. Subsequently the efficiency of the transfer was checked by staining the membranes with Ponceau red. Thereafter the membrane was washed with TBST-T buffer, and saturated with 5 % milk powder dissolved in TBS-T buffer for 1 h at room temperature. After repeated washing the membrane was incubated with the primary antibody (Table 2.1) overnight at 4 °C. The Path Scan Multiplex Western Cocktail® (Cellsignaling, Boston, USA) was used to detect the proteins phospho Akt (Ser473) and phospho p44/42 MAPK (Thr202/204). The Multiplex Western Cocktail contained an additional eukaryotic initiation factor 4E (eIF4E) antibody, which was used to control protein loading. This antibody detects endogenous levels of total eIF4E protein and does not cross-react with other proteins. In addition, phospho eNOS was also detected by using a specific phospho eNOS antibody (Biolabs, Frankfurt am Main, Germany).

After washing with TBS-T buffer, the membrane was incubated with specifically horseradish peroxidase (HRP)-conjugated secondary antibodies for 1 h at room temperature. After washing and adding ECL western blotting substrate (Pierce, Rockford, USA), a luminol-based chemiluminescent substrate for the detection of HRP on immunoblots, the protein bands were visualized via X-ray film exposure. Bands were analyzed by densitometry with the Gene Tool software.

2.5 Cytotoxicity Assay

A cytotoxicity detection kit (Roche, Grenzbach-Whylen, Germany) was used to investigate the cytotoxicity potential of the tested compounds. This assay is based on the measurement of lactate dehydrogenase (LDH) activity from damaged cells. In the first step NAD^+ is reduced to $NADH/H^+$ by the LDH-catalyzed conversion of lactate to pyruvate. In the second step the catalyst transfers H/H^+ from $NADH/H^+$ to the tetrazolium salt 2-[4-iodohenyl]-3-[4-nitrophenyl]-5-phenyltetrazolium chloride (INT), which is reduced to formazan. The increase in supernatant LDH-activity directly correlates to the amount of formazan over time. The formazan dye formed shows an absorption maximum at about 500 nm, whereas the tetrazolium salt INT shows no significant absorption at this wavelength. In accordance to the manufacturer's protocol HDMECs were let to incubate on a collagen-coated 96 well plates and treated for 5 h with the test substances. Afterward the culture supernatant was collected and centrifugate to remove cells. The cell-free supernatant were transferred into corresponding wells of an optically clear bottom 98-well microplate and incubated with added Reaction mixture from the kit for 30 min at room temperature. The absorption of the samples were measured using an ELISA reader. The maximum amount of releasable LDH enzyme activity was determined by lysing the cells with 1 % Triton X-100.

2.6 Chromatographic Methods for Analysis of 8-iso-PGA_2 Transformation *in Vitro*

2.6.1 High-Performance Liquid Chromatography for Analysis of 8-iso-PGA_2 Transformation *in Vitro*

Reversed phase high performance-liquid chromatography (RP-HPLC) of cyclopentenone isoprostanes was performed using a Dionex ASI-100 autosampler and a Dionex P 680 HPLC pump (Idstein, Germany) equipped with a column (250 x 4.6 mm ID) packed with 100-5C18 Nucleosil from Macherey-Nagel (Düren, Germany). Free acids were analysed isocratically using a mobile phase consisting of 10 mM NaH_2PO_4/acetonitrile/2-propanol (67:21:12, v/v/v), the pH was adjusted to 3.5 by *o*-phosphoric acid. The flow rate was

1.0 mL/min and the effluent was detected at 205 nm using a DAD detector UVD 340 U from Dionex. The following retention times were obtained from separate analyses of each isoprostane: 23.9±0.2 min for 8-iso-PGA_2, 26.3±0.4 min for compound X, 14.4±0.3 min for compound Y (mean ± SD, n=5). Compound X and Y were obtained after 24 h and 48 h incubation of 8-iso-PGA_2 in cell culture medium at 37 °C, respectively. Compounds were extracted from cell culture supernatants by SPE. For this purpose the cell culture supernatants were diluted 1:1 (v/v) with water, the pH was adjusted to 2-3 by 5 M HCOOH. Subsequently the samples were vortexed and stored on ice for 30 min. Octadecylsilica (C_{18})-SPE columns (500 mg, Chromabond, Macherey-Nagel, Düren) were conditioned with 10 mL of MeOH then with 10 mL of 0.05 M HCOOH, before samples were applied. Columns were subsequently washed with 10 mL of 0.5 M HCOOH then with 2 mL of heptane. Samples were eluted with 2 mL ethylacetate. Solvent present in the eluate from solid phase extraction was evaporated to dryness. Subsequently the residue was diluted in 200-µL aliquot of the mobile phase and 25 µL of this solution was injected into the RP-HPLC system.

2.6.2 Liquid Chromatography-Tandem Mass Spectrometry for Analysis of 8-iso-PGA_2 Transformation *in Vitro*

The transformation products of cyclopentenone isoprostane 8-iso-PGA_2 were analysed via liquid chromatography-tandem mass spectrometry (LC-MS/MS). Aliquots of the RP-analysis of transformed isoprostanes were collected at the retention times indicated for compounds X and Y and subsequently subjected either to LC-MS/MS. LC-MS/MS anlysis was performed with negative ion electrospray ionisation (ESI) using a Varian 1200 triple quadrupole spectrometer equipped with Varian Pro Star 230 HPLC pumps (Darmstadt, Germany). Isoprostanes were analysed isocratically using a mobile phase consisting of 33 % 1 mM ammonium acetate, pH 4.5 and 66 % acetonitrile. Mass spectra obtained were compared with the spectra of cyclopentenone 15-deoxy-Δ12,14-prostaglandin J_2 (15-deoxy-PGJ_2, Cayman Chemical).

2.6.3 Gas Chromatography-Mass Spectrometry for Analysis of 8-iso-PGA$_2$ Transformation *in Vitro*

The transformation products of cyclopentenone isoprostane 8-iso-PGA$_2$ were also analysed with GC-MS. Aliquots of the RP-analysis of transformed isoprostanes were collected at the retention times indicated for compounds X and Y. Prior to GC-MS analysis compounds X and Y as well as 8-iso-PGE$_2$ were converted to their pentafluorobenzyl (PFB) *O*-methoxime (MO) trimethylsilyl (TMS) derivatives (Figure 2.4).

For that purpose the collected aliquots were evaporated down to 0.4-0.5 mL under nitrogen and at 40 °C, then transferred into silanised vials and desiccated, under nitrogen and at room temperature, until crystallization. For the first derivatization, 10 µL MeOH, 100 µL acetonitril, 10 µL Hünig's base (N,N-diisopropylethylamine) and 10 µL 2,3,4,5,6-pentafluorobenzyl (PFB) bromide 33 % (v/v) in acetonitrile were added in each sample. Subsequently samples were incubated at 30 °C for 1 and desiccated under nitrogen at room temperature until they crystallised. For the second derivatization, 100 µL waterfree, saturated *O*-methylhydroxylamine hydrochloride (MOX)/pyridine solution was added to each sample. After incubation at 60 °C for 1 h, the reaction mixtures were desiccated under nitrogen and at room temperature, until crystallization. For the third derivatization, 100 µL of N,O-bis(trimethylsilyl)(TMS)trifluoroacetmaide (BSTFA) was added in each sample and they were incubated at 60 °C for 1 h. Subsequently the residuum of each sample was dissolved in 200 µL *aqua ad injectabilia* and extracted with 500 µL diethyl ether twice. The upper phase was transferred into a silanised vials and the sample was desiccated under nitrogen again. Samples were dissolved in methanol and analysed via GC-MS.

GC-MS analyses was performed by means of a quadrupole mass spectrometer 1200 (Varian, Walnut Creek, USA), equipped with a gas chromatograph CP-3800 (Varian). The gaseous separation occurred by means of a 30 m x 0.25 mm (length x diameter) FactorFour^{TM}-5MS capillary column (Varian), with a film thickness of 0.25 µm. The capillary column was heated according the following temperature sequence: 70 °C for 2 min, heating to 280 °C at a rate of 25 °C/min, heating at 325 °C at a rate of 5 °C/min. The carrier gas was helium, with a constant flow of 1 mL/min. The temperature o the injector, 150 °C at the injection, was increased immediately thereafter to 300 °C at a rate of 100 °C/min. Injection volume was 2.0 µL in the split/splitless mode. A 1:10

split was used at injection time and closed after 20 sec. The transferline and the ion source were heated at a constant temperature of 300 °C and 170 °C respectively. Under the chosen NICI conditions, the ionization energy was 70 eV and the electron current 160 µA. Methane was used for chemical ionization in the ion source. For detection of the ions, the electron-multiplier was set to a tension of 1.4 kV.

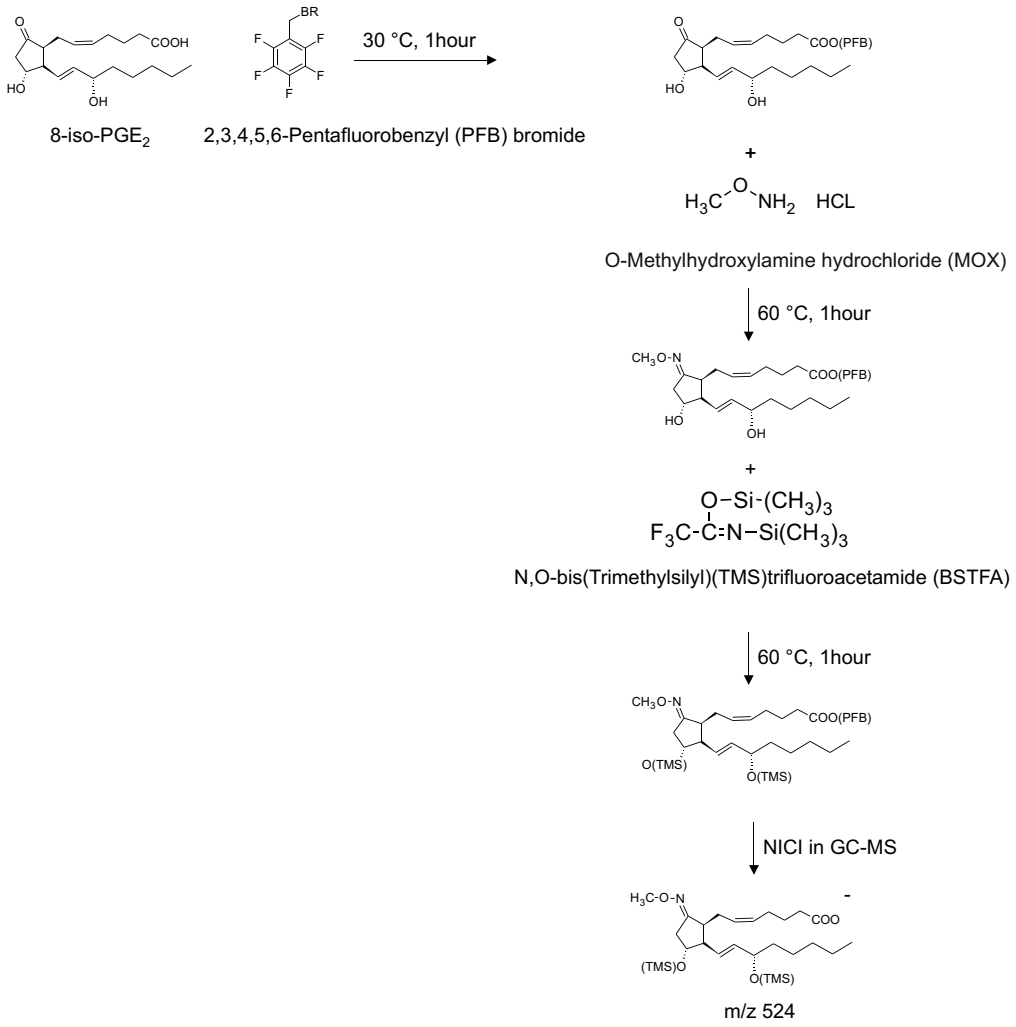

Figure 2.4: Derivatization and ionization of 8-iso-PGE$_2$ via GC-MS.

2.7 Statistical Analysis

All data are expressed as mean ± SD. Statistical analysis was performed by 1-way ANOVA followed by the Fisher's protected least significant difference test using GraphPad Prism 4 software. Probability values were considered significant at $P<0.05$.

3 Results

3.1 Influence of Isoprostanes and the Thromboxane A_2 Mimetic U-46619 on Basal Migration of Endothelial Cells

EC migration represents a crucial step in the process of angiogenesis. To explore the effect of isoprostanes on angiogenic potential, transwell migration assays with increasing concentrations of 8-iso-$PGF_{2\alpha}$ were performed. 8-iso-$PGF_{2\alpha}$ exerted a biphasic effect on basal migration of HDMECs with a moderate stimulation of migration at lower concentrations (122.1±9.9% (mean±SD) [8-iso-$PGF_{2\alpha}$ at $3{\cdot}10^{-7}$M]; $P<0.01$ versus vehicle) and an inhibitory effect at higher concentrations (72.7±11.2% [8-iso-$PGF_{2\alpha}$ at $3{\cdot}10^{-4}$M]; $P<0.01$ versus vehicle) (Figure 3.1).

This biphasic response to 8-iso-$PGF_{2\alpha}$ was also present in HCAECs (130.8±14.4% [$1{\cdot}10^{-6}$M]; $P<0.001$ versus vehicle and 72.7±9% [$1{\cdot}10^{-4}$M]; $P<0.001$ versus vehicle) and mimicked by the isoprostane 8-iso-PGA_2 (114.8±11.4% [$1{\cdot}10^{-6}$M]; $P<0.01$ versus vehicle and 86.8±5.1% [$1{\cdot}10^{-4}$M]; $P<0.05$ versus vehicle). In contrast, the isoprostane 8-iso-PGE_2 did not induce a significant pro-migrative effect at low concentrations (107±9.7% [$1{\cdot}10^{-6}$M]; $P>0.05$ versus vehicle). But 8-iso-PGE_2 inhibited the basal migration at high concentrations (83.1±16.6% [$3{\cdot}10^{-5}$M]; $P<0.05$ versus vehicle) as well (Figure 3.2).

Moreover, the 8-iso-$PGF_{2\alpha}$-induced biphasic modification of HDMEC migration was reversed by costimulation with the TBXA2R antagonist SQ-29548 (Figure 3.1). SQ-29548 itself had no significant effect on the basal migration of HDMECs (101.±8.7% [$3{\cdot}10^{-5}$M]; $P>0.05$ versus vehicle).

Also the thromboxane A2 mimetic U-46619 dose-dependently reduced the basal migration of HDMECs with a maximum at the highest concentration tested (50.7±6.3% [$3{\cdot}10^{-5}$M]; $P<0.001$ versus vehicle). This effect was completely reversed when U-46619 was incubated with equimolar concentrations of SQ-29548. In contrast to 8-iso-$PGF_{2\alpha}$, U-46619 at low concentrations did not enhance the basal migration in HDMECs (78.38± 9.27% [$1{\cdot}10^{-7}$M]; $P<0.05$ versus vehicle).

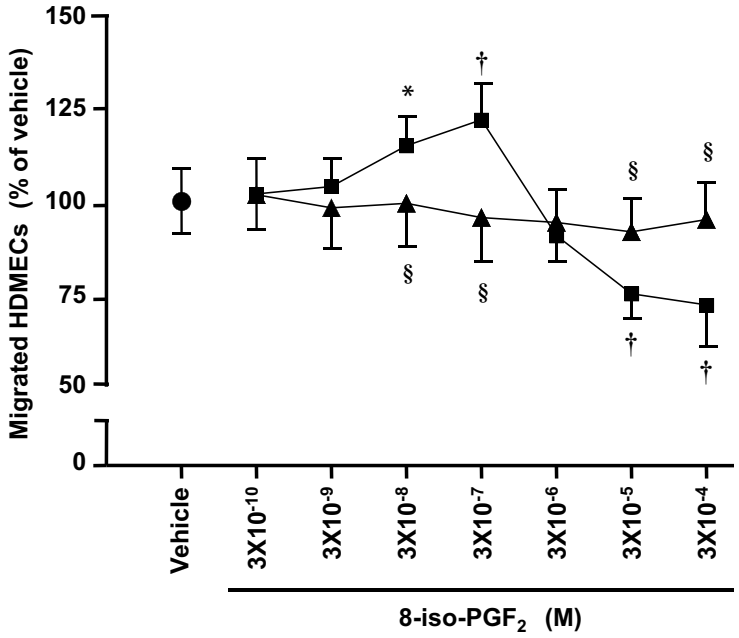

Figure 3.1: Effect of 8-iso-$PGF_{2\alpha}$ on basal migration of HDMECs. 8-iso-$PGF_{2\alpha}$ exerts a biphasic effect on basal migration of HDMECs. The TBXA2R antagonist SQ-29548 abolishes the stimulatory- and inhibitory effects of 8-iso-$PGF_{2\alpha}$.
● Vehicle, ■ 8-iso-$PGF_{2\alpha}$ (M), ▲ 8-iso-$PGF_{2\alpha}$ (M) + SQ-29548 ($3{\cdot}10^{-5}$M). Results are expressed as means ± SD of 2 separate experiments performed at least in triplicate, n=6 to 12. * $P<0.05$, † $P<0.01$ vs. vehicle; § $P<0.01$ vs. 8-iso-$PGF_{2\alpha}$ alone.

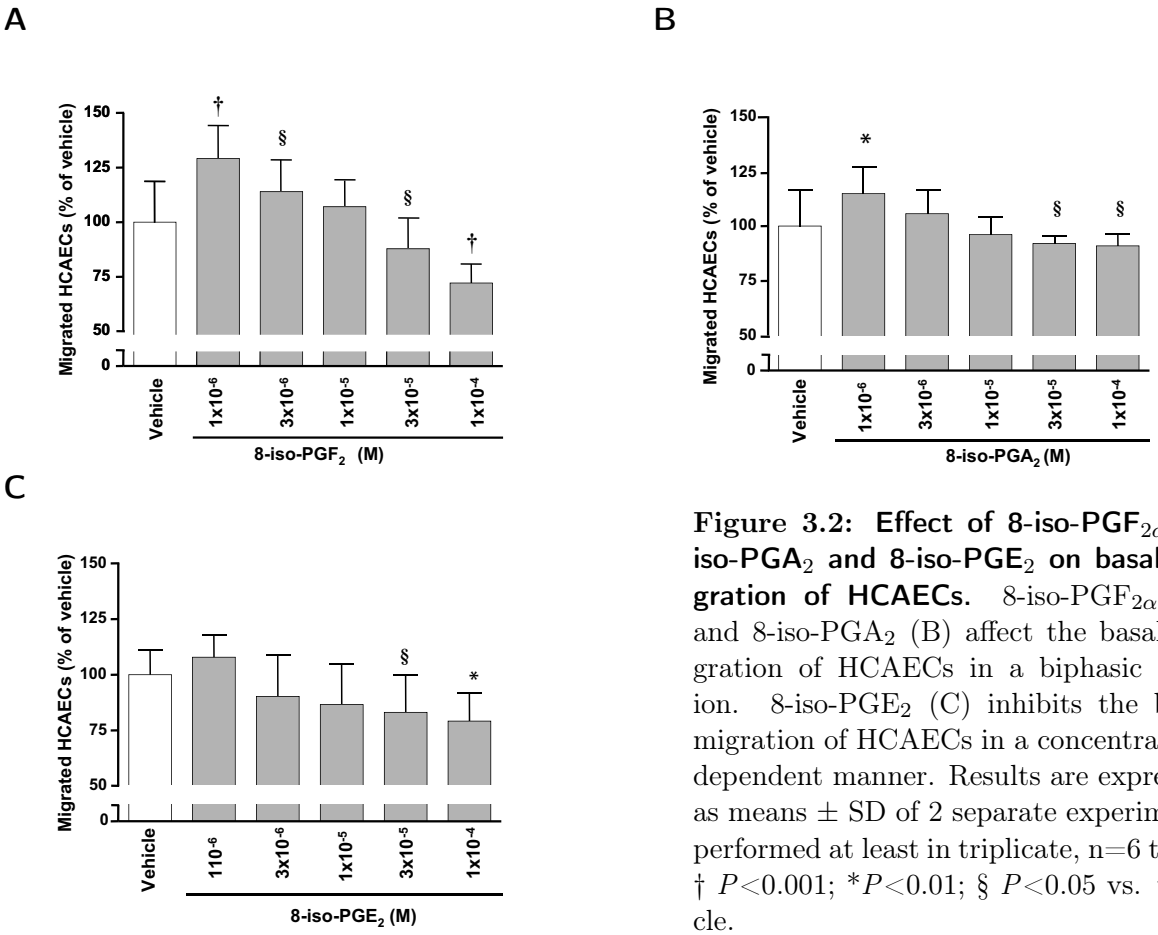

Figure 3.2: Effect of 8-iso-$PGF_{2\alpha}$, 8-iso-PGA_2 and 8-iso-PGE_2 on basal migration of HCAECs. 8-iso-$PGF_{2\alpha}$ (A) and 8-iso-PGA_2 (B) affect the basal migration of HCAECs in a biphasic fashion. 8-iso-PGE_2 (C) inhibits the basal migration of HCAECs in a concentration-dependent manner. Results are expressed as means ± SD of 2 separate experiments performed at least in triplicate, n=6 to 12. † $P<0.001$; *$P<0.01$; § $P<0.05$ vs. vehicle.

3.1.1 Effect of AH-6809 on 8-iso-$PGF_{2\alpha}$-Influenced Basal Migration of Endothelial Cells

It has been reported that 8-iso-PGE_2 is able to evoke substantial contractions in the presence of the TBXA2R antagonist ICI-192605 in the porcine pulmonary vein. In addition, it has been shown that this effect could be blocked by the unspecific $DP/EP_1/EP_2$ (prostaglandin D/prostaglandin E_1/prostaglandin E_2) receptor antagonist AH-6809 [154]. To examine the possible involvement of another receptor beside the TBXA2R in 8-iso-$PGF_{2\alpha}$ stimulated migration, HDMECs were pre-incubated with AH-68093 ($3{\cdot}10^{-5}$M)

for 24 h, then migration assays were performed with AH-6809 and increasing concentrations of 8-iso-$PGF_{2\alpha}$. The results showed that treatment with AH-6809 did not influence the biphasic effect of 8-iso-$PGF_{2\alpha}$ on HDMEC migration compared to non-treated cells (Figure 3.3).

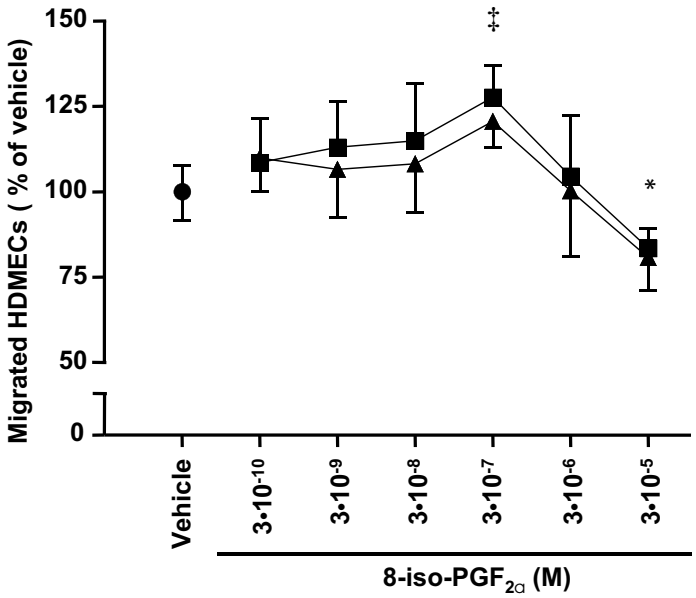

Figure 3.3: Effect of AH-6809 on 8-iso-$PGF_{2\alpha}$-influenced basal migration of HDMECs. AH-6809 does not alter the response of HDMECs to 8-iso-$PGF_{2\alpha}$. ● Vehicle, ■ 8-iso-$PGF_{2\alpha}$ (M), ▲ 8-iso-$PGF_{2\alpha}$ (M) + AH-6809 ($3{\cdot}10^{-5}$M). Results are expressed as mean ± SD of 2 separate experiments performed at least in triplicate, n=9 to 12. * $P<0.01$, ‡ $P<0.05$ vs. vehicle.

3.1.2 Influence of PI3K, ERK-1/2 and Rho-kinase on the pro-Migratory Effect of 8-iso-$PGF_{2\alpha}$

G-protein-coupled receptors and receptor tyrosine kinases are known to promote cell migration. Several critical signaling components including the small G-protein RhoA are involved in this process. RhoA activates the Rho kinase ROCK, which is regarded as a key regulator of cell motility. Other signaling pathways include the activation of

PI3K and ERK-1/2. To explore the potential role of Rho kinase in 8-iso-$PGF_{2\alpha}$ mediated pro-migrative effect at low concentrations ($1{\cdot}10^{-7}$M), further migration assays were performed in the presence of the Rho kinase inhibitor Y-27632 (10 µM). Moreover, a possible involvement of PI3K and ERK-1/2 was investigated by performing migration assays in the presence of the PI3K inhibitors LY-294002 (25 µM) and Wortmannin (10 µM) as well as the ERK-1/2 inhibitor PD-98059 (60 µM). As shown in Figure 3.4, neither PD-98059, Ly-294002, and Wortmannin nor Y-27623 interfered with the pro-migrative effect of 8-iso-$PGF_{2\alpha}$.

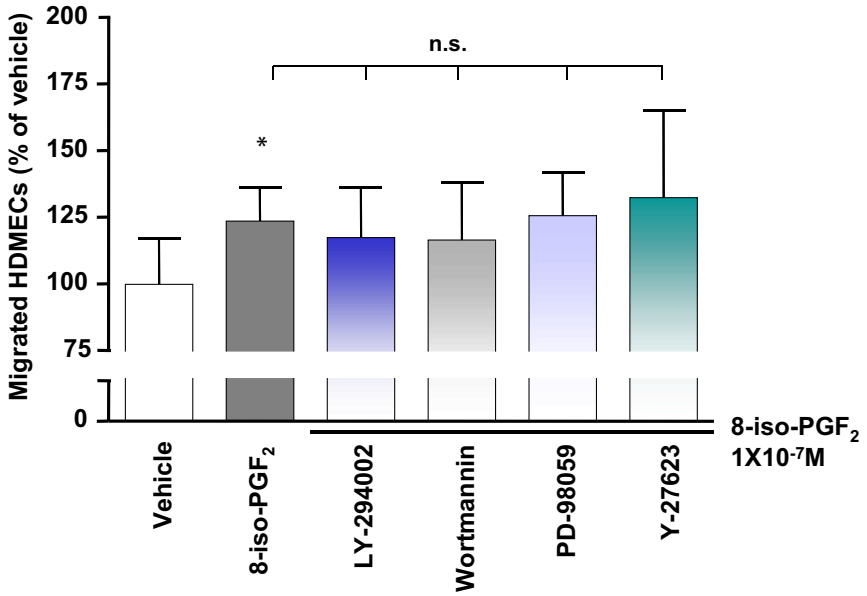

Figure 3.4: Influence of the PI3K inhibitors Ly-294002 and Wortmannin, ERK-1/2 inhibitor PD-98059 and Rho kinase inhibitor Y-27623 on the pro-migrative effect of 8-iso-$PGF_{2\alpha}$. Ly-294002 (25 µM), Wortmannin (10µM), PD-98059 (60 µM), and Y-27623 (10µM) do not influence the pro-migrative effect of 8-iso-$PGF_{2\alpha}$ at $1{\cdot}10^{-7}$M on HDMECs. Results are expressed as mean ± SD of 2 separate experiments performed at least in triplicate, n=9 to 12. * $P<0.01$ vs. vehicle.

3.1.3 The Influence of ERK-1/2 and Rho-kinase on the Anti-Migratory Effect of 8-iso-$PGF_{2\alpha}$ and U-46619

We investigated the potential role of Rho kinase and ERK-1/2 in 8-iso-$PGF_{2\alpha}$-mediated anti-migratory effects on HDMEC basal migration at high concentrations. For this purpose the influence of Y-27632 (10 μM) and PD-98059 (60 μM) on the inhibiting effect of 8-iso-$PGF_{2\alpha}$ ($3{\cdot}10^{-5}$M) was investigated. Interestingly the Rho kinase-inhibitor Y-27632 almost completely abolished the inhibitory effect of 8-iso-$PGF_{2\alpha}$ on HDMEC migration (91.1±7.4% [8-iso-$PGF_{2\alpha}$ + Y-27632] versus 76.5±6.5% [8-iso-$PGF_{2\alpha}$ alone]; $P<0.001$)(Figure 3.5, A), whereas control experiments showed that Y-27632 itself had no effect on basal migration. In contrast, PD-98059 did not impact the anti-migratory effect of 8-iso-$PGF_{2\alpha}$.

Similar results were obtained when these experiments were conducted with the TBXA2R agonist U-46619. Y-27632 almost completely abolished the U-46619-induced inhibition of basal migration (96.5±9.6% [Y-27632 + U-46619] versus 45.9±7.6% [U-46619 alone]; $P<0.001$), whereas PD-98059 did not induce any effect (Figure 3.5, B).

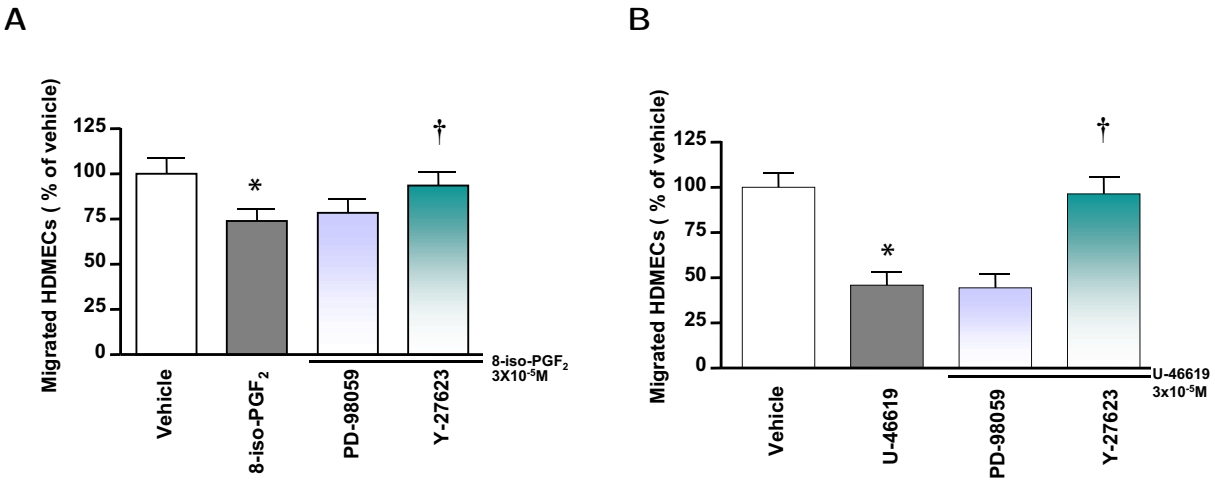

Figure 3.5: Effect of the ERK-1/2 inhibitor PD-98059 and the Rho kinase inhibitor Y-27623 on the anti-migrative effect of 8-iso-$PGF_{2\alpha}$ (A) and U-46619 (B) on HDMEC basal migration. The Rho kinase inhibitor Y-27623 (10 μM) completely reverses the inhibitory effect of 8-iso-$PGF_{2\alpha}$ ($3{\cdot}10^{-5}$M) and U-46619 ($3{\cdot}10^{-5}$M) on basal migration, whereas PD-98059 (60 μM) does not induce any effect. Results expressed as mean ± SD of 2 separate experiments performed at least in triplicate, n=6 to 12. *$P<0.001$ vs. vehicle; † $P<0.001$ vs. 8-iso-$PGF_{2\alpha}$/ U-46619 alone.

3.1.4 The Influence of Gα_i on the pro- and Anti-Migratory Effect of 8-iso-PGF$_{2\alpha}$

To elucidate the role of the Gα_i in 8-iso-PGF$_{2\alpha}$-mediated effects on basal migration, HDMECs were pre-incubated with PTX (0.1 ng/mL)-containing basal medium for 24 h. PTX catalyses the ADP-ribosylation of Gα_i and circumvents therefore Gα_i-mediated signaling. After pre-incubation migrationassays were conducted with 8-iso-PGF$_{2\alpha}$ at $1{\cdot}10^{-5}$M, $1{\cdot}10^{-7}$M, and $1{\cdot}10^{-8}$M, respectively. 8-iso-PGF$_{2\alpha}$ at $1{\cdot}10^{-7}$M did not exert a pro-migratory effect on basal migration of PTX-treated HDMECs (Figure 3.6, B). In contrast 8-iso-PGF$_{2\alpha}$ at $1{\cdot}10^{-7}$M stimulated the basal migration of control cells which were pre-incubated with PTX-free medium (Figure 3.6, A). This pro-migratory effect was reversible by the TBXA2R antagonist SQ-29548. The inhibitory effect of 8-iso-PGF$_{2\alpha}$ at $1{\cdot}10^{-5}$M could be shown in both groups of HDMECs, those which were treated with PTX and those which were not. In both cases SQ-29548 ($3{\cdot}10^{-5}$M) reversed these anti-migratory effects (Figure 3.6, A/B).

A

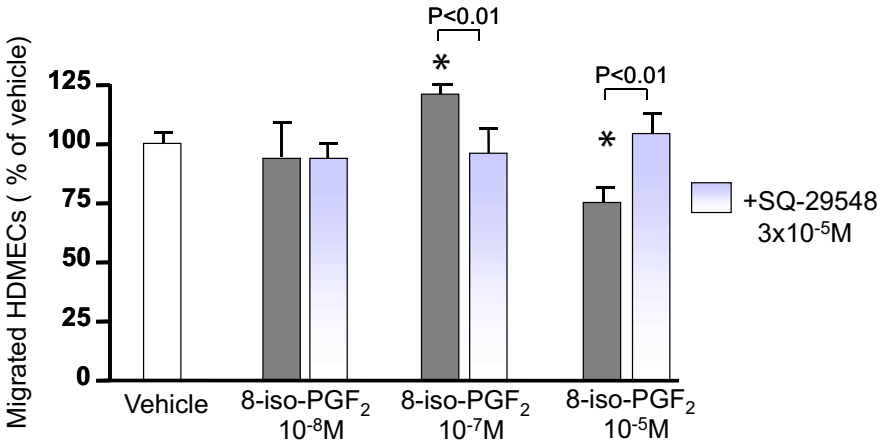

B

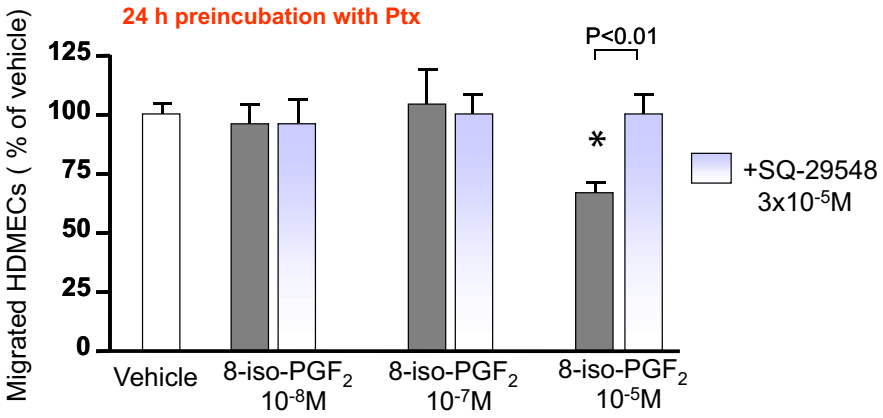

Figure 3.6: Influence of Gα_i on the pro- and anti-migratory effect of 8-iso-PGF$_{2\alpha}$. 8-iso-PGF$_{2\alpha}$ at $1{\cdot}10^{-7}$M exerted a pro-migratory effect on basal HDMEC migration (A). In contrast 8-iso-PGF$_{2\alpha}$ at $1{\cdot}10^{-7}$M did not induce a pro-migratory effect on basal HDMEC migration, when cells were pre-incubated with PTX (0.1 ng/mL) for 24 h (B). Results expressed as mean ± SD of 2 separate experiments performed at least in triplicate, n=9 to 12. *P<0.01 vs. vehicle.

3.2 Influence of 8-iso-PGF$_{2\alpha}$ and U-46619 on Basal Tube Formation of Endothelial Cells

Endothelial tube formation represents a further important step in the angiogenic process. To elucidate the effect of isoprostanes on endothelial tube formation we performed matrigel-based tube formation assays in the presence of 8-iso-PGF$_{2\alpha}$. In line with our findings from the migration assays, 8-iso-PGF$_{2\alpha}$ exerted a stimulating effect on basal tube formation of HCAECs at low concentrations (120.2±4.2% [$1{\cdot}10^{-7}$M] versus vehicle; P<0.001). To explore the potential role of PI3K, ERK-1/2, and Rho-kinase on this stimulating effect further tube formation assays in the presence of the PI3K-inhibitor Ly-294002 (25 µM), the ERK-1/2 inhibitor PD-98059 (60 µM), and the Rho kinase inhibitor Y-27623 (10 µM) were performed. Noteworthy, Ly-294002 and PD-98059 reversed the stimulating effect of 8-iso-PGF$_{2\alpha}$ at low concentrations (97.0±11.8% [8-iso-

$PGF_{2\alpha}$ + Ly-294002]; $P<0.01$ and 104.7±12.1% [8-iso-$PGF_{2\alpha}$ + PD-98059]; $P<0.01$ versus 120.2±4.2% [8-iso-$PGF_{2\alpha}$ alone], respectively), whereas the Rho kinase inhibitor Y-27623 did not influence the 8-iso-$PGF_{2\alpha}$-mediated stimulating effect on basal tube formation (Figure 3.7). Control experiments showed that neither Ly-294002 and PD-98059 nor Y-27623 had any effects themselves on basal tube formation under the choosen conditions (108.3±11.6% [Ly-294002], 103.5±4.4% [PD-98059], 104.8±5.9% [Y-27623]; p>0.05 versus vehicle, respectively).

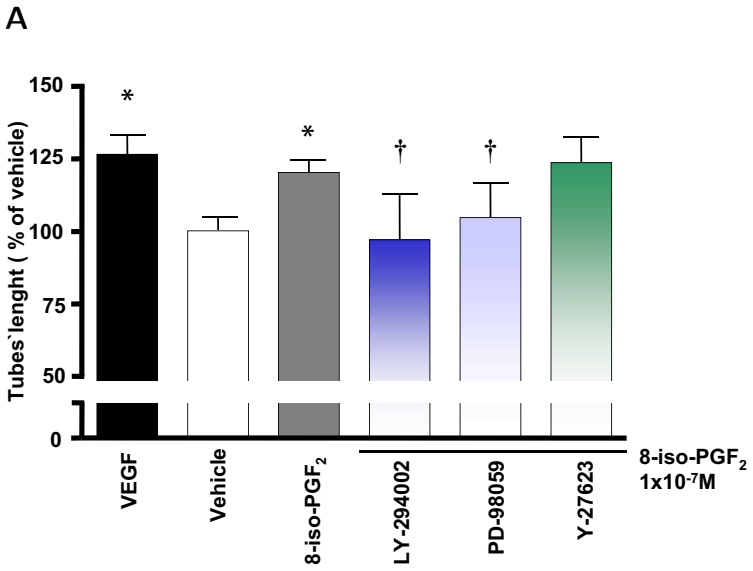

B

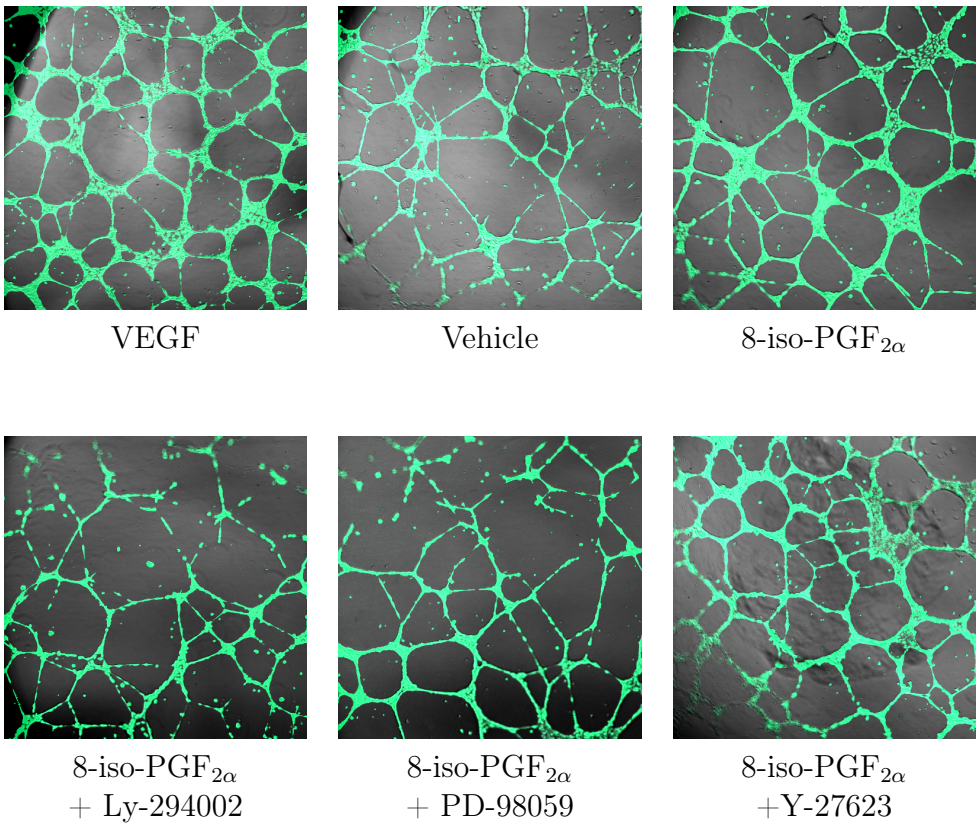

Figure 3.7: Influence of Ly-294002, PD-98059 and Y-27623 on the stimulating effect of 8-iso-PGF$_{2\alpha}$ at $1{\cdot}10^{-7}$M on HCAEC tube formation. Bar graph shows the results of quantitative analysis of HCAEC tube formation (A). 8-iso-PGF$_{2\alpha}$ exerts a stimulating effect on basal tube formation at $1{\cdot}10^{-7}$M. This effect is abolishable by Ly-294002 (25 µM) and PD-98059 (60 µM), but not by Y-27623 (10 µM). VEGF serves as positive control. Photographs show representative effects of substances on tube formation of HCAECs (B). Results are expressed as mean ± SD of 2 separate experiments performed at least in triplicate, n=6 to 9. *P<0.001 vs. vehicle; †P<0.01 vs. 8-iso-PGF$_{2\alpha}$ alone.

Further investigations revealed that 8-iso-$PGF_{2\alpha}$ at high concentrations reduced the basal tube formation of HCAECs (68.2±11.9% [$3{\cdot}10^{-5}$M] versus vehicle; $P<0.001$) (Figure 3.8). This inhibitory effect was almost completely abolished by the Rho kinase inhibitor Y-27632 (119.1±19.6% [8-iso-$PGF_{2\alpha}$ + Y-27632] versus 68.2±11.9% [8-iso-$PGF_{2\alpha}$ alone]; $P<0.001$), whereas neither PD-98059 nor Ly-294002 influenced the inhibiting effect of 8-iso-$PGF_{2\alpha}$.

A

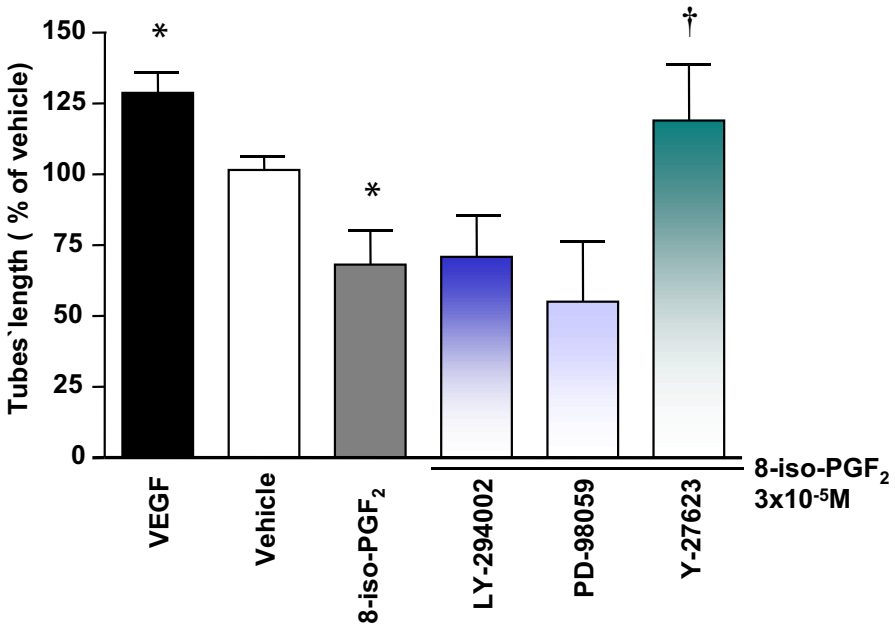

B

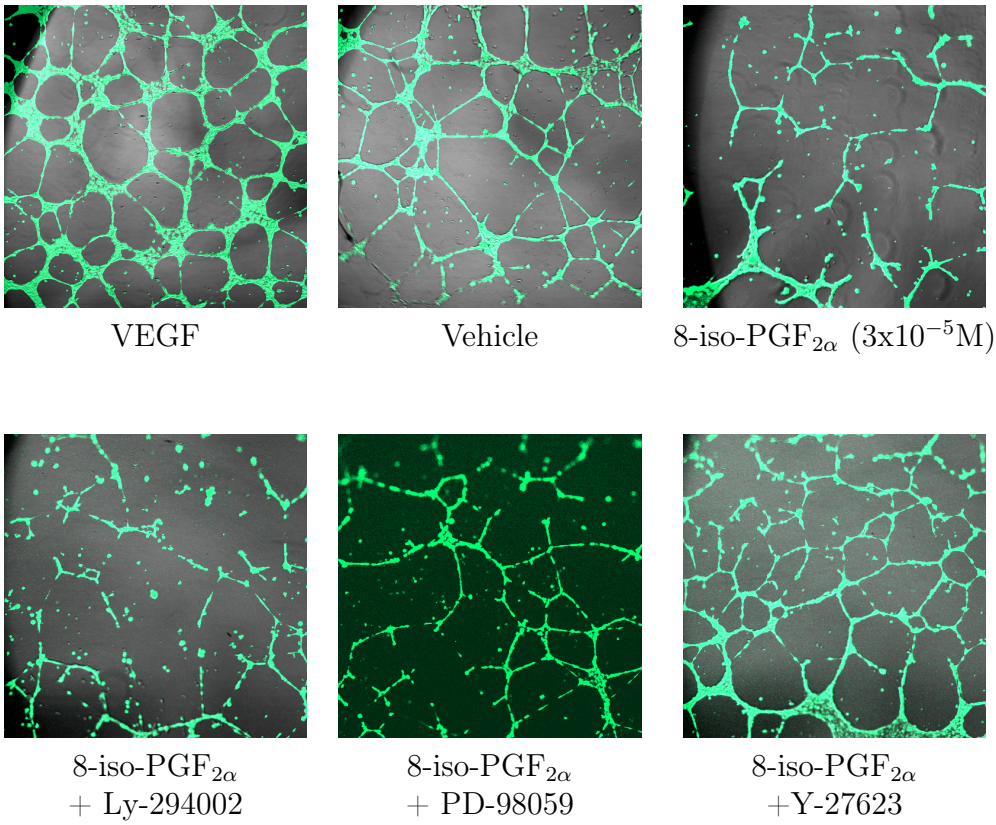

Figure 3.8: The influence of Ly-294002, PD-98059 and Y-27623 on the inhibiting effect of 8-iso-PGF$_{2\alpha}$ at high concentrations on HCAEC tube formation. Bar graph shows the results of quantitative analysis of HCAEC tube formation (A). The inhibiting effect of 8-iso-PGF$_{2\alpha}$ ($3{\cdot}10^{-5}$M) is abolishable by Y-27623 (10 µM), whereas Ly-294002 (25 µM) and PD-98059 (60 µM) do not influence this effect. Photographs show representative effects of substances on HCAEC tube formation of (B). Results are expressed as mean ± SD of 2 separate experiments performed at least in triplicate, n=6 to 9. *P<0.001 vs. vehicle; †P<0.001 vs. 8-iso-PGF$_{2\alpha}$ alone.

Similar data were obtained when tube formation assays were performed with the TBXA2R agonist U-46619. Like 8-iso-$PGF_{2\alpha}$ ($3{\cdot}10^{-5}$M), U-46619 inhibited the basal tube formation of HCAECs (53,8±6,9% [$3{\cdot}10^{-5}$M]; $P<0.001$) versus vehicle). This effect was again abolished by the Rho kinase inhibitor Y-27632 (95,0±9,1% [U-46619 + Y-27632] vs. 53,8±6,9% [U-46619 alone]; $P<0.001$). PD-98059, LY-294002 and Wortmannin did not influence the inhibiting effect of U-46619 (Figure 3.9).

A

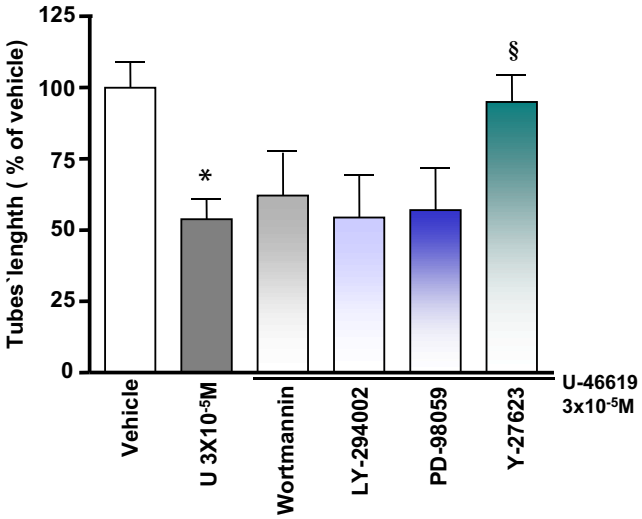

B

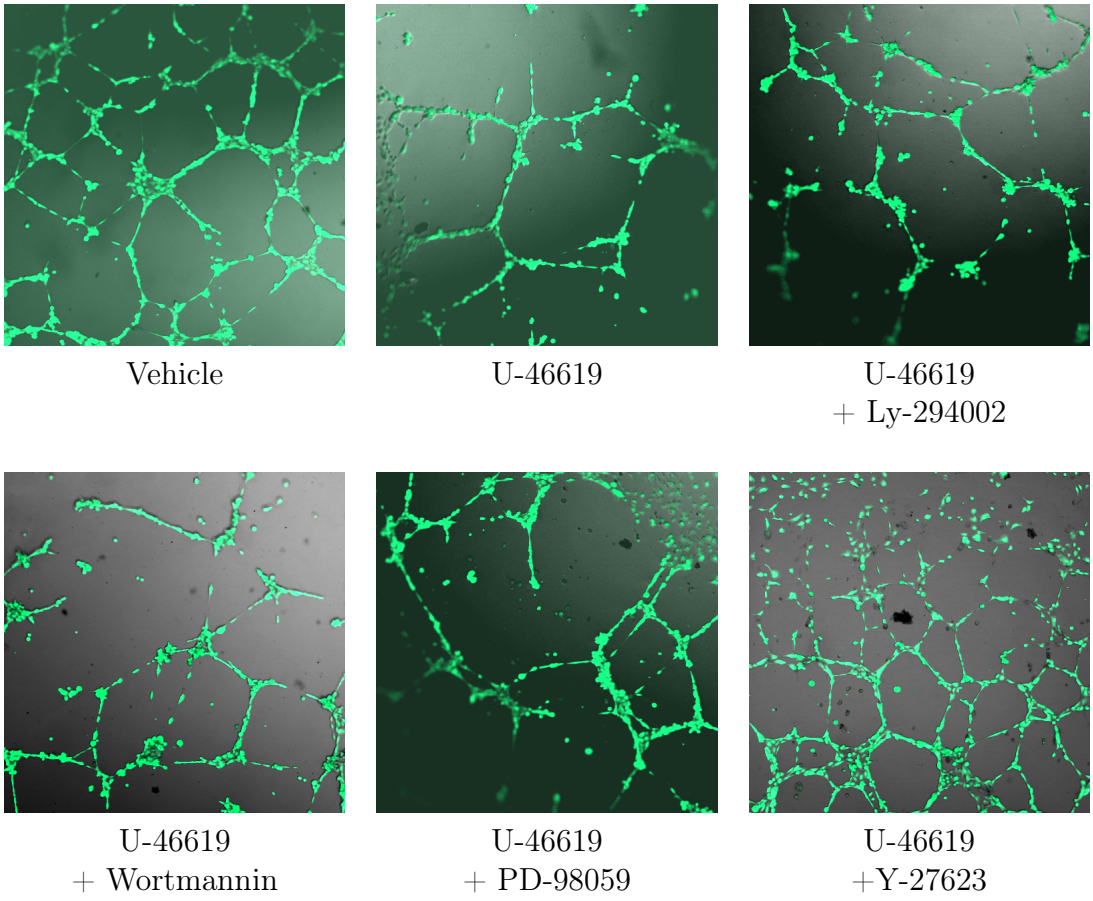

Figure 3.9: Effect of U-46619 on basal tube formation of HCAECs. Bar graph shows the results of quantitative analysis (A). U-46619 inhibits the basal HCAEC tube formation. This effect is abolishable by Y-27632, whereas PD-98059, LY-294002 and Wortmannin do not induce any effect. Photographs show representative effects of substances on HCAEC tube formation (B). Results are expressed as means ± SD of 2 separate experiments performed at least in triplicate, n=6. $^{*}P<0.001$ vs. vehicle; §$P<0.001$ vs. U-46619 alone.

3.3 Influence of Isoprostanes and U-46619 on VEGF-Induced Angiogenesis in Vitro

3.3.1 Influence of 8-iso-$PGF_{2\alpha}$, 8-iso-PGE_2, 8-iso-PGA_2 and U-46619 on VEGF-Induced Migration and Tube Formation of Endothelial Cells

Since VEGF stimulates almost all steps of angiogenesis *in vivo*, we subsequently examined the effect of isoprostanes on VEGF-induced EC migration. For this purpose HDMECs were subjected to transwell migration assays and incubated with VEGF (50 ng/mL) in the presence of increasing concentrations of 8-iso-$PGF_{2\alpha}$. 8-iso-$PGF_{2\alpha}$ significantly inhibited the pro-migrative effect of VEGF in a concentration-dependent manner. A significant inhibition was observed starting at concentrations as low as 10^{-9}M (162.3±20.0% [8-iso-$PGF_{2\alpha}$ + VEGF] versus 185.7±14.2% [VEGF alone]; $P<0.05$), which increased in a concentration-dependent manner (125.1±9.8% [8-iso-$PGF_{2\alpha}$ at 10^{-4}M) + VEGF]; $P<0.001$). The TBXA2R antagonist SQ-29548 ($3{\cdot}10^{-5}$M) reversed the inhibitory effect of 8-iso-$PGF_{2\alpha}$ (Figure 3.10).

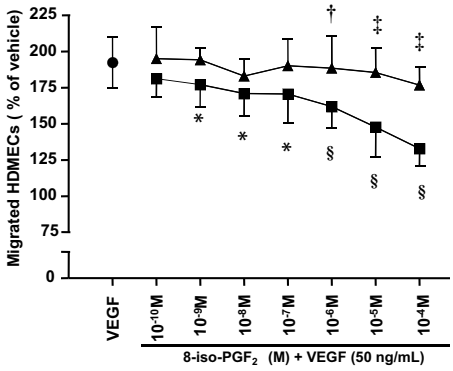

Figure 3.10: Influence of 8-iso-$PGF_{2\alpha}$ on VEGF-induced migration of HDMECs. 8-iso-$PGF_{2\alpha}$ inhibits the VEGF-induced migration of HDMECs in a concentration-dependent manner. This effect is abolished by the TBXA2R antagonist SQ-29548. ● VEGF only (50 ng/mL), ■ 8-iso-$PGF_{2\alpha}$ (M) + VEGF (50 ng/mL), ▲ 8-iso-$PGF_{2\alpha}$ (M) + VEGF (50 ng/mL) + SQ-29548 ($3{\cdot}10^{-5}$M). Results are expressed as means ± SD of 2 separate experiments performed at least in triplicate, n=6 to 12. *$P<0.05$, § $P<0.001$ vs. VEGF alone; † $P<0.01$, ‡ $P<0.001$ vs. VEGF + 8-iso-$PGF_{2\alpha}$.

The concentration-dependent inhibitory effect of 8-iso-$PGF_{2\alpha}$ on VEGF-induced migration was also shown in HCAECs and mimicked by the isoprostanes 8-iso-PGA_2 and 8-iso-PGE_2 (Figure 3.11).

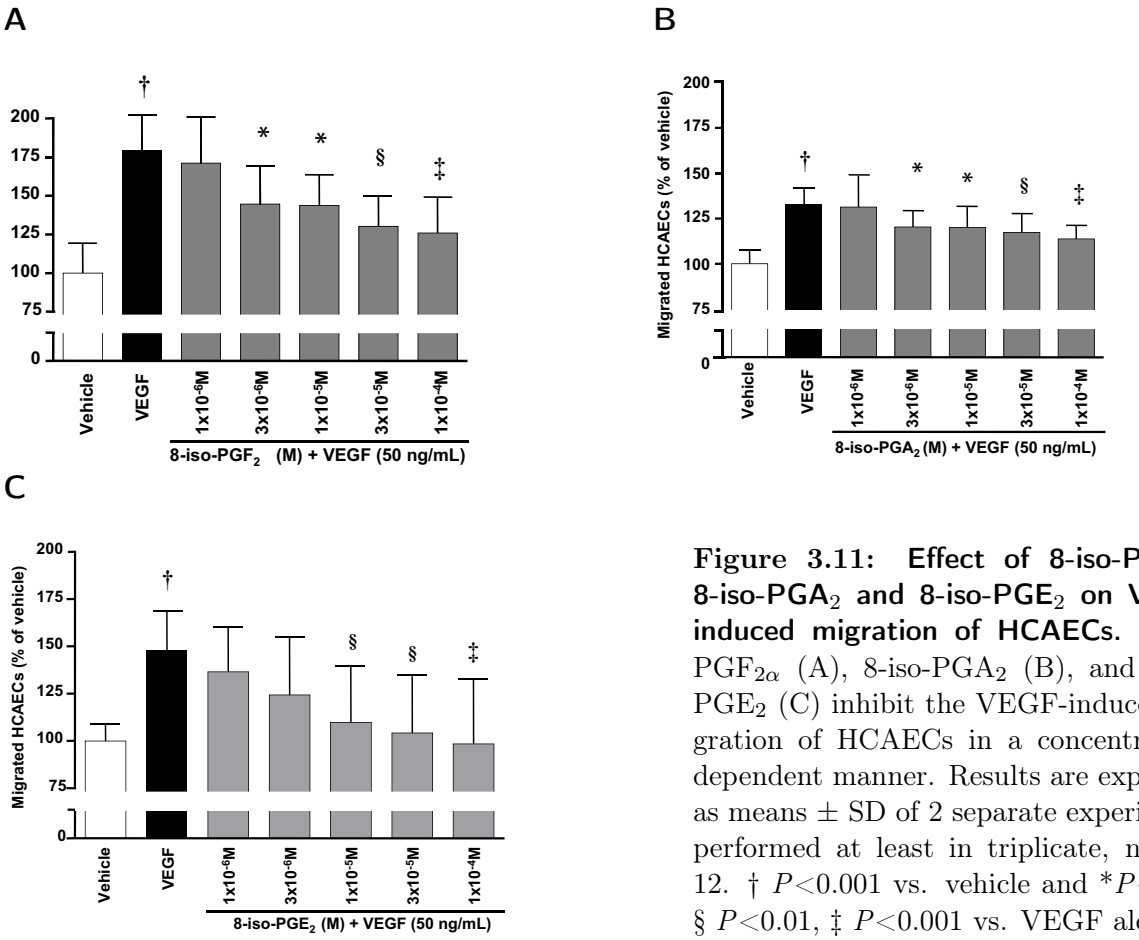

Figure 3.11: Effect of 8-iso-$PGF_{2\alpha}$, 8-iso-PGA_2 and 8-iso-PGE_2 on VEGF-induced migration of HCAECs. 8-iso-$PGF_{2\alpha}$ (A), 8-iso-PGA_2 (B), and 8-iso-PGE_2 (C) inhibit the VEGF-induced migration of HCAECs in a concentration-dependent manner. Results are expressed as means ± SD of 2 separate experiments performed at least in triplicate, n=6 to 12. † $P<0.001$ vs. vehicle and $*P<0.05$, § $P<0.01$, ‡ $P<0.001$ vs. VEGF alone.

It has been reported that 8-iso-$PGF_{2\alpha}$ induced neuro-microvascular cell death, which was associated with increased endothelial thromboxane A_2 formation [155]. To find out if isoprostane-mediated inhibition of VEGF-induced migration is caused by an isoprostane-induced production or release of thromboxane A_2, HDMECs were pre-incubated with the specific thromboxane A_2 synthase inhibitor ozagrel (4.5 µM) for 12 h. Subsequently the effect of 8-iso-$PGF_{2\alpha}$, 8-iso-PGA_2, 8-iso-PGE_2, and U-46619 on VEGF-induced mi-

gration of HDMECs were investigated in the presence of ozagrel. However, ozagrel did not alter the inhibitory effect of 8-iso-$PGF_{2\alpha}$, 8-iso-PGA_2, 8-iso-PGE_2, and U-46619 on VEGF-induced HDMEC migration (Figure 3.12).

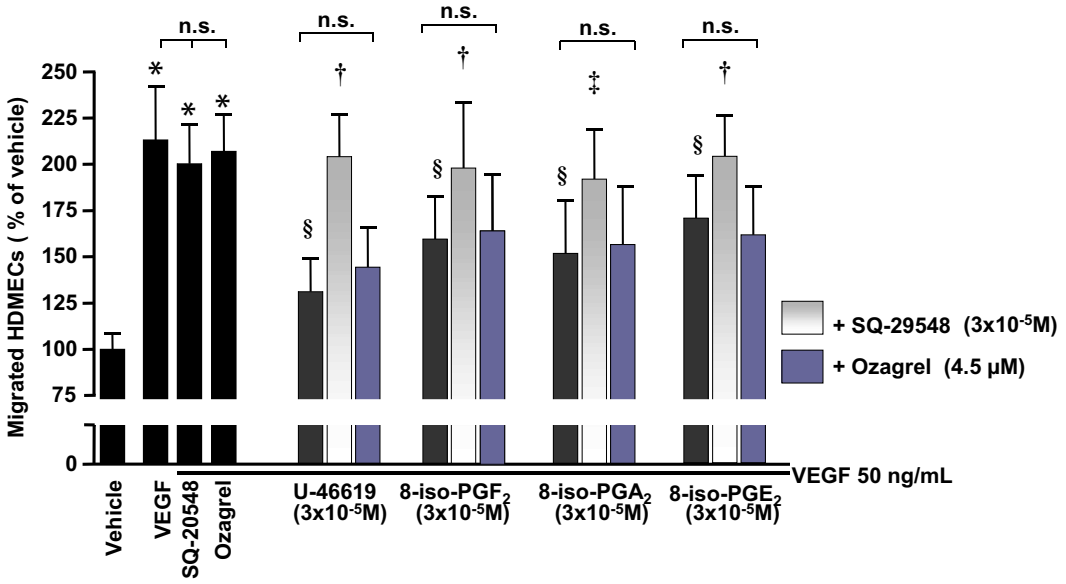

Figure 3.12: The effect of the isoprostanes 8-iso-$PGF_{2\alpha}$, 8-iso-PGA_2, and 8-iso-PGE_2 as well as the TBXA2R agonist U-46619 on VEGF-induced migration of HDMECs. All tested isoprostanes (each $3{\cdot}10^{-5}$M) and U-46619 ($3{\cdot}10^{-5}$M) inhibit the VEGF-induced migration of HDMECs. These effects are reversible by the TBXA2R antagonist SQ-29548 ($3{\cdot}10^{-5}$M). Pre-incubation and presence of the thromboxane A_2 synthase inhibitor ozagrel (4.5 µM) does not alter the inhibitory effect of isoprostanes on VEGF-induced HDMEC migration. Results are expressed as means ± SD of 2 separate experiments performed at least in triplicate, n=9 to 12. *P<0.001 vs. vehicle, § P<0.001 vs. VEGF, † P<0.01, ‡ P<0.05 vs. any isoprostane/U-46619 + VEGF.

Many different kinds of isoprostanes can be formed via the isoprostane pathway *in vivo*. To investigate if several isoprostanes could exert additive biological effects, simultaneous addition of 8-iso-$PGF_{2\alpha}$, 8-iso-PGA_2, and 8-iso-PGE_2 was examined in VEGF-induced EC migration. 8-iso-$PGF_{2\alpha}$, 8-iso-PGA_2, and 8-iso-PGE_2 (each $3{\cdot}10^{-5}$M) reduced the VEGF-induced migration of HDMECs (114.3±26.0% [8-iso-$PGF_{2\alpha}$], 77.0±12.9% [8-iso-PGA_2], 78.3±10.4% [8-iso-PGE_2] versus 162.0±10.2% [VEGF alone]; $P<0.001$ versus VEGF, respectively). Actually, simultaneous addition of 8-iso-$PGF_{2\alpha}$, 8-iso-PGA_2, and 8-iso-PGE_2 resulted in a significantly stronger inhibition of HDMEC migration compared with the inhibition induced by any of the isoprostanes alone (59.1±8.32%; $P<0.01$ versus 8-iso-$PGF_{2\alpha}$-, 8-iso-PGA_2-, or 8-iso-PGE_2 alone), indicating a synergistic inhibitory effect of isoprostanes on VEGF-induced migration of ECs *in vitro* (Figure 3.13). Furthermore, the influence of 8-iso-$PGF_{2\alpha}$, 8-iso-PGA_2, and 8-iso-PGE_2 on VEGF-induced tube formation of HCAECs were investigated. Simultaneous addition of 8-iso-$PGF_{2\alpha}$, 8-iso-PGA_2, and 8-iso-PGE_2 ($3{\cdot}10^{-5}$M, respectively) reduced the VEGF-induced tube formation of HCAECs (81±13% [8-iso-$PGF_{2\alpha}$], 74±10% [8-iso-PGA_2] and 84±11% [8-iso-PGE_2] versus 118±16% [VEGF alone]; $P<0.001$ versus VEGF, respectively). Again, simultaneous addition of 8-iso-$PGF_{2\alpha}$, 8-iso-PGA_2, and 8-iso-PGE_2 resulted in a significantly stronger inhibition of EC tube formation compared with the inhibition induced by any of the isoprostanes alone (54±9%; $P<0.01$ versus 8-iso-$PGF_{2\alpha}$/8-iso-PGA_2/8-iso-PGE_2 alone) suggesting a synergistic inhibitory effect of isoprostanes on tube formation of ECs *in vitro* (Figure 3.14).

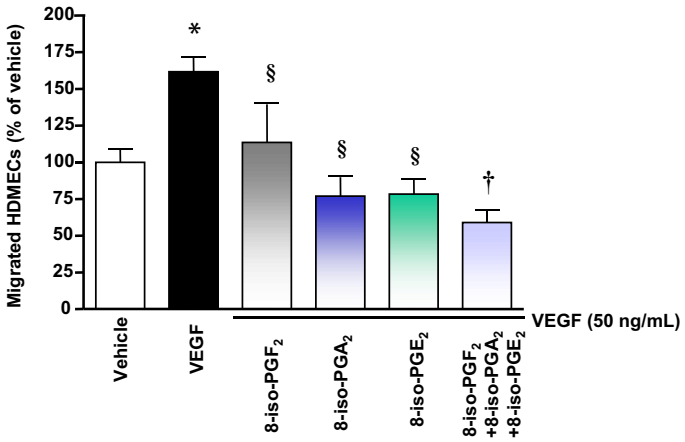

Figure 3.13: Effect of 8-iso-PGF$_{2\alpha}$, 8-iso-PGA$_2$, and 8-iso-PGE$_2$ on VEGF-induced migration of HDMECs. 8-iso-PGF$_{2\alpha}$, 8-iso-PGA$_2$, and 8-iso-PGE$_2$ (each $3{\cdot}10^{-5}$M) inhibit the VEGF-induced migration of HDMECs. A simultanous addition of all three isoprostanes results in a stronger inhibition compared with the inhibition induced by any of the isoprostanes alone. Results are expressed as means ± SD of 2 separate experiments performed at least in triplicate, n=6 to 12. * $P<0.001$ vs. vehicle; § $P<0.01$ vs. VEGF; † $P<0.001$ vs. any isoprostane + VEGF.

A

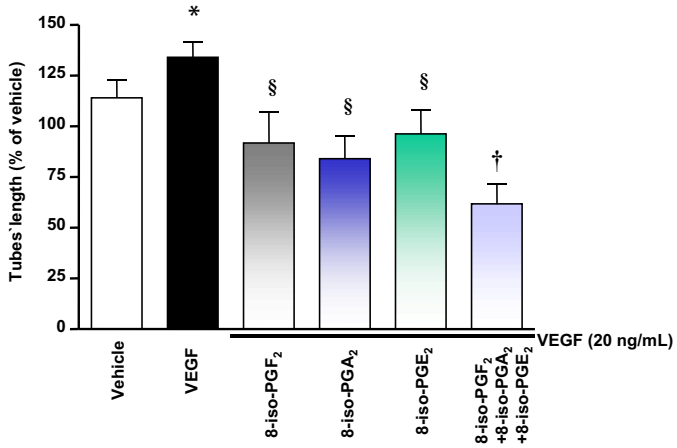

B

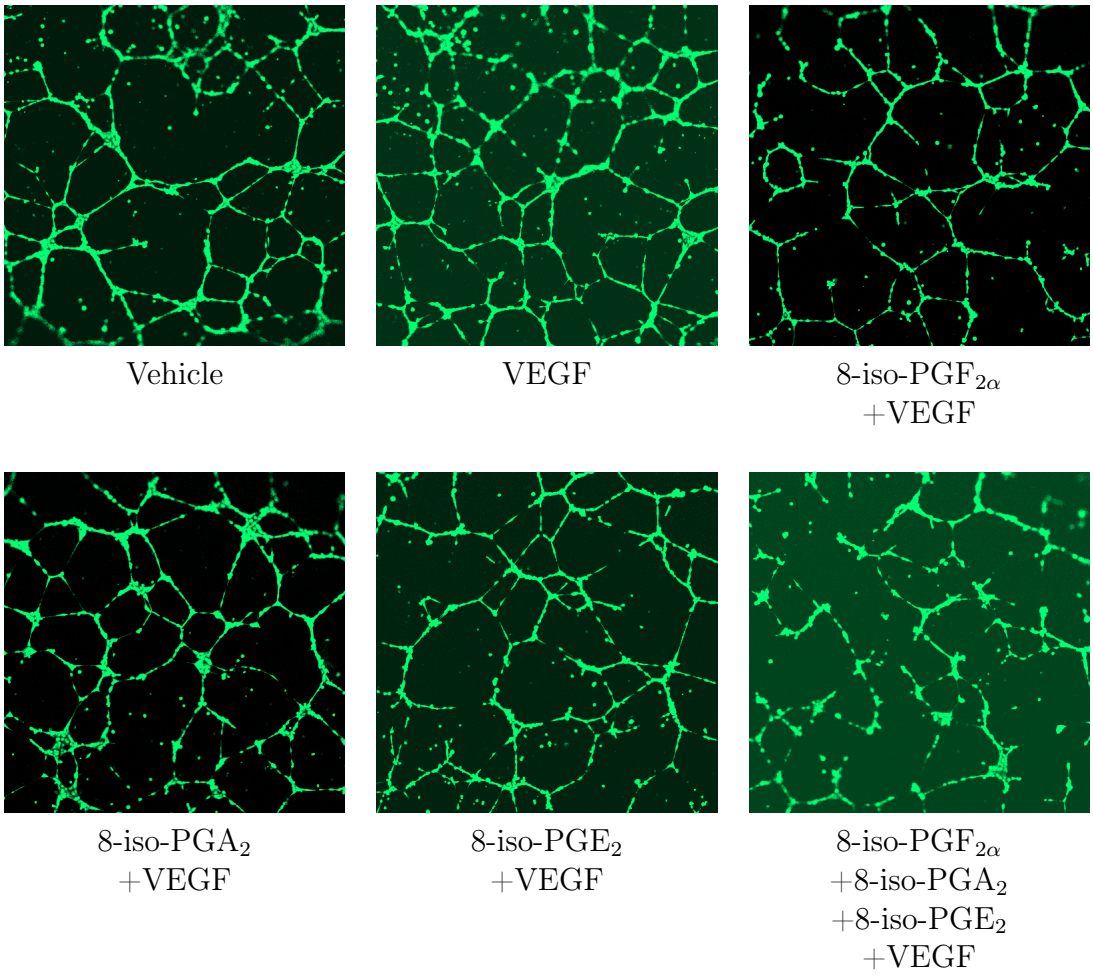

Figure 3.14: Effect of 8-iso-PGF$_{2\alpha}$, 8-iso-PGA$_2$, and 8-iso-PGE$_2$ on VEGF-induced tube formation of HCAECs. The Bar graph shows the results of quantitative analysis (A). 8-iso-PGF$_{2\alpha}$, 8-iso-PGA$_2$, and 8-iso-PGE$_2$ (each $3{\cdot}10^{-5}$M) inhibit the VEGF-induced tube formation of HCAECs. A simultaneous addition of all three isoprostanes results in a stronger inhibition compared with the inhibition induced by any of the isoprostanes alone. Photographs show representative effects of substances on HCAEC tube formation (B). Results are expressed as means ± SD of 2 separate experiments performed at least in triplicate, n=6 to 12. * $P<0.001$ vs. vehicle; § $P<0.001$ vs. VEGF; † $P<0.001$ vs. VEGF + any isoprostane alone.

3.3.2 Effects of Compound X and Y on VEGF-Induced Migration and Tube Formation of Endothelial Cells

In contrast to the isoprostane 8-iso-$PGF_{2\alpha}$, which has been shown to be rather stable under *in vivo* conditions, the stability of further isoprostanes remaines elusive. 8-iso-PGE_2 is known to degrade spontaneously to 8-iso-PGA_2. Hence, the stability of cyclopentone 8-iso-PGA_2 under "physiological" conditions (pH 7,4, 37 °C) *in vitro* was investigated. Via HPLC analysis, a decomposition of 8-iso-PGA_2 within 24 h into an unknown compound, termed X, which again completely transformed within 24 h into compound Y could be observed (Figure 3.15).

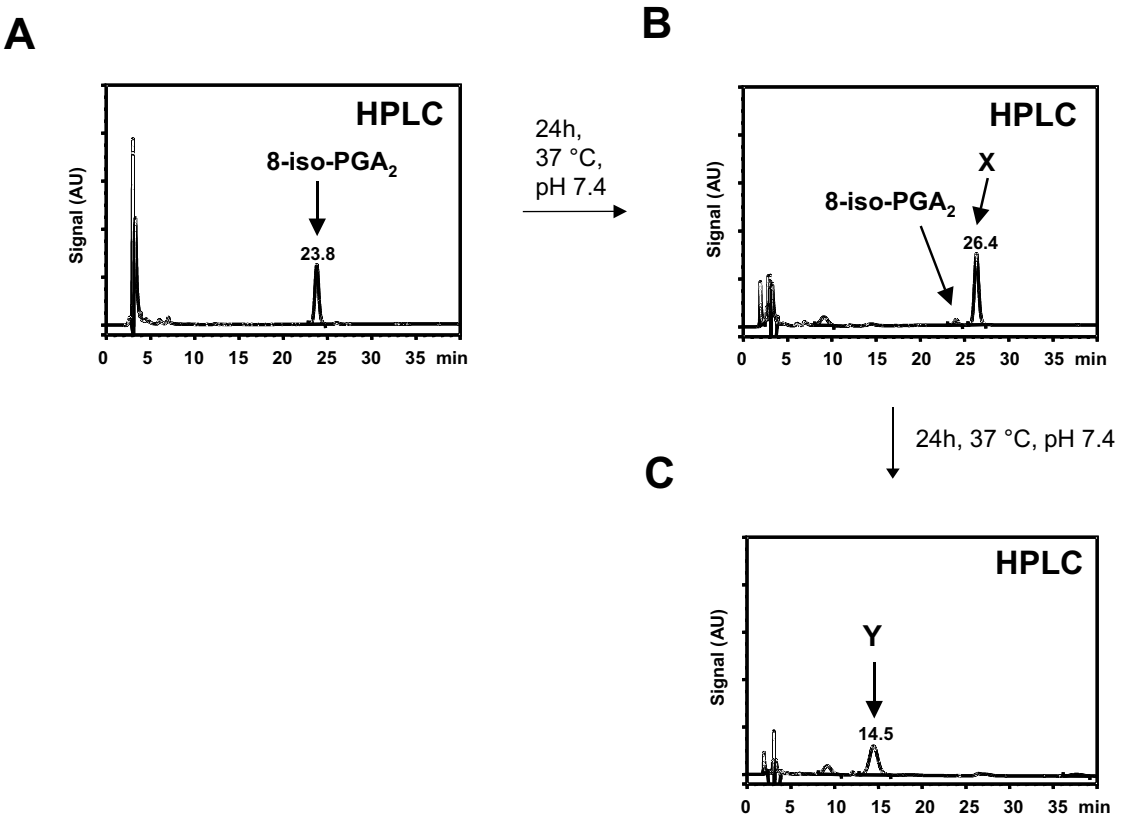

Figure 3.15: Decomposition of 8-iso-PGA_2. HPLC analysis demonstrates that 8-iso-PGA_2 (A) decomposes to the unknown compound X (B) within 24 h, which in turn is transformed to compound Y (C) within further 24 h.

To investigate if these substances are also able to exert biological activity, we investigated the effects of compound X and Y on VEGF-induced migration and tube formation of ECs. Compound X exerted a potent inhibitory effect on VEGF-induced EC migration, which again was partly reversed by the TBXA2R antagonist SQ-29548 (104±32% [X + VEGF] versus 181±5% [VEGF alone]; $P<0.001$). In contrast, compound Y did not show a significant effect on VEGF-induced migration (Figure 3.16, A). Both compounds inhibited the VEGF-induced tube formation (77±4% [X + VEGF], 68±4% [Y + VEGF]; $P<0.001$ versus VEGF, respcetively), which was again partly reversed by the TBXA2R antagonist SQ-29548 (Figure 3.16, B). These findings strongly suggest that specific instable isoprostanes may non-enzymatically form more or less biologically active derivates *in vivo*, which may exert synergistic effects together with further endogenous isoprostanes via the TBXA2R.

A

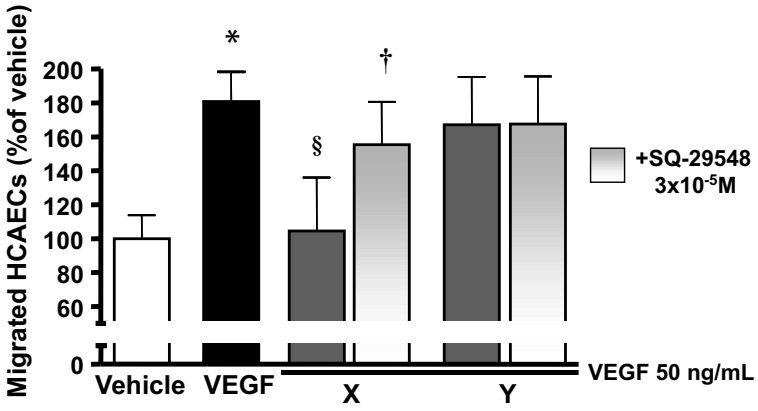

B

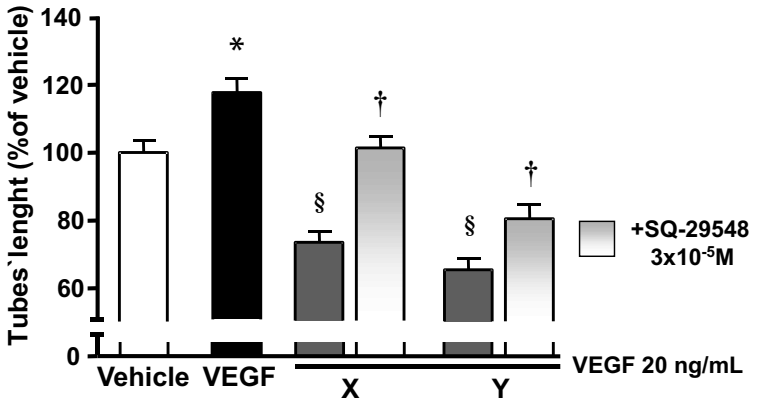

Figure 3.16: The effect of compound X and Y on VEGF-induced migration and tube formation of HCAECs. Compound X, but not Y, inhibits the VEGF-induced migration of HCAECs (A). This effect is reversible by the TBXA2R antagonist SQ-29548. Both, compound X and Y exert an inhibitory effect on VEGF-induced tube formation of HCAECs that is reversible by SQ-29548 (B). Results are expressed as means ± SD of 2 separate experiments performed at least in triplicate, n=6 to 9. * $P<0.001$ vs. vehicle; § $P<0.001$ vs. VEGF alone; † $P<0.01$ vs. VEGF + compound X or Y.

LC-MS/MS and GC-MS analysis were performed to identify the transformation products of 8-iso-PGA_2 referred to as compound X and Y. LC-MS/MS analysis revealed that compound X generated a molecular ion $[M\text{-}H]^-$ with a mass to charge ratio (m/z) at 333 under ESI conditions in the negative-ion mode (Figure 3.17, A). This negatively charged molecule ion underwent collision -induced dissociation (CID), leading to fragmentation patters at m/z 315, m/z 271, and m/z 217, corresponding to loss of water, subsequent carboxylation, and cleavage at the Z-double bound, respectively. Compound Y generated the molecular ion $[M\text{-}H]^-$ m/z 315 and also the fragmentation patterns m/z 271 and m/z 217 (Figure 3.17, B). Exactly the same molecular ion and the same fragmentation patterns could be observed by the cyclopentenone isomer 15-deoxy-PGJ_2 (Figure 3.17, C).

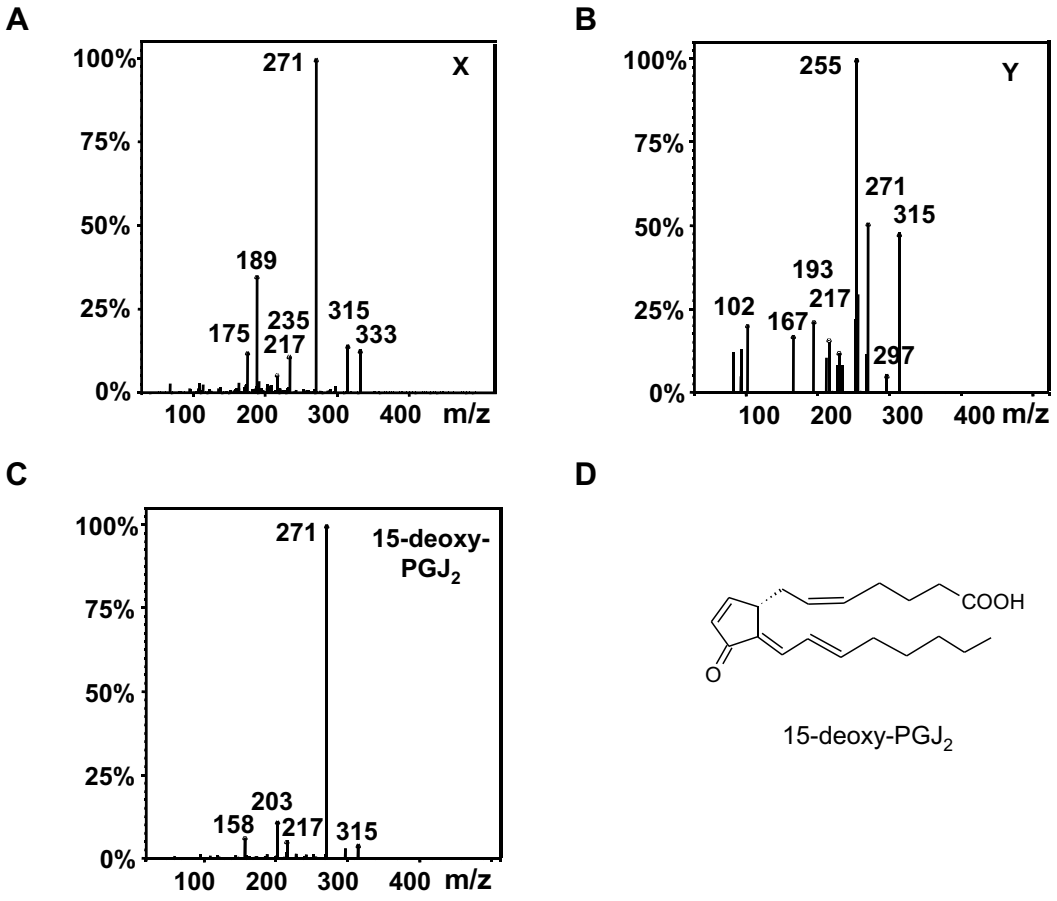

Figure 3.17: LC/ESI-MS/MS (liquid chromatographic/electrospray ionization-tandem mass spectrometric) analysis of compound X (A), compound Y (B), and 15-deoxy-PGJ_2 (C). Chemical structure of 15-deoxy-PGJ_2 (D).

GC-MS analysis of the PFB-MO-(TMS) derivatives of 8-iso-PGE_2, compound X and Y revealed the most abundant ion at m/z 524, m/z 434, and m/z 344, respectively. The m/z difference between 8-iso-PGE_2 and compound X as well as between compound X and Y exhibit 90 m/z, respectively. This is in accordance with a loss of one TMS group, respectively and let conclude that the chemical structure of compound X exhibits one hydroxyl group less than 8-iso-PGE_2, and compound Y exhibit one hydroxyl group less that compound X.

A potential chemical fate of compounds investigated is outlined in Figure 3.18. According to this 8-iso-PGA_2 isomerises into 8-iso-Δ^{12}-PGA_2 (X) within 24h incubation under physiological conditions. In line with this theory compound X exhibited a molecular ion of m/z 333 via LC-MS/MS analysis. In addition GC/MS analysis of the corresponding PFB-MO-TMS derivative revealed an ion of m/z 434 ($[M\text{-}PFB]^-$). Further 24 h incubation of 8-iso-Δ^{12}-PGA_2 (X) leads to a loss of water resulting in the formation 15-deoxy-8-iso-PGA_2 (Y). This theory is confirmed by the molecular ion of m/z 315 detected via LC-MS/MS analysis. Furthermore LC-MS/MS analysis of the cyclopentenone isomer 15-deoxy-PGJ_2 revealed the same molecular ion and fragmentation pattern like compound Y. In this regard 15-deoxy-PGA_2 exhibits a similar chemical structure like 15-deoxy-PGJ_2. Only the position of the keto group in the cyclopentenone ring is interchanged. Finally GC/MS analysis of the corresponding PFB-MO-TMS derivative revealed an ion of m/z 344 ($[M\text{-}PFB]^-$).

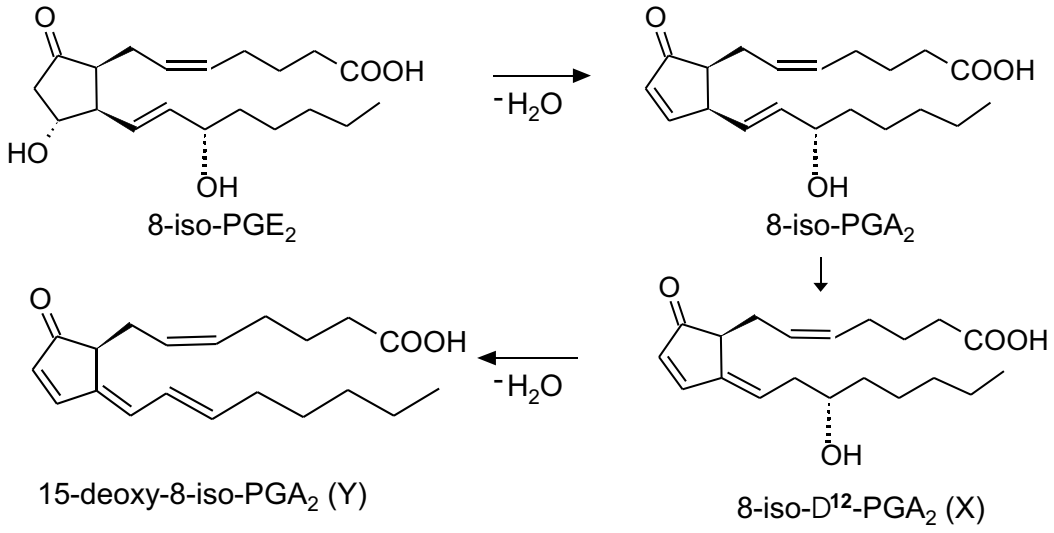

Figure 3.18: Proposed chemical fate of 8-iso-PGA_2 through a sequence of isomerization and dehydration reactions.

3.3.3 Effect of 5-series Isoprostanes on VEGF-Induced Migration of Endothelial Cells

We investigated the effect of two 5-series isoprostanes (5-F_{2t}-IsoP and 5-epi-5-F_{2t}-IsoP) on VEGF-induced migration. They are considered as being attractive markers of oxidative stress due to the fact that they are chemically stable like 8-iso-$PGF_{2\alpha}$ and present in urine in greater concentration than 8-iso-$PGF_{2\alpha}$. We could show that 5-epi-5-F_{2t}-IsoP is able to inhibit the VEGF-induced migration of HCAECs and HDMECs. This effect was reversible by the TBXA2R antagonist SQ-29548 (only tested in HCAECs). 5-F_{2t}-IsoP did not show any effect in that respect (Figure 3.19).

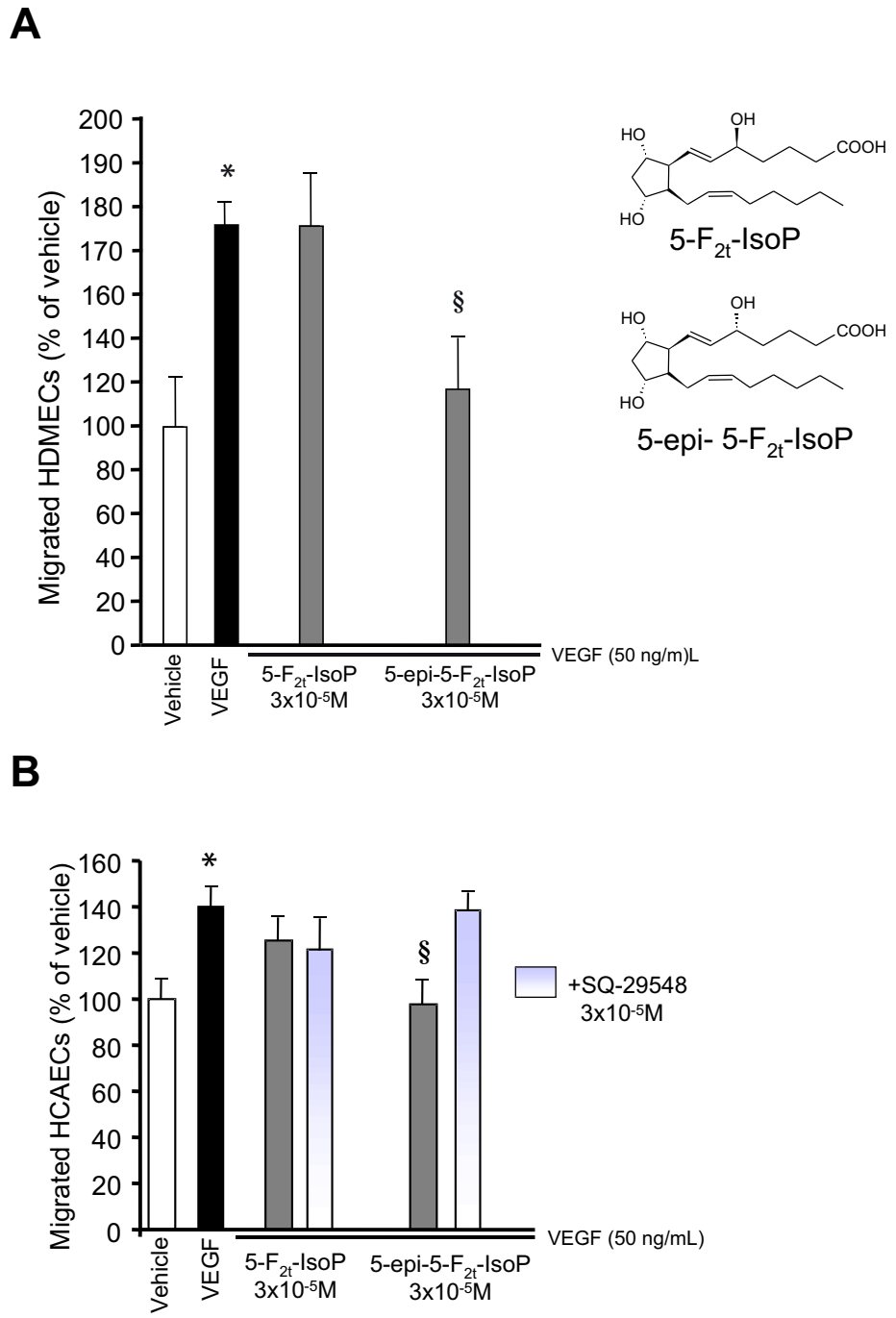

Figure 3.19: Effect of 5-F_{2t}-IsoP and 5-epi-5-F_{2t}-IsoP on VEGF-induced migration of ECs. 5-epi-5-F_{2t}-IsoP inhibits the VEGF-induced Migration of HDMECs (A) and HACAECs (B), whereas 5-F_{2t}-IsoP does not exert any effect. Results are expressed as means ± SD of 2 separate experiments performed at least in triplicate, n= 12. * P<0.001 vs. vehicle; § P<0.05 vs. VEGF alone.

3.3.4 Effect of Phytoprostanes on VEGF-Induced Migration of HDMECs

Finally, we tested the response of VEGF-induced HDMEC migration to a variety of phytoprostanes. B_1-PhytoP II and ent-B_1-PhytoP II inhibited the VEGF-induced migration. In contrast, B_1-PhytoP I and ent-B_1-PhytoP I evoked no effect. In addition, all tested F_1-PhytoPs caused an inhibiting effect on VEGF-induced migration, except ent-F_1-PhytoP (Figure 3.20).

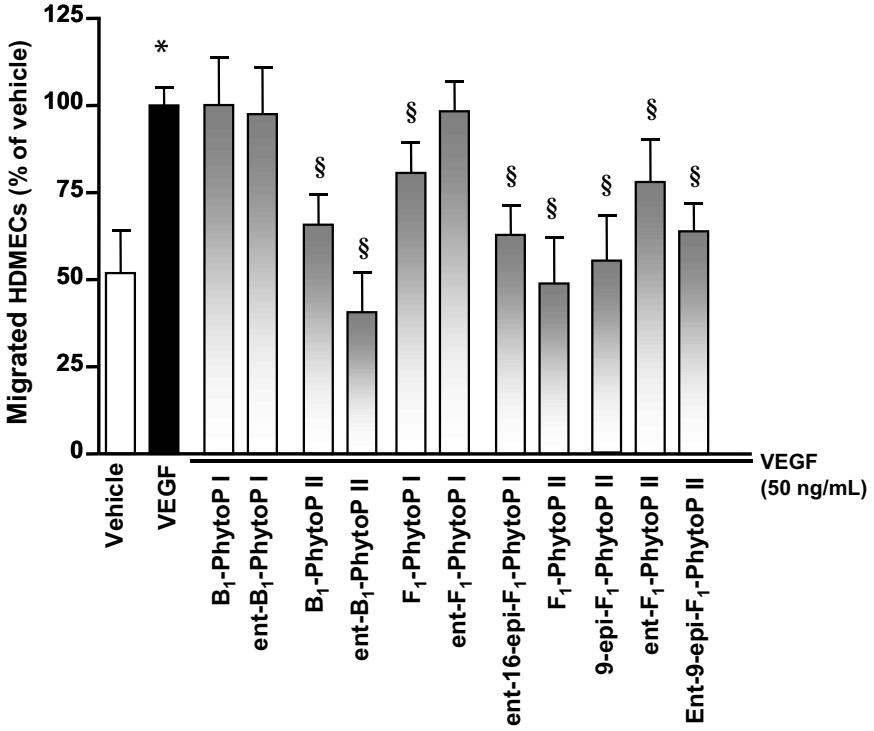

Figure 3.20: Effect of several Phytoprostanes on VEGF-induced migration of HDMECs. All tested phytoprostanes except B_1-PhytoP I, ent-B_1-PhytoP I, and ent-F_1-PhytoP I inhibit the VEGF-induced migration of HDMECs. Results are expressed as means ± SD of 2 separate experiments performed at least in triplicate, n= 12. * P<0.001 vs. vehicle; § P<0.05 vs. VEGF alone.

3.4 Determination of Signaling Pathways Involved in the Isoprostanes-Mediated Effects on VEGF-Induced Migration and Tube Formation of Endothelial Cells

One goal of this work was to find out via which mechanisms 8-iso-$PGF_{2\alpha}$ influences the VEGF-induced EC migration and tube formation. VEGF stimulation leads to activation of a number of downstream signaling cascades including the ERK-1/2- and PI3K/Akt pathway, which manage the multifaceted processes occurring during angiogenesis. Recently, the Rho-familiy of small GTPases was identified as an essential downstream effector of VEGF signaling in the angiogenic process.

3.4.1 The Role of PI3K, ERK-1/2, and Rho kinase on the Inhibiting Effect of 8-iso-$PGF_{2\alpha}$ on VEGF-Induced Migration and Tube Formation of Endothelial Cells

To explore the potential role of PI3K, ERK-1/2, and Rho-kinase on the 8-iso-$PGF_{2\alpha}$-mediated inhibiting effect on VEGF-induced cell migration, further migration assays were performed in the presence of the PI3K-inhibitors LY-294002 (25 μM) and Wortmannin (10 μM), the ERK-1/2 inhibitor PD-98059 (60 μM), and the Rho kinase inhibitor Y-27632 (10 μM). Control experiments showed that addition of PD-98059, LY-294002 and Wortmannin themselves reduced the VEGF-induced migration of HDMECs (125±8.88% [PD-98059], 132±16.9% [Ly-294002] and 140±15.8% [Wortmannin] versus 162±10.2% [VEGF]; P< 0.001, P<0.001, P<0.01 versus VEGF, respectively)(Figure 3.21, A). But they did not influence the inhibiting effect of 8-iso-$PGF_{2\alpha}$ on VEGF-induced migration of HDMECs (Figure 3.21, B). In contrast, the inhibiting effect of 8-iso-$PGF_{2\alpha}$ on VEGF-induced migration (114±26.0% [VEGF + 8-iso-$PGF_{2\alpha}$ alone] versus 162±10.2 [VEGF]; P<0.001) was strongly attenuated by Y-27632 (141±27,4% [VEGF + Y-27632 + 8-iso-$PGF_{2\alpha}$] versus 114±26.0% [VEGF + 8-iso-$PGF_{2\alpha}$]; P<0.05)(Figure 3.21, B). Y-27632 itself did not influence the VEGF-induced migration of HDMECs (Figure 3.21, A).

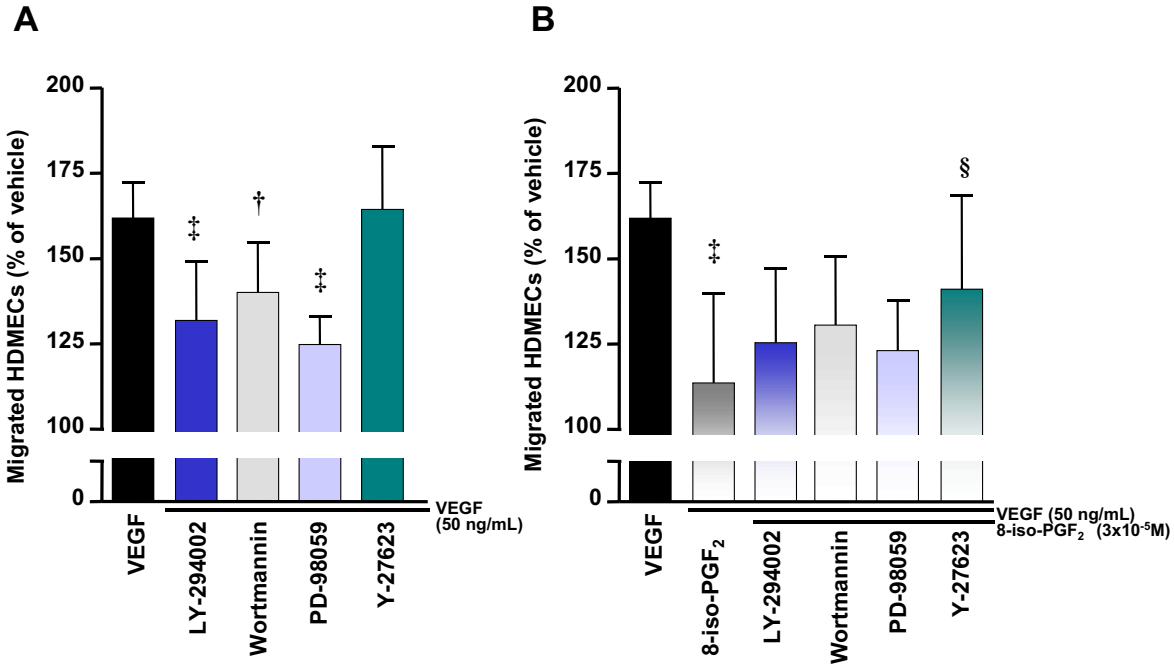

Figure 3.21: Effect of the PI3K inhibitors Ly-294002 and Wortmannin, the ERK-1/2 inhibitor PD-98059, and the Rho kinase inhibitor Y-27623 on the inhibiting effect of 8-iso-PGF$_{2\alpha}$ on VEGF-induced migration. Control experiments show that LY-294002 (10 μ), Wortmannin (10 μM), and PD-98059 (60 μM) themselves reduce the VEGF-induced migration of HDMECs (A), but do not influence the inhibiting effect of 8-iso-PGF$_{2\alpha}$ ($3{\cdot}10^{-5}$M) on VEGF-induced migration (B). In contrast Y-27623 (10 μM) has no effect on VEGF-induced migration itself (A), but it reverses the inhibiting effect of 8-iso-PGF$_{2\alpha}$ on VEGF-induced migration (B). Results are expressed as mean ± SD of 2 separate experiments performed at least in triplicate, n=6 to 12. ‡ $P<0.001$, † $P<0.01$ versus VEGF; § $P<0.05$ versus 8-iso-PGF$_{2\alpha}$ + VEGF.

We also investigated the role of PI3K, ERK-1/2 and Rho-kinase on the inhibiting effect of 8-iso-$PGF_{2\alpha}$ on VEGF-induced tube formation of HCAECs (92.0±116.2% [8-iso-$PGF_{2\alpha}$+ VEGF] versus 128.0±116.2 [VEGF alone]; P<0.001). Again, this effect was abolished by Y-27632 (146±27.8% [VEGF + Y-27632 + 8-iso-$PGF_{2\alpha}$] versus 92.0±116.2% [VEGF + 8-iso-$PGF_{2\alpha}$ alone]; P<0.001), whereas PD-98059, LY-294002 and Wortmannin did not influence the inhibiting effect of 8-iso-$PGF_{2\alpha}$ on VEGF-induced tube formation (104±10.3%, 95.4±24.3% and 102±7.14% versus 92.0±116.2% [VEGF + 8-iso-$PGF_{2\alpha}$ alone]; P>0.05 respectively)(Figure 3.22). Control experiments showed that neither Wortmannin, LY-294002, and PD-98059 nor Y-27632 had any effect on VEGF-induced tube formation themselves (112.2±8.2% [Wortmannin], 111.5±12.4% [LY-294002], 114.3±9.1% [PD-98059]; 118.1±17.9% [Y-276329] p>0.05 versus VEGF [120.7±3.5%], respectively).

A

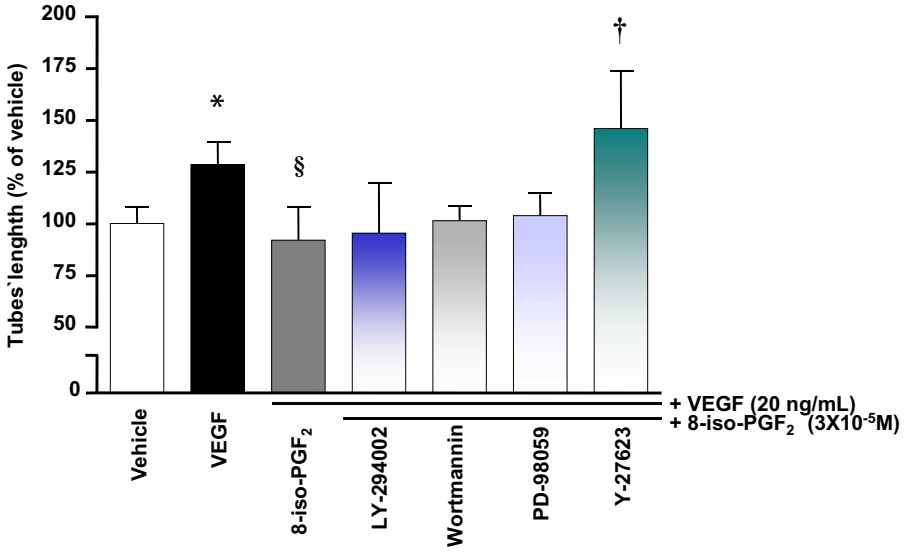

B

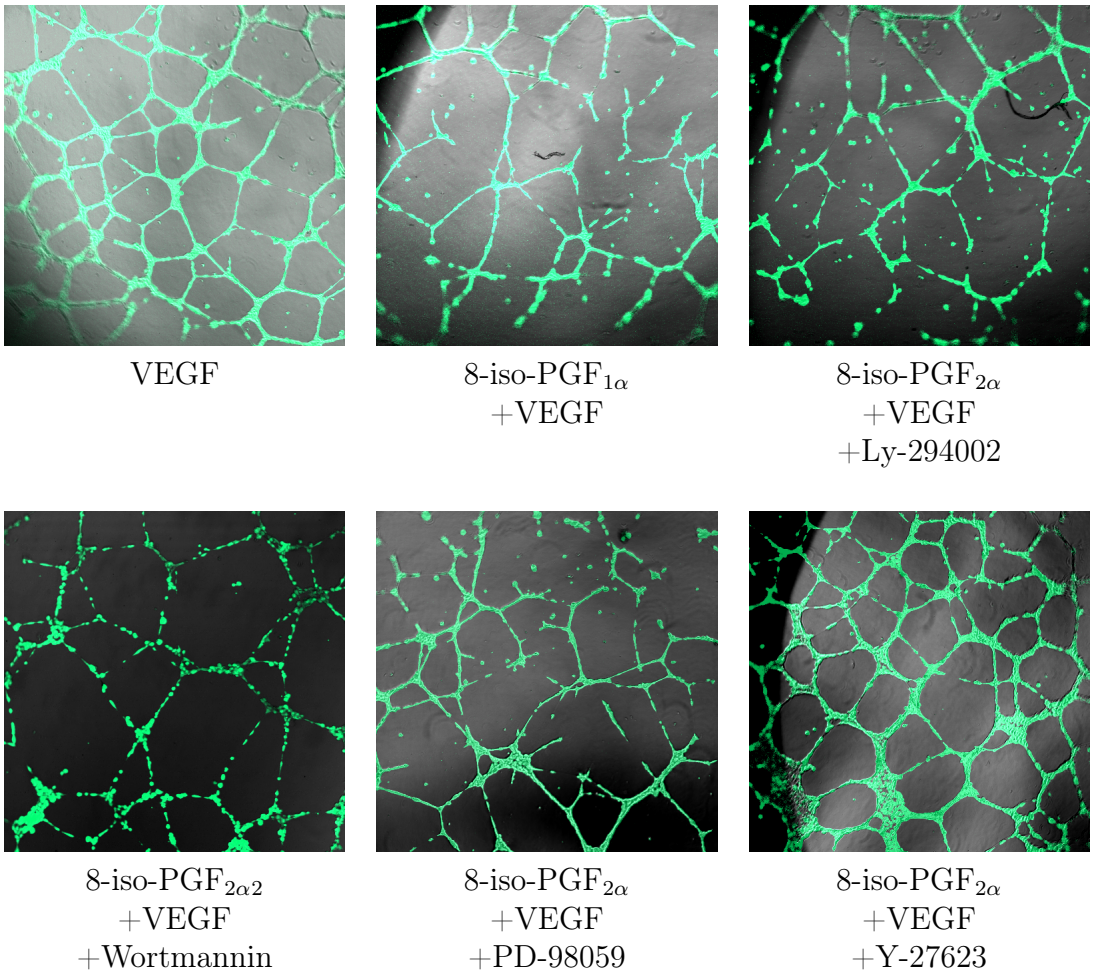

Figure 3.22: Effect of Ly-294002, Wortmannin, PD-98059 and Y-27623 on 8-iso-$PGF_{2\alpha}$-inhibiting effect on VEGF-induced tube formation of HCAECs. Bar graph shows results of quantitative analysis (A). Y-27623 (10 µM), but not Ly-294002 (10 µM), Wortmannin (10 µM) and PD-98059 (60 µM), reverses the inhibiting effect of 8-iso-$PGF_{2\alpha}$ ($3{\cdot}10^{-5}$M) on VEGF-induced tube formation of HCAEC. Photographs show representative effects of substances on tube formation of HCAECs (B). Results are expressed as mean ± SD of 2 separate experiments performed at least in triplicate, n=6 to 9. *P<0.001 vs. vehicle, § P<0.001 vs. VEGF; †P<0.001 vs. 8-iso-$PGF_{2\alpha}$ + VEGF alone.

Like 8-iso-$PGF_{2\alpha}$, U-46619 inhibited the VEGF-induced tube formation of HCAECs (55.3±14.3% [VEGF + U-46619] versus 121±3.9 [VEGF alone]; $p<0.001$). This effect was again abolished by Y-27632 (94.1±8.22% [VEGF + Y-27632 + U-46619] versus 55.3±14.3% [VEGF + U-46619], $P<0.001$). Again, PD-98059, LY-294002 and Wortmannin did not influence the inhibiting effect of U-46619 on VEGF-induced tube formation (53.7±6.1%, 47.4±6.6% and 48.4±5.02%, $P>0.05$, respectively)(Figure 3.23).

A

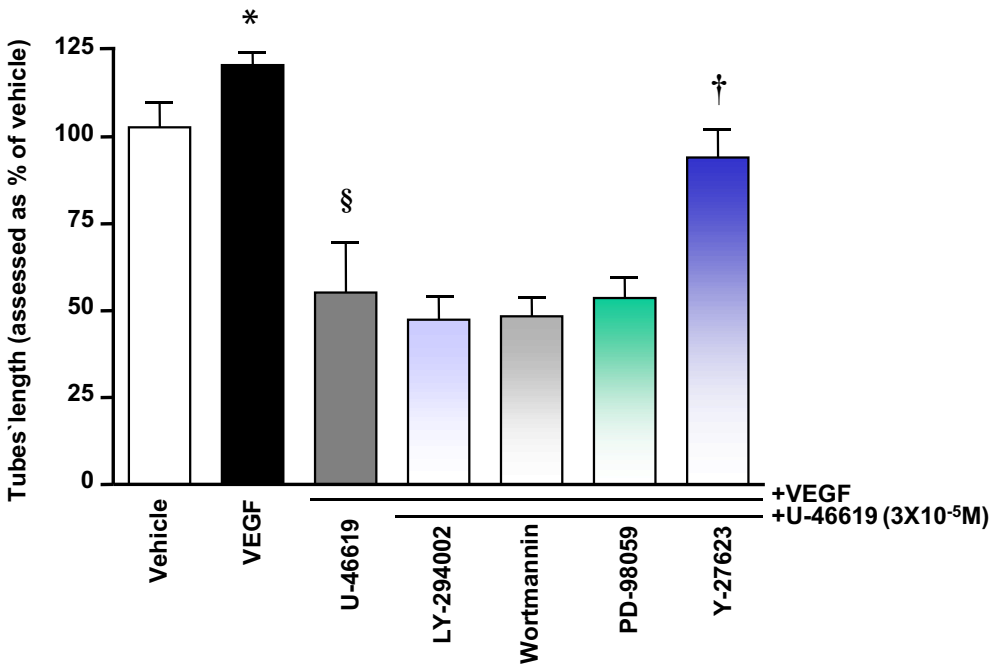

B

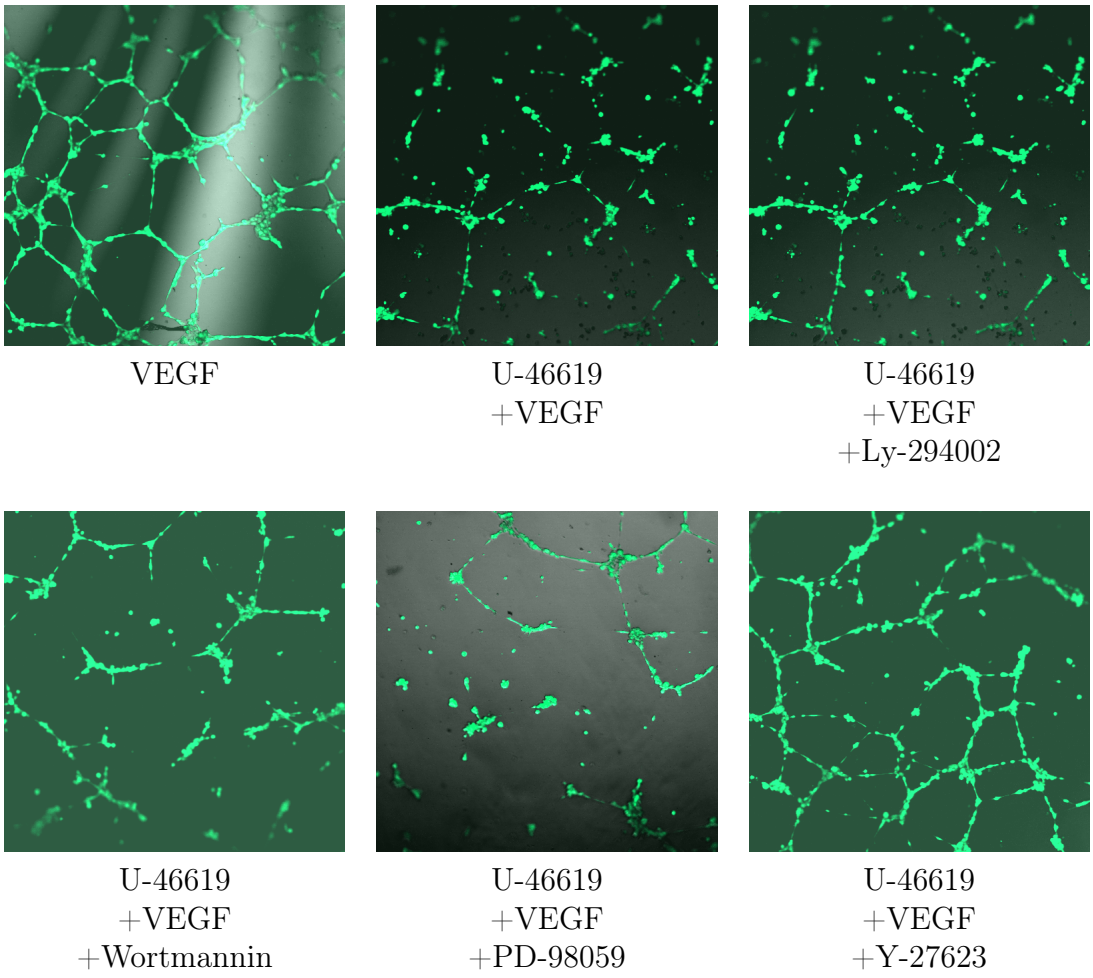

Figure 3.23: The influence of Ly-294002, Wortmannin, PD-98059 and Y-27623 on the inhibiting effect of U-46619 on VEGF-induced tube formation of HCAECs. Bar graph shows results of quantitative analysis (A). Y-27623 (10 µM), but not Ly-294002 (10 µM), Wortmannin (10 µM) and PD-98059 (60 µM), reverses the inhibiting effect of U-46619 ($3{\cdot}10^{-5}$M) on VEGF-induced tube formation of HCAECs. Photographs show representative effects of substances on tube formation of HCAECs (B). Results are expressed as mean ± SD of 2 separate experiments performed at least in triplicate, n=6 to 9. * P<0.01 vs. vehicle; § P<0.001 vs. VEGF; †P<0.001 vs. 8-iso-$PGF_{2\alpha}$ + VEGF alone.

3.4.2 Cytotoxicity Assay

To clarify if the inhibitory effects of 8-iso-$PGF_{2\alpha}$ and U-46619 were related to cytotoxic effects in HDMECs, a cytotoxicity assay based on the measuring of LDH activity in supernatant of incubated cells were conducted. The quantification of the LDH activity revealed that neither 8-iso-$PGF_{2\alpha}$ nor U-46119 induced an increase in LDH release compared to vehicle. Also the TBXA2R antagonist SQ-29548, the ERK-1/2 inhibitor PD-98059, and the Rho kinase inhibitor Y-27623 did not affect an increased LDH release. In contrast, Triton X serves as positive control, inducing remarkable LDH-release (Figure 3.24).

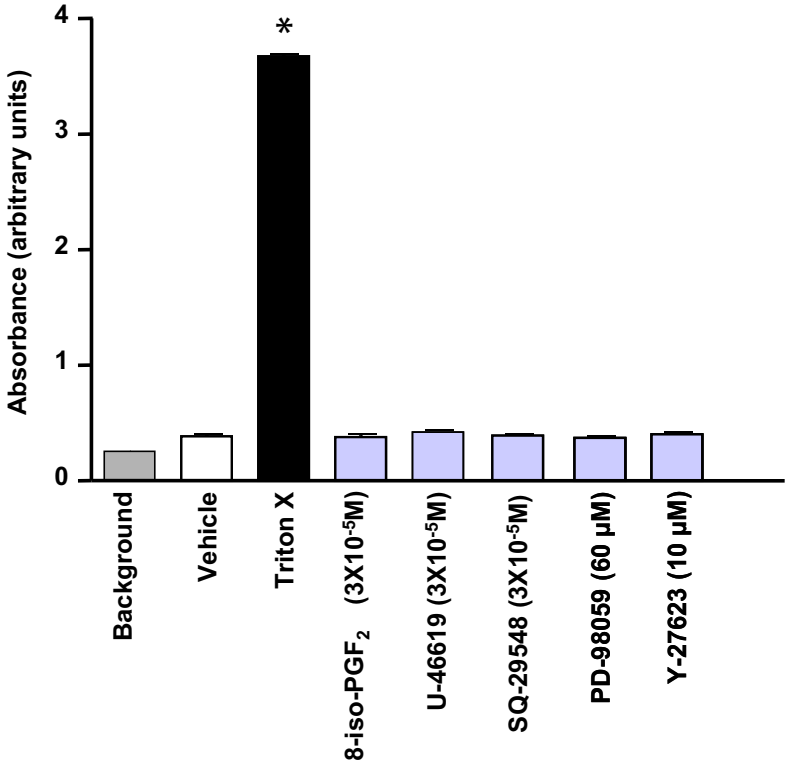

Figure 3.24: Cytotoxicity effects of 8-iso-$PGF_{2\alpha}$, U-46619, SQ-29548, PD-98059, and Y-27623 on HDMECs. Non of the tested substances exert an LDH release compared to vehicle in HDMCECs. Results are expressed as means ± SD of 2 separate experiments performed at least in triplicate, n=6 to 9. * $P<0.001$ vs. vehicle.

3.5 Investigation of Signaling Pathways of Isoprostanes in Endothelial Cells by Western Blot Analysis

To get more information via which mechanism 8-iso-$PGF_{2\alpha}$ influence EC migration and tube formation the effect of 8-iso-$PGF_{2\alpha}$ on eNOS (Ser-1177), PI3K/Akt (Ser-473) and ERK-1/2 (Thr202/Tyr204) phosphorylation was investigated via Western blot analysis as described in 2.4.3. The influence of the TBXA2R agonist U-46619 was investigated as well. The quantitative analysis of phosphorylated eNOS, Akt and ERK-1/2 was normalized to the control protein eIF4E and related to the vehicle.

3.5.1 Effect of 8-iso-$PGF_{2\alpha}$ and U-46619 on Basal Akt and ERK-1/2 Signaling in HDMECs

To find out if Akt activation is involved in isoprostanes-mediated effects, the influence of 8-iso-$PGF_{2\alpha}$ on Akt (Ser-473) phosphorylation in HDMECs was investigated. Noteworthy, lower pro-migrative concentrations of 8-iso-$PGF_{2\alpha}$ ($1{\cdot}10^{-7}$M) induced basal phosphorylation of Akt (Figure 3.25). The TBXA2R antagonist SQ-29548, which abolished the pro-migrative effect of low-concentrated 8-iso-$PGF_{2\alpha}$, also reversed the 8-iso-$PGF_{2\alpha}$-induced Akt phosphorylation. Moreover, HDMECs treated with high (ant-imigrative) concentrations of 8-iso-$PGF_{2\alpha}$ ($3{\cdot}10^{-5}$M) exhibited levels of phosphorylated Akt comparable to those of unstimulated control cells. The TBXA2R agonist U-46619, which did not stimulate basal migration of HDMECs at low concentrations, did not induce significant phosphorylation of Akt at $1{\cdot}10^{-7}$M either (Figure 3.26).

In contrary to Akt-, ERK-1/2 (Thr202/Tyr204) phosphorylation increased in HDMECs treated with 8-iso-$PGF_{2\alpha}$ in a dose-dependent manner. This effect was reversible by the TBXA2R antagonist SQ-29548 ($3{\cdot}10^{-5}$M) (Figure 3.25). HDMECs treated with U-46619 also exhibited an increased phosphorylation of ERK-1/2 (Thr202/Tyr204). Comparable with 8-iso-$PGF_{2\alpha}$ this effect was reversible by the TBXA2R antagonist SQ-29548 ($3{\cdot}10^{-5}$M)(Figure 3.26).

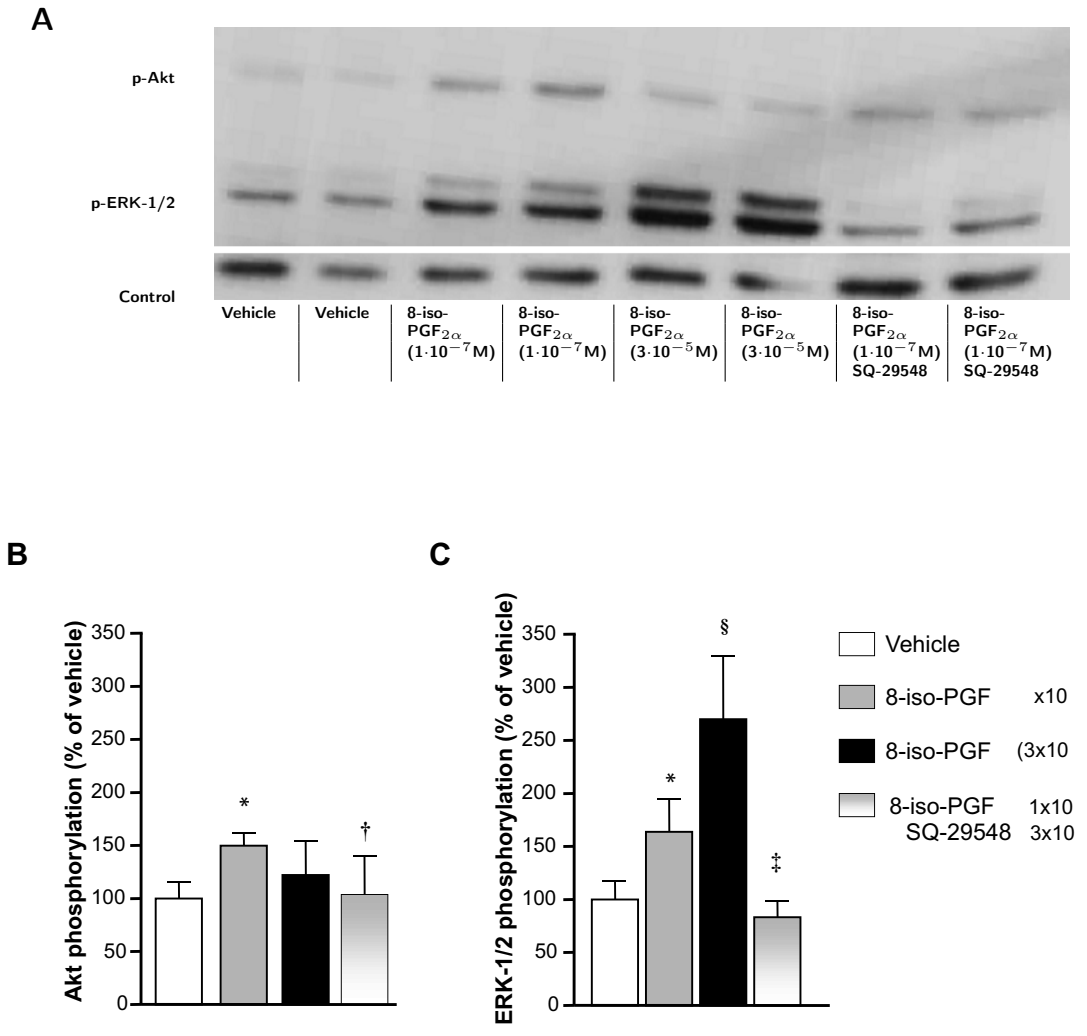

Figure 3.25: The effect of 8-iso-PGF$_{2\alpha}$ on Akt and ERK-1/2 signaling in HDMECs. Proteins were extracted from HDMECs treated with 0.1% EtOH-solution (vehicle) or 8-iso-PGF$_{2\alpha}$ ± SQ-29548 for 15 min. A representative Western blot (A) and the quantitative analysis of phosphorylated Akt (B) and ERK-1/2 (C) normalized to control protein and related to vehicle are shown. 8-iso-PGF$_{2\alpha}$ induces Akt posphorylation at low concentrations ($1{\cdot}10^{-7}$M). 8-iso-PGF$_{2\alpha}$ at high concentrations ($3{\cdot}10^{-5}$M) counteracts this effect. In contrast, 8-iso-PGF$_{2\alpha}$ increased ERK-1/2 phosphorylation in a concentration-dependent manner. The TBXA2R antagonist SQ-29548 ($3{\cdot}10^{-5}$M) blocks 8-iso-PGF$_{2\alpha}$ induced Akt- and ERK-1/2 phosphorylation. Bars represent the mean ± SD. * $P<0.01$, § $P<0.001$ vs. vehicle; † $P<0.05$, ‡ $P<0.01$ vs. 8-iso-PGF$_{2\alpha}$ ($1{\cdot}10^{-7}$M) alone. Four independent experiments were performed.

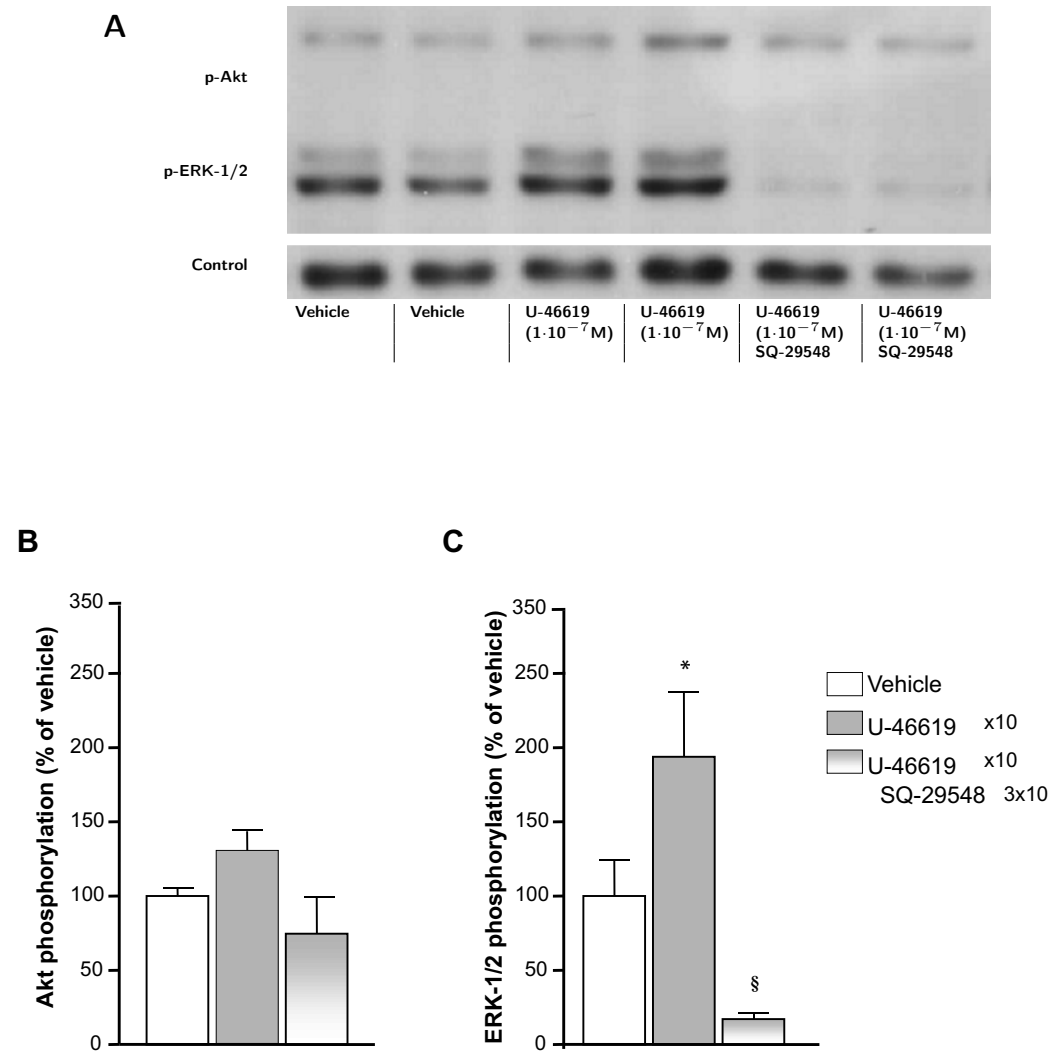

Figure 3.26: The effect of U-46619 on Akt and ERK-1/2 signaling in HDMECs. Proteins were extracted from HDMECs treated with 0.1% EtOH-solution (vehicle) or U-46619 ($1{\cdot}10^{-7}$M) ± SQ-29548 ($3{\cdot}10^{-5}$M) for 15 min. A representative Western blot (A) and the quantitative analysis of phosphorylated Akt (B) and ERK-1/2 (C) normalized to control protein and related to vehicle are shown. U-46619 induces ERK-1/2 phosphorylation. This effect is abolished by SQ-29548. In contrast Akt phosphorylation is not significantly affected by U-36619. Bars represent the mean ± SD. † $P<0.05$, * $P<0.001$ vs. vehicle; ‡ $P<0.05$, § $P<0.001$ vs. U-46619 ($1{\cdot}10^{-7}$M) alone. Four independent experiments were performed.

3.5.2 Effect of 8-iso-$PGF_{2\alpha}$ and U-46619 on VEGF-Induced eNOS-, Akt-, and ERK-1/2 Signaling in HDMECs

Due to the predominant role of VEGF in eNOS-, Akt-, and ERK-1/2 signaling *in vivo*, the effect of 8-iso-$PGF_{2\alpha}$ on eNOS (Ser-1177), Akt (Ser-473) and ERK-1/2 (Thr202/Tyr-204) phosphorylation in the presence of VEGF (50 ng/mL) was investigated. HDMECs treated with VEGF for 15 min exhibit increased levels of phosphorylated eNOS, Akt, and ERK-1/2 compared to vehicle. Costimulation with 8-iso-$PGF_{2\alpha}$ ($3{\cdot}10^{-5}$M) ± SQ-29548 ($3{\cdot}10^{-5}$M) did not affect VEGF-induced eNOS-, Akt-, and ERK-1/2 phosphorylation (Figure 3.27, A; 3.28, A). Similar results were observed when cells were treated with the TBXA2R agonist U-46619 at $3{\cdot}10^{-5}$M (Figure 3.27, B; 3.28, B).

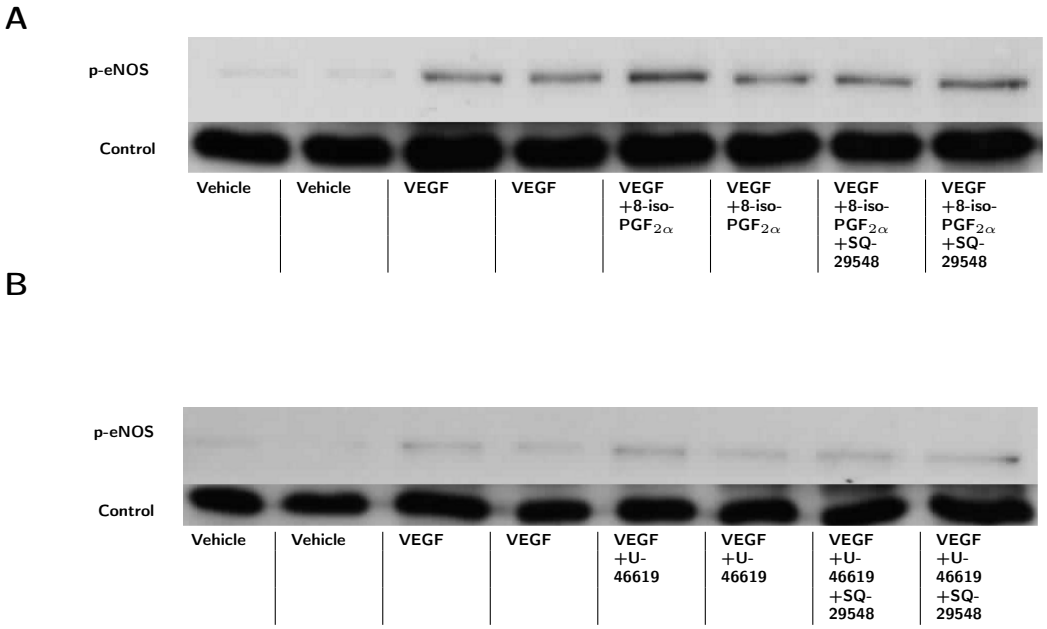

Figure 3.27: VEGF-induced eNOS phosphorylation in HDMECs. Proteins were extracted from HDMECs treated with 0.1% EtOH-solution (vehicle) and VEGF (50 ng/mL) ± 8-iso-$PGF_{2\alpha}$ ($3{\cdot}10^{-5}$M) or U-46619 ($3{\cdot}10^{-5}$M) for 15 min. These representative western blots show that neither 8-iso-$PGF_{2\alpha}$ (A) nor U-46619 (B) influenced the VEGF-induced phosphorylation of eNOS.

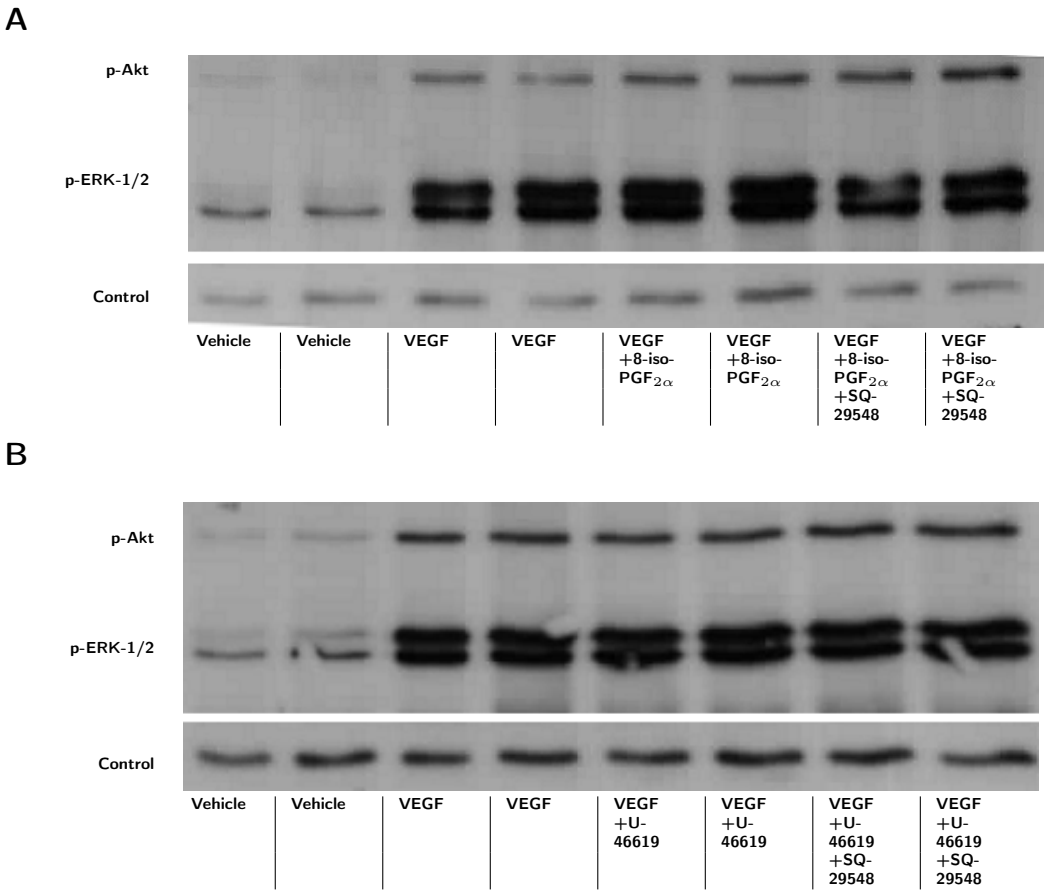

Figure 3.28: VEGF-induced Akt and ERK-1/2 phosphorylation in HDMECs. Proteins were extracted from HDMECs treated with 0.1% EtOH-solution (vehicle) and VEGF (50 ng/mL) ± 8-iso-$PGF_{2\alpha}$ ($3{\cdot}10^{-5}$M) or U-46619 ($3{\cdot}10^{-5}$M) for 15 min. These representative western blots show that neither 8-iso-$PGF_{2\alpha}$ (A) nor U-46619 (B) influenced VEGF-induced phosphorylation of Akt and ERK-1/2.

To clarify, if in the above mentioned experiments the effects of 8-iso-$PGF_{2\alpha}$ were overlayed by VEGF overstimulation, the incubation time for VEGF was decreased to 5 min. For the following experiments HDMECs were incubated with 0.1% EtOH solution (vehicle) and 8-iso-$PGF_{2\alpha}$ ($1{\cdot}10^{-7}$M) ± SQ-29548 ($3{\cdot}10^{-5}$M) for 10 min, then VEGF added and the cells incubated for further 5 min with all substances. Western blots were performed with extracted proteins and the phosphorylation levels of eNOS, Akt, and ERK-1/2 were assessed anew. No significant effect could be observed in eNOS phosphorylation. Furthermore, VEGF alone did not induce a significant Akt phosphorylation, presumably due to the short incubation time (Figure 3.29). However, 8-iso-$PGF_{2\alpha}$ + VEGF caused a distinct Akt phophorylation. In contrast, addition of SQ-29548 did not counteract p-Akt in this settings, presumably due to the impact of VEGF. Investigation of ERK-1/2 signaling showed that VEGF increased phosphorylation of ERK-1/2. Additional stimulation with 8-iso-$PGF_{2\alpha}$ did not increase ERK-1/2 phosphorylation significantly. SQ-29548 decreased ERK-1/2 phosphorylation induced by 8-iso-$PGF_{2\alpha}$ + VEGF to levels which lower than those induced by VEGF alone. (Figure 3.29).

A

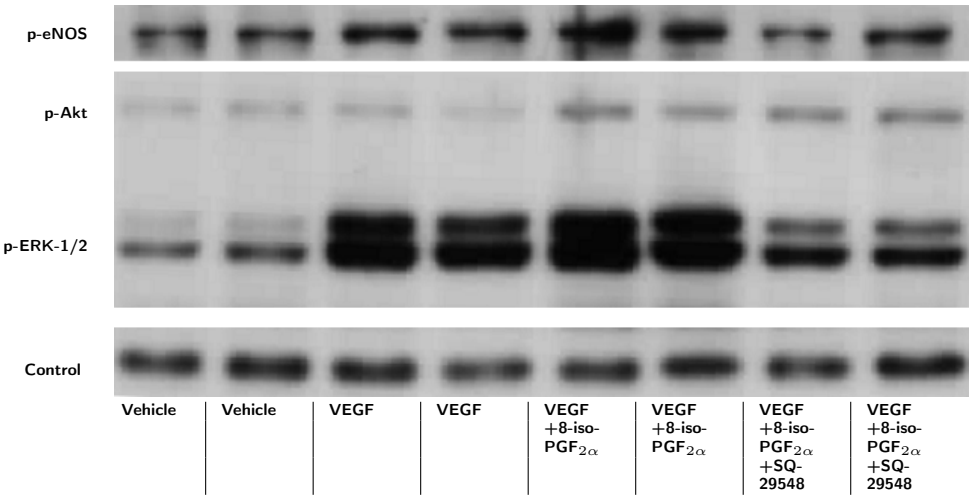

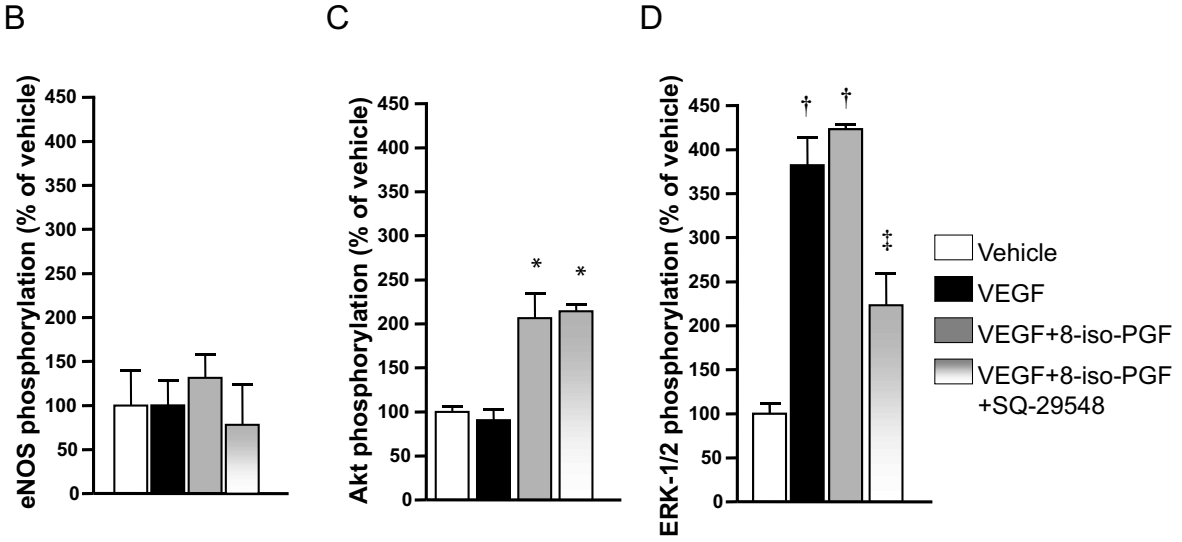

Figure 3.29: Effect of 8-iso-$PGF_{2\alpha}$ on VEGF-induced eNOS, Akt and ERK-1/2 phosphorylation in HDMECs. Cells were incubated with 8-iso-$PGF_{2\alpha}$ ($1{\cdot}10^{-7}$M) ± SQ-29548 ($3{\cdot}10^{-5}$M) for 15 min + VEGF (50 ng/mL) for 5 min. A representative western blot (A) and the quantitative analysis of phosphorylated eNOS (B), Akt (C) and ERK-1/2 (D) normalized to control protein and related to vehicle are shown. Under these conditions 8-iso-$PGF_{2\alpha}$ + VEGF cause increased phosphorylation of Akt compared to levels induced by VEGF alone. VEGF and 8-iso-$PGF_{2\alpha}$ + VEGF induce strong ERK-1/2 phophorylation, both effects are abolishable by SQ-29548. In contrast, no changes in eNOS phosphorylation is observed. Bars represent the mean ± SD. * $P<0.01$, † $P<0.001$ vs. vehicle; ‡$P<0.01$ vs. 8-iso-$PGF_{2\alpha}$ ($1{\cdot}10^{-7}$M) + VEGF (50 ng/mL) alone. Three independent experiments were performed.

3.5.3 Effect of PD-98059 and Y-27634 on 8-iso-$PGF_{2\alpha}$ and U-46619 Influenced Akt, eNOS and ERK-1/2 Signaling in HDMECs

The influence of the ERK-1/2 inhibitor PD-98059 on 8-iso-$PGF_{2\alpha}$ mediated Akt and ERK-1/2 phosphorylation was investigated. Therefore HDMECs were treated with 8-iso-$PGF_{2\alpha}$ ($1{\cdot}10^{-7}$M) ± PD-98059 (60 µM) for 15 min, before proteins were extracted for western blot analysis. As seen in Figure 3.30, PD-98059 decreased p-Akt as well as p-ERK-1/2. The influence of Rho kinase inhibitor Y-27623 (10 µM) on 8-iso-$PGF_{2\alpha}$ me-

diated Akt and ERK-1/2 phosphorylation was also determined (Figure 3.30). Y-27623 decreased Akt and ERK-1/2 phosphorylation.

In addition the effect of PD-98059 and Y-27623 on U-46619 ($1 \cdot 10^{-7}$M) mediated Akt and ERK-1/2 phosphorylation was examined and similar results were obtained. As well PD-98059 (60 µM) as Y-27623 (10 µM) reduced Akt- and ERK-1/2 phosphorylation (Figure 3.31). In addition, the influence of 8-iso-$PGF_{2\alpha}$ and U-46619 on eNOS phosphorylation under basal conditions was investigated, but no effects were detectable (Figure 3.30 and 3.31).

A

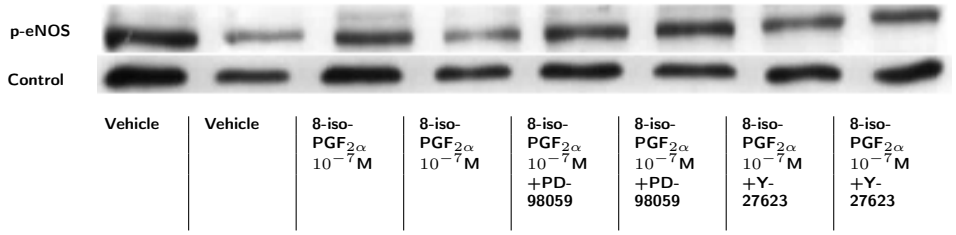

B

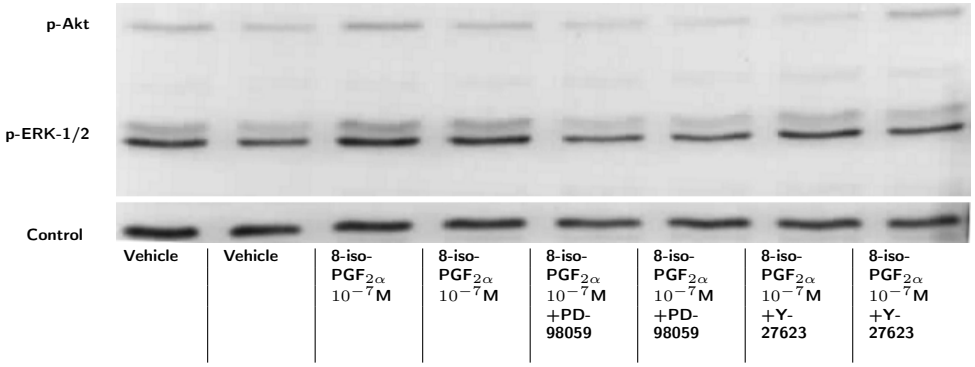

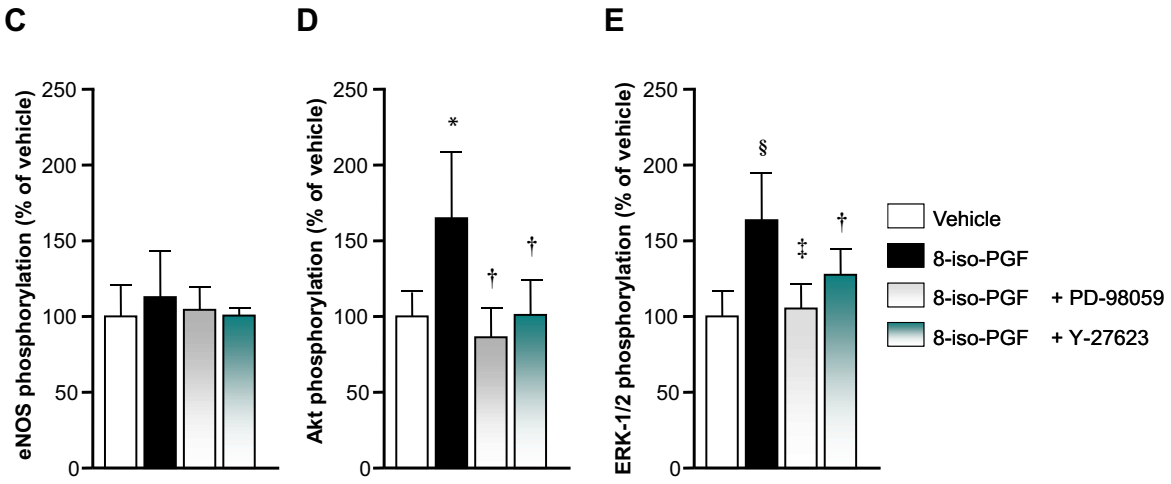

Figure 3.30: Effect of the ERK-1/2 inhibitor PD-98059 and the rho kinase inhibitor on 8-iso-PGF$_{2\alpha}$-influenced eNOS-, Akt-, and ERK phosphorylation in HDMECs. Cells were incubated with 8-iso-PGF$_{2\alpha}$ ($1{\cdot}10^{-7}$M) ± PD-98059 (60 µM) and Y-27623 (10 µM) for 15 min. Representative western blots demonstrate levels of p-eNOS (A) and p-Akt/p-ERK-1/2 (B). The quantitative analysis of phosphorylated eNOS (C), Akt (D), and ERK-1/2 (E) are shown normalized to control protein and related to vehicle. PD-98059 as well as Y-27623 reverses both the 8-iso-PGF$_{2\alpha}$-induced Akt- and ERK-1/2 phosphorylation. No changes can be detected in eNOS phosphorylation. Bars represent the mean ± SD. * $P<0.01$, § $P<0.001$ vs. vehicle; † $P<0.05$, ‡ $P<0.01$ vs. 8-iso-PGF$_{2\alpha}$ ($1{\cdot}10^{-7}$M) alone. Four independent experiments were performed.

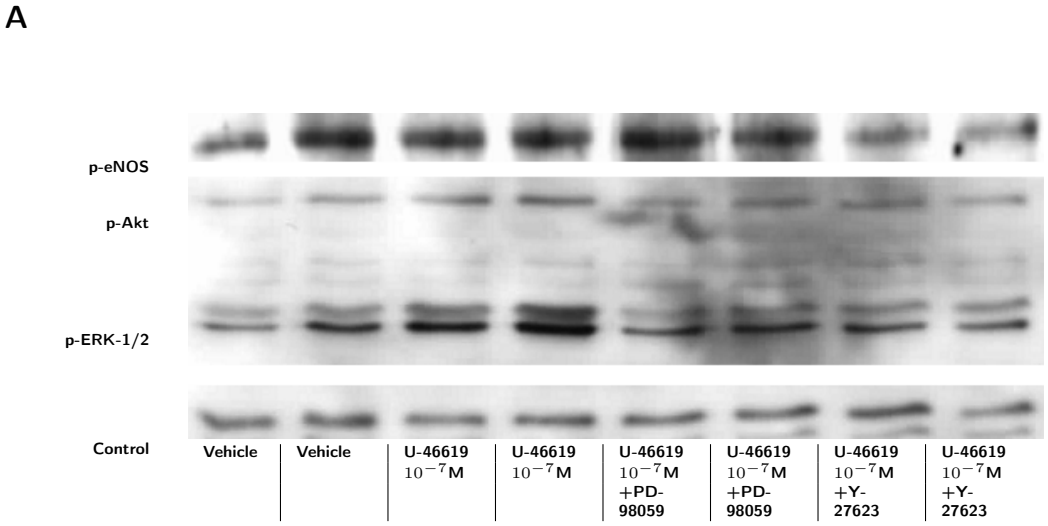

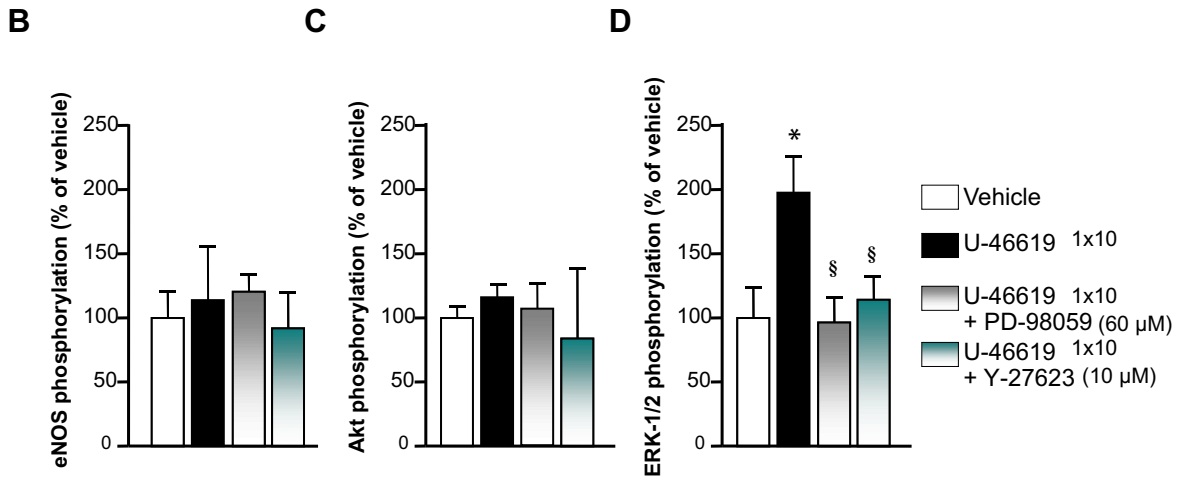

Figure 3.31: Effect of the ERK-1/2 inhibitor PD-98059 and rho kinase inhibitor Y-27623 on U-46619-influenced eNOS-, Akt- and ERK-1/2 phosphorylation. Cells were incubated with U-46619 ($1{\cdot}10^{-7}$M) ± PD-98059 (60 µM) and Y-27623 (10 µM) for 15 min. A representative western blot (A) and quantitative analysis of phosphorylated eNOS (B), Akt (C), and ERK-1/-2 (D) normalized to control protein and related to vehicle are shown. U-46619-induced ERK-1/2 phosphorylation was abrogated by PD-98059 and Y-27623 costimulation. No significant changes can be detected for p-eNOS and p-Akt levels. Bars represent the mean ± SD. * $P<0.05$ vs. vehicle; § $P<0.01$ vs. U-46619 ($1{\cdot}10^{-7}$M) alone. Four independent experiments were performed.

4 Discussion

The main focus of this work was to investigate the influence of isoprostanes on angiogenesis. Therefore, the effects of isoprostanes on EC migration as well as tube formation under basal- and VEGF-induced conditions were examined. Another objective included the investigation of possibly signaling pathways. First of all migration assays were performed with HCAECs. Unfortunately they did not always show a strong response to VEGF. The reason for this is not clear, but an explanation could be that they lost some quality characteristics during refreezing. Another explanation could be the age of donors. HCAECs were taken from adult patients during heart surgeries (23-77 years old). Therefore several migration assays were also performed with HDMECs from young donors (0-9 years old), which were cultered and used for experiments immediately after delivery. They consistently exhibited an intensive response to VEGF.

4.1 Influence of Isoprostanes on Basal-Induced Angiogenesis *In Vitro*

8-iso-$PGF_{2\alpha}$ and 8-iso-PGA_2 at low concentrations ($1{\cdot}10^{-7}$M) exerted a biphasic response on basal migration of ECs with lower concentrations moderately inducing basal EC migration. These effects were mediated via TBXA2R activation because the TBXA2R antagonist SQ-29549 abrogated the 8-iso-$PGF_{2\alpha}$-induced pro-migratory effect in HDMECs (Figure 3.1). Due to the fact that isoprostanes could also act via activation of the DP (prostaglandin D receptor) and EP (prostaglandin E receptor) [154, 156, 157] we examined a possible involvement of these receptors in isoprostanes-mediated pro-migratory effects on HDMECs and found out that the unspecific $DP/EP_1/EP_2$ receptor

antagonist AH-6809 did not influence the biphasic effect of 8-iso-$PGF_{2\alpha}$ (Figure 3.3). Hence, we exclude an involvement of the DP and EP in this setting.

When cells were pre-incubated with PTX (0.1 ng/mL) for 24 h the pro-migratory effect of 8-iso-$PGF_{2\alpha}$ was abolished (Figure 3.6). These results provide a strong argument for an involvement of the G-protein subunit $G\alpha_i$ in 8-iso-$PGF_{2\alpha}$-mediated pro-migratory effects because PTX prevents $G\alpha_i$-mediated signaling by inhibiting $G\alpha_i$ receptor-coupling.

In agreement with its pro-migratory effect, 8-iso-$PGF_{2\alpha}$ stimulates also the basal tube formation of ECs at low concentrations. This effect was abrogated by the PI3K inhibitor LY-294002 and the ERK-1/2 inhibitor PD-98059 (Figure 3.7). However LY-294002 and PD-98059 did not influence the pro-migrative effect of 8-iso-$PGF_{2\alpha}$ (Figure 3.4).

The PI3K/Akt pathway regulates cell survival through the phosphorylation of multiple substrates involved in the regulation of apoptosis [158]. ERK-1/2 is known to regulate diverse cellular processes, such as cell growth, cell motility, cell survival, and cell proliferation [159]. The reason why PI3K- and ERK-1/2 inhibition abrogated the stimulating effect of 8-iso-$PGF_{2\alpha}$ only in the tube formation and not in the migration assay may come from different test conditions, particularly with regard to different incubation times. The migration assay lasted 5 h, whereas the tube formation assay ended not until 24 h, which makes higher demands on the cells. In this regard abilities like PI3K/Akt-mediated cell survival as well as ERK-1/2 induced cell proliferation seem to play a crucial role in EC tube formation. These findings suggest that 8-iso-$PGF_{2\alpha}$ at low concentrations exerts its stimulating effects on basal migration and tube formation via TBXA2R activation and these effects were mediated through PTX-sensitive $G\alpha_i$-signaling. Furthermore, the stimulating effect of 8-iso-$PGF_{2\alpha}$ on basal tube formation requires additionally $G\beta\gamma$-mediated PI3K/Akt-induced cell survival as well as ERK-1/2-induced cell proliferation (Figure 4.1).

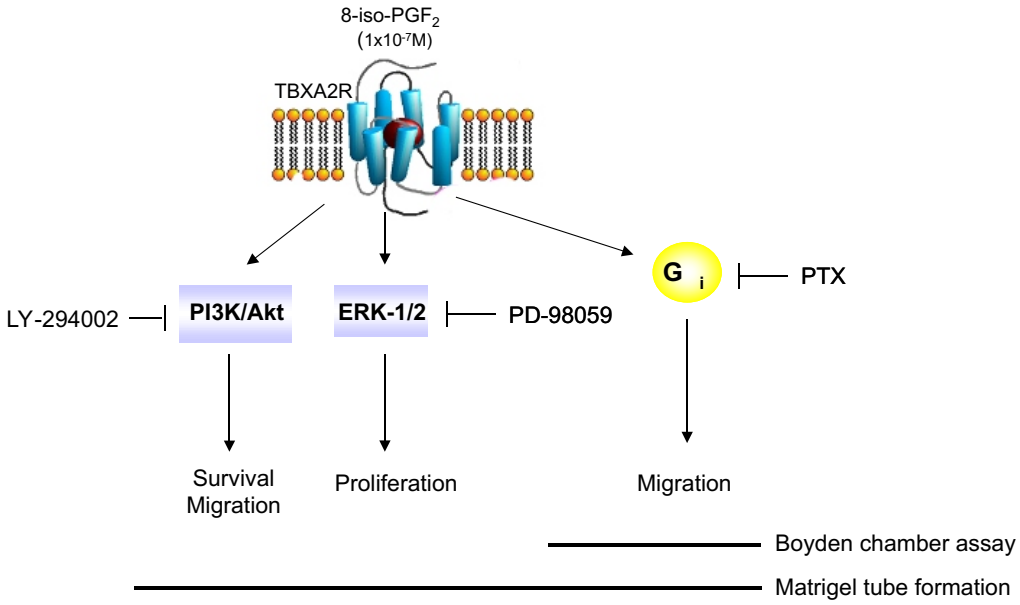

Figure 4.1: Proposed signaling of 8-iso-PGF$_{2\alpha}$ at low concentrations in EC migration and tube formation. 8-iso-PGF$_{2\alpha}$ at low concentrations exerts a stimulating effect on basal migration and tube formation via TBXA2R activation through PTX-sensitive Gα_i-signaling. The stimulating effect of 8-iso-PGF$_{2\alpha}$ on basal tube formation requires additionally PI3K/Akt-induced cell survival as well as ERK-1/2-induced cell proliferation.

Western Blot analysis revealed that 8-iso-PGF$_{2\alpha}$ at low concentrations induced Akt phosphorylation in HDMECs after 15 min incubation. This effect was reversed by costimulation with SQ-29548 (Figure 3.25). These data are in accordance with the abovementioned stimulating effect of 8-iso-PGF$_{2\alpha}$ on EC tube formation and confirmed that these effects were mediated at least in part via Akt activation through the TBXA2R. Furthermore, it was shown that 8-iso-PGF$_{2\alpha}$-induced Akt phosphorylation was also reversed by the ERK-1/2 inhibitor PD-98059 (Figure 3.30), suggesting that PD-98059 affects PI3K/Akt signaling.

In addition, 8-iso-PGF$_{2\alpha}$ induced ERK-1/2 phosphorylation in a concentration-dependent manner (Figure 3.25). This effect was also mediated via TBXA2R activation because the

TBXA2R antagonist SQ-29548 completely reversed this effect. In line with these findings it has been reported that 8-iso-$PGF_{2\alpha}$ mediates biological effects via ERK-1/2 phosphorylation, such as inducing inflammatory chemokines expression in human macrophages [160] and stimulating mitogenesis of human VSMCs (vascular smooth muscle cells) [161].

In addition, we showed that 8-iso-$PGF_{2\alpha}$-induced ERK-1/2 phosphorylation was completely reversed by the ERK-1/2 inhibitor PD-98059 and partly reversed by the Rho kinase inhibitor Y-27623. These findings support the assumption that ERK-1/2 signaling can be affected by two different signaling ways which are both mediated via the TBXA2R. First, TBXA2R activation leads to ERK-1/2 activation involving $G\beta\gamma$ [132]. Due to the observation that PD-98059 abolished Akt- as well as ERK-1/2 phosphorylation it is imaginable that PD-98059 inactivates PI3K, which may function as intermediate switch. In this case PI3K inactivation would result in decreased Akt and ERK-1/2 phosphorylation. Second, TBXA2R activation leads also to $G\alpha_{12/13}$-mediated Rho activation, which in turn may affect ERK-1/2. Little is known about a potential crosstalk between PI3K and ERK-1/2. It has been shown that in neuronal cells the epidermal growth factor (EGF) induces ERK-1/2 activation via a pathway involving PI3K. On the other hand, activation of the PI3K/Akt pathway seems to inhibit ERK-1/2 activation in human colon cancer cell lines [162]. The second pathway is supported by several groups, which have described that ERK-1/2 phosphorylation is Rho-dependent [163]. For instance Renshaw and colleagues have shown that Rho is an important component in the integrin-dependent activation of ERK-1/2 [164].

8-iso-$PGF_{2\alpha}$ at high concentrations and U-46619 inhibited basal migration and tube formation of ECs. Both effects were reversed by costimulation with SQ-29548 and Y-27623, indicating that TBXA2R activation leads to a Rho kinase activation, which in turn inhibits angiogenesis *in vitro* (Figure 3.5). Confirming that isoprostanes are able to mediate biological effects via this mechanism Mueed et al. showed that isoprostanes constrict human radial artery by stimulation of the TBXA2R and RhoA activation [165].

Concordant with other publications we detected only an inhibiting effect of U-46619 on basal EC migration and tube formation. Several studies demonstrated the antiangiogenic effect of TBXA2R activation in ECs [166, 167, 168]. In contrast to our results,

there is one publication from Nie et al. which described that the TBXA2R agonist U-46619 stimulated human umbilical vein endothelial cell (HUVEC) migration at low concentrations (300 nM) and inhibited HUVEC migration at high concentrations (30 μM) [169]. The authors suggested that this biphasic response of the TBXA2R could be due to receptor desensitization at high concentrations. Receptor desensitization is a critical aspect of G protein coupled receptors (GPCRs) signaling mechanism that occurs in response to the continued presence of receptor ligands and results in a termination of the cellular response. Indeed it has been established that both TBXA2R subtypes TBXA2R-α and TBXA2R-β undergo U-46619-induced desensitization [170, 171]. Furthermore a biphasic response to U-46619 in human prostate cancer (PC-3) cell migration was reported. This effect was also reversible by SQ-29548 [169]. These data suggest that TBXA2R signaling may effect cell migration through Rho activation. During cell migration lamellipoda and filopodia are formed at the leading edge of the cell to drive the cell forward. At the trailing end the cell has to detach and retract to enable a forward motion. This coordinated process requires a temporal and spatial activation of the Rho GTPases RhoA, Cdc42, and Rac [152]. Whereas Cdc42 is required for filopodial protrusions and Rac promotes lamellipodial protrusions, RhoA regulates the contraction at the trailing edge [152]. A sustained TBXA2R activation induces a persistent RhoA activation, which disturbed the elaborated interplay between the three Rho GTPases and therefore results in an inhibition of cell migration. Taking into account the short half life of the physiological TBXA2R agonist thromboxane A_2 *in vivo* (approximately 30 sec), isoprostanes may represent important stable ligands of the TBXA2R, especially in pathophysiological states of increased oxidative stress.

We demonstrated that the inhibiting effects of U-46619 and 8-iso-$PGF_{2\alpha}$ at high concentrations on basal EC migration and tube formation were also mediated via Rho kinase activation. The stimulating effects of isoprostanes at low concentrations were only observed in the absence of VEGF, a scenario unlikely to occur *in vivo*, where growth factors are continuously secreted. However, the effects of 8-iso-$PGF_{2\alpha}$ at high concentrations on ECs in the absence of VEGF were identical with those of 8-iso-$PGF_{2\alpha}$ on VEGF-stimulated ECs. They are discussed in detail in the chapter 4.4.

4.2 The Role of VEGF on Angiogenesis *in Vitro*

VEGF plays a central role in angiogenesis. It initiates a complex network of signaling pathways including ERK-1/2 and Akt phosphorylation. Both have been implicated in mediating VEGF functions, including survival, proliferation, and migration of ECs. The influence of VEGF on EC migration was investigated and as expected VEGF exerted a strong stimulating effect on HDMEC migration at 50 ng/mL (Figure 3.12). We tested the possibility of an involvement of ERK-1/2 activation in this setting and found out that VEGF-induced EC migration was partly reversed by the ERK-1/2 inhibitor PD-98059 (Figure 3.21). These results correlate well with the literature. PD-98059 has been shown to inhibit the migration of diverse cell types in response to growth factors such as VEGF, fibroblast growth factor (FGF), and EGF [147]. Eliceiri et al. demonstrated that PD-98059 blocked the VEGF-induced migration of ECs [172]. We also elucidated the role of the PI3K/Akt pathway in VEGF-induced migration and find out that two inhibitors of PI3K, LY-294002 and Wortmannin reduced the VEGF-induced migration of HDMECs (Figure 3.21). These observations are in accordance with Morales-Ruiz et al. who have described that LY-294002 and Wortmannin reduced VEGF-induced cell migration in ECs [141]. In conclusion, VEGF-dependent EC migration is mediated at least partly via PI3K activation. PI3K is known to induce Akt phosphorylation which causes NO release by eNOS activation and this pathway may be essential for VEGF-induced migration [173]. Since the small GTPase RhoA has been implicated in the VEGF-enhanced EC migration, we investigated the influence of the Rho kinase inhibitor Y-27623 on VEGF-induced migration. Y-27623 did not influence the VEGF-induced migration, although other groups demonstrated an involvement of Rho kinase in EC migration [174]. In this regard conflicting findings are reported in the literature. A detailed discussion about the function of RhoA/Rho kinase is given in the chapter 4.4.

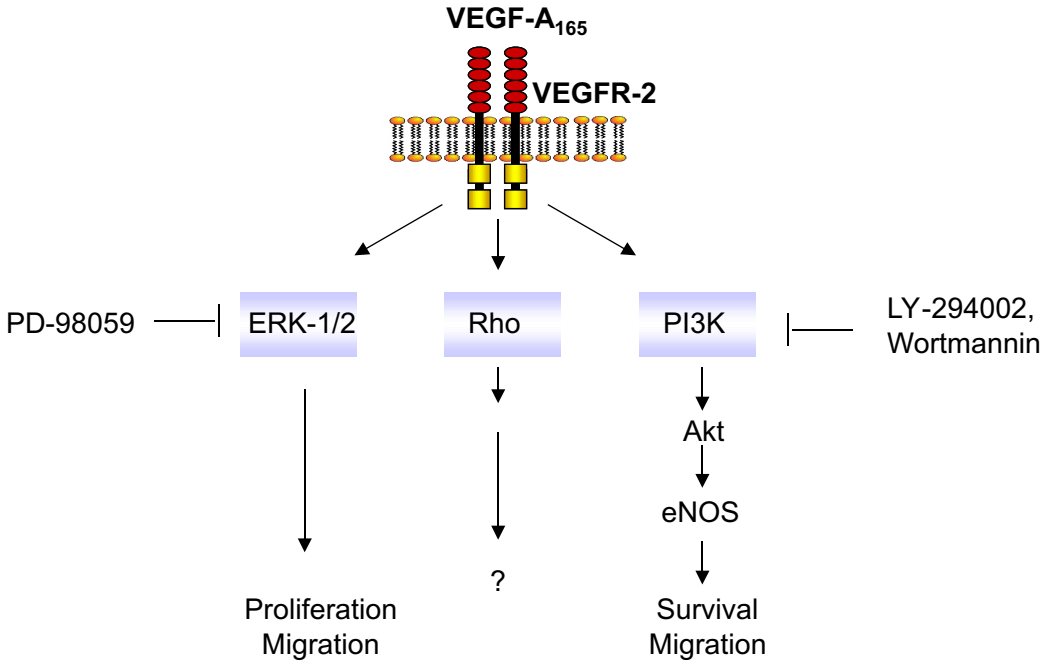

Figure 4.2: VEGF-mediated signaling in EC migration.

We showed that VEGF exerted also a stimulating effect on EC tube formation. In contrast to the data obtained from the migration assays neither Wortmannin and LY-294002, nor PD-98059 had any effect on VEGF-induced tube formation. The reason for this discrepancy is not clear. An explanation could be that the tube formation assays were conducted on matrigel containing several growth factors. These growth factors might compensate potential inhibiting effects of PI3K- and ERK-1/2 inhibitors by inducing other pro-angiogenic pathways.

Western blot analysis showed that VEGF induces a strong phosphorylation of Akt and eNOS. This is also evidenced by other groups which have reported that VEGF leads to Akt- and eNOS phosphorylation [137]. In addition, VEGF showed a strong stimulating effect on ERK-1/2 phosphorylation, which confirms that ERK-1/2 is one of the most important targets of VEGF.

4.3 Signaling Effects of 8-iso-$PGF_{2\alpha}$ at low Concentrations in the Presence of VEGF

8-iso-$PGF_{2\alpha}$ at low concentrations as well as at high concentrations inhibited the VEGF-induced migration and tube formation. This chapter debates the signaling effects of 8-iso-$PGF_{2\alpha}$ at low concentrations in the presence of VEGF. Effects at high concentrations in the presence of VEGF are subject of discussion in the next chapter.

Due to the observations that VEGF induced such a strong phosphorylation of eNOS, Akt, and ERK-1/2 which seems not capable of being influenced by 8-iso-$PGF_{2\alpha}$ and U-46619 by 15 min costimulation (Figure 3.27/28), we assumed that VEGF were overstimulated under the chosen conditions and covered therefore potential effects of 8-iso-$PGF_{2\alpha}$ and U-46619. Hence, we altered the test conditions to 5 min VEGF stimulation. VEGF alone did not induce Akt phosphorylation (Figure 3.29). This result indicated that VEGF-induced Akt phosphorylation is time-dependent having in mind that VEGF induced strong Akt phophorylation after 15 min incubation time (Figure 3.27). VEGF + 8-iso-$PGF_{2\alpha}$ caused a distinct Akt phophorylation, which was not reversible by addition of SQ-29548. These results underline the findings obtained from the experiments performed under basal conditions that 8-iso-$PGF_{2\alpha}$ is able to induce Akt phosphorylation. In contrast to the findings under basal conditions, Akt phosphorylation was not blocked by the TBXA2R antagonist SQ-29548 in the presence of VEGF (Figure 3.29).

Investigation of ERK-1/2 signaling revealed that VEGF induced strong ERK-1/2 phosphorylation after 5 min incubation time (Figure 3.29). Addition of 8-iso-$PGF_{2\alpha}$ did not increase ERK-1/2 phosphorylation significantly, presumably ERK-1/2 activation induced by 8-iso-$PGF_{2\alpha}$, which was already shown in the experiments under basal conditions, was covered by the strong stimulus of VEGF. Noteworthy, SQ-29548 decreased ERK-1/2 phosphorylation levels induced by VEGF + 8-iso-$PGF_{2\alpha}$ to levels which were lower than those induced by VEGF alone, indicating that SQ-29548 did not only abolish the effect of 8-iso-$PGF_{2\alpha}$. Inactivation of the TBXA2R by SQ-29548 decreased the VEGF-induced ERK-1/2 phosphorylation via an unknown mechanism. In this regard a cross talk between the TBXA2R and the VEGFR2 is imaginable. In this case TBXA2R inhibition could not only inhibited ERK-1/2 phosphorylation induced by 8-iso-$PGF_{2\alpha}$ but also inhibited the ERK-1/2 phosphorylation induced by VEGF.

4.4 Influence of 8-iso-$PGF_{2\alpha}$ at High Concentrations on VEGF-Induced Angiogenesis *in Vitro*

Since VEGF is a major stimulus of angiogenesis *in vivo*, we investigated the influence of 8-iso-$PGF_{2\alpha}$ on VEGF-stimulated ECs. The inhibiting effect of 8-iso-$PGF_{2\alpha}$ on the VEGF-induced migration of ECs was mimicked by the TBXA2R agonist U-46619 and abolished by the TBXA2 antagonist SQ-29548 (Figure 3.12), indicating that isoprostanes mediate their anti-angiogenic effects via activation of the TBXA2R.

A further goal of this work was to find out which signaling pathways downstream of the TBXA2R could be involved in the anti-angiogenic effects of isoprostanes. For that purpose we investigated the role of the PI3K/Akt pathway in isoprostanes-mediated inhibition of VEGF-induced migration and tube formation. Our results showed that the PI3K inhibitors LY-294002 and Wortmannin did not influence the inhibiting effect of 8-iso-$PGF_{2\alpha}$ and U-46619 on VEGF-induced migration and tube formation of ECs (Figure 3.21/B, 3.22). Moreover, Western blotting revealed that VEGF-induced eNOS- and Akt-phosphorylation were not inhibited by 8-iso-$PGF_{2\alpha}$ after 15 min costimulation in HDMECs (Figure 3.27, 3.29). Based on our data, isoprostanes do not mediate their inhibiting effects through inactivation of the PI3K/Akt pathway. These findings differ from previous data, which reported that the thromboxanes A_2 mimetic IBOP inhibited angiogenesis by suppressing NO release from VEGF-treated ECs through decreased activation of Akt and eNOS [167]. The reason for this discrepancy may be due to different cell types studied (HDMECs versus HUVECs). First of all, the TBXA2R can activate several different signaling cascades, whereas the relative signaling preference for a given cascade is cell/tissue specific. Furthermore, the TBXA2R expresses two isoforms in human ECs, the TBXA2R-α and TBXA2R-β [175, 128]. They display critical differences in their signaling and exhibit distinct patterns of expression in a variety of cell/tissue types.

We also investigated if 8-iso-$PGF_{2\alpha}$ mediated its anti-angiogenic effects through activation of the ERK-1/2 pathway. The ERK-1/2 inhibitor PD-98059 did not influence the inhibiting effect of 8-iso-$PGF_{2\alpha}$ and U-46619 on VEGF-induced migration and tube formation (Figure 3.21/B, 3.22). Same applies for the inhibiting effect of 8-iso-$PGF_{2\alpha}$ at high concentrations on basal migration and tube formation (Figure 3.5/A, 3.7). Fur-

thermore, 8-iso-$PGF_{2\alpha}$ and U-46619 did not ablated the VEGF-induced ERK-1/2 phosphorylation after 15 min costimulation in HDMECs (Figure 3.29). Hence the ERK-1/2 pathway does not play a role in isoprostanes-mediated inhibition of angiogenesis.

Finally we found out that the Rho kinase inhibitor Y-27632 almost completely abolished the inhibitory effect of 8-iso-$PGF_{2\alpha}$ and U-46619 on VEGF-induced migration (Figure 3.21/B) and tube formation (Figure 3.22/A), advocating that a pronounced and persistent RhoA activation may be responsible for isoprostanes-induced inhibition of VEGF-stimulated angiogenesis. The same applies for the experiments that showed that Y-27632 also reversed the inhibitory effect of 8-iso-$PGF_{2\alpha}$ at high concentrations and U-46619 on basal migration and tube formation (Figure 3.5, 3.8, 3.9). These findings are supported by further experiments from our group, which demonstrated an increased and more persistent RhoA activation induced by concomitant stimulation with 8-iso-$PGF_{2\alpha}$ in ECs compared to the observed transient RhoA activation induced by VEGF alone [119]. The hypothesis that the TBXA2R takes part in a persistent activation of RhoA is in accordance with a recent publication from Wikström and colleagues [176]. They demonstrated that both receptor subtypes, TBXA2R-α and TBXA2R-β readily induced RhoA activation, which in turn lead to F-actin polymerization in response to the TBXA2R agonist U-46619. In this regard, RhoA and its downstream target Rho kinase are known to play a crucial role in EC motility by reorganization of the cytoskeleton leading to stress fibers formation and focal adhesion turnover. The activation of RhoA and Rho kinase has been shown to inhibit or stimulate cell motility depending on cell type and culture conditions [177, 178, 179]. On one hand, basal activity of Rho kinase is important for cell body contraction and a necessary step in cell migration [152]. On the other hand, persistent activation leads to high levels of cell adhesion to the substratum through pronounced stress fibers-associated focal adhesions, which in turn leads to a decreased focal adhesion turnover and therefore to an inhibition of cell movement [180, 178]. In this line histological analysis performed from our group demonstrated in histological analysis that 8-iso-$PGF_{2\alpha}$ and U-46619 disturbed the VEGF-induced directional stress fiber generation and focal adhesion formation in HDMECs [119]. Furthermore, it has been reported that Rho kinase decreases eNOS expression and may, by this mechanism, additionally counteract VEGF-induced angiogenesis [181]. Therefore, our data suggest that activation of RhoA/Rho kinase by VEGF leads to a basal activation level which results in a stimulation of cell migration, whereas RhoA/Rho kinase activation by iso-

prostanes leads to a robust and persistent activation level resulting in an inhibition of EC migration (Figure 4.3). In this regard VEGF regulated RhoA/Rho kinase activation has been shown to be short lived in ECs *in vitro*, therefore it is unlikely that such short time signaling exerts persistent effects [182].

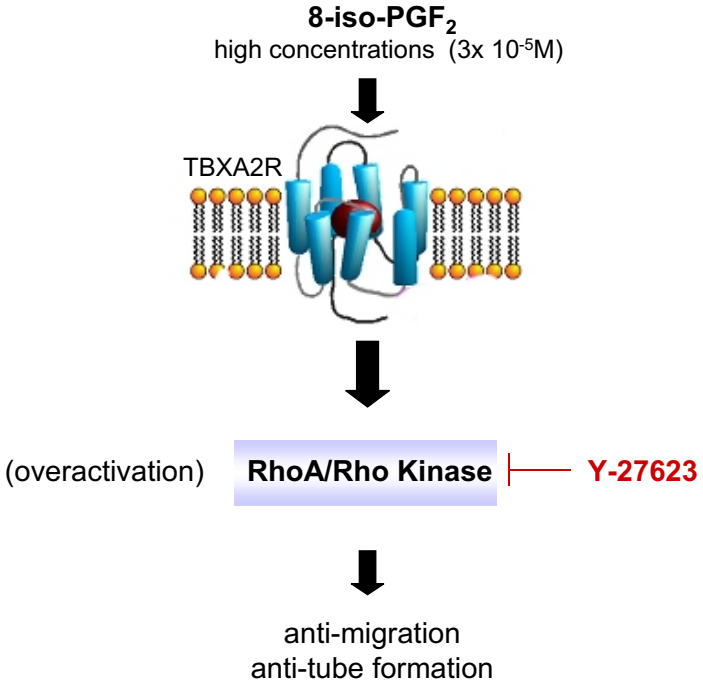

Figure 4.3: 8-iso-PGF$_{2\alpha}$ -mediated signaling in HDMECs. 8-iso-PGF$_{2\alpha}$ induces persistent Rho kinase activation resulting in an inhibition of EC migration and tube formation.

These data have important implications in settings where release of VEGF and increased isoprostanes formation coincide, such as myocardial ischemia in patients suffering from CHD. Indeed the human heart has developed mechanisms to adapt to changes in its environment. One of these mechanisms is the formation of new blood capillaries into ischemic areas to maintain the blood supply and to ensure myocardial function. Animal models have shown that VEGF enhances the development of small coronary arteries supplying ischemic myocardium, resulting in an increase in maximal collateral blood flow delivery [183, 184]. Moreover, another study has shown that patients with acute

ischemia exhibit HIF1α- and VEGF m-RNA in specimens from the affected myocardial territory but not in control specimens [185]. Furthermore, patients exhibited increased VEGF serum levels from day 7-14 after acute myocardial infarction [186]. Hence, VEGF stimulates myocardial collateral vessel formation under ischemia conditions, thus improving the oxygen supply. This work clearly demonstrates that isoprostanes inhibit the VEGF-induced migration and tube formation of ECs. Furthermore, experimental findings of our group have shown that 8-iso-$PGF_{2\alpha}$ also inhibits VEGF-induced cardiac vessel sprouting *in vitro* and angiogenesis in the chick chorioallantoic membrane (CAM) assay *in vivo* [119]. In line with this data we hypothezise that isoprostanes might counteract VEGF-induced revascularization processes during myocardial ischemic conditions and thus exacerbate vessel rarefications within CVD.

4.5 8-iso-$PGF_{2\alpha}$, 8-iso-PGA_2, 8-iso-PGE_2, and Derivatives

The physiological concentration of free 8-iso-$PGF_{2\alpha}$ *in vivo* range between 10^{-11}M to 10^{-10}M in human plasma [187] and is 2- to 3-fold increased in patients suffering from CHD [59, 65]. We observed a significant inhibiting effect of 8-iso-$PGF_{2\alpha}$ on VEGF-induced migration starting at $1{\cdot}10^{-9}$M. However, there are possibly 64 F_2- isoprostanes *in vivo*, and several other isoprostanes families. Beside 8-iso-$PGF_{2\alpha}$, we demonstrated that the isoprostanes 8-iso-PGE_2 and 8-iso-PGA_2 also inhibited the VEGF-induced EC migration and tube formation (Figure 3.12, 3.14). Moreover, we could show that a simultaneous addition of all three isoprostanes resulted in a stronger inhibition of VEGF-induced EC migration and tube formation compared with the inhibition induced by any of the isoprostanes alone, suggesting that isoprostanes can potentiate each other. In addition, recently published data showed that isoketals, which are also formed by the isoprostane pathway via H_2-isoprostanes rearrangement, accumulate in the hypoxic myocardium [60]. Furthermore, 8-iso-$PGF_{2\alpha}$ has also been shown to accumulate in coronary arteries in patient suffering from CHD [58]. These data show that pathological concentrations of isoprostanes are higher than in healthy individuals, with concentrations *in situ* being possibly even higher than systemic concentrations. Consequential, the concentrations used in our experiments are relevant *in vivo*, thus underlining the clinical

relevance of our findings.

In addition, it was demonstrated that 8-iso-PGA_2 decays under physiological conditions into an unknown product X within 24 h, which in turn decomposes into another product Y within further 24 h (Figure 3.15). Interestingly X, but not Y, inhibits the VEGF-induced migration (Figure 3.16/A). In contrast, both products induced an inhibiting effect on VEGF-induced tube formation (Figure 3.16/B). Hence, it can be concluded that X and Y act on different stages of angiogenesis. Whereas compound X inhibits EC migration and therefore EC tube formation as well, compound Y inhibits components which are only required for EC tube formation. These data let infer that isoprostanes could be transformed into unknown decomposition products, which are also biologically active and thus might contribute to anti-angiogenic effects *in vivo*. On the other hand, 8-iso-PGA_2 is a cyclopentenone isoprostane that contains a highly reactive α,β-unsaturated carbonyl group, which readily binds by a Michael-type addition reaction to various thiol-containing molecules such as proteins and GSH. [188]. 8-iso-PGA_2 is known to be generated in large amounts *in vivo* [189], but due to its high reactivity, it can not be detected in its free form. Therefore it is questionable if compound X and Y are generated in appreciable amounts *in vivo*. In rats, the major urinary metabolite of 8-iso-PGA_2 was identified as a N-acetyl cysteine sulfoxide conjugate arising from the conjugation of 8-iso-PGA_2 with GSH and subsequent reduction of the carbonyl group on the prostane ring. Conjugation of cyclopentenone eicosanoids with GSH has been shown to negate their bioactivity, due to the loss of the highly reactive α,β-unsaturated carbonyl group [40]. A similar conjugate could presumably be an appropriate biomarker to assess the 8-iso-PGA_2 production in humans.

The inhibiting effect of 8-iso-$PGF_{2\alpha}$, 8-iso-PGE_2, and 8-iso-PGA_2 on the VEGF-induced migration and tube formation was mimicked by the TBXA2R agonist U-46618 and abolished by the TBXA2R antagonist SQ-29548, indicating that isoprostanes mediate their anti-angiogenic effects via activation of the TBXA2R. It is well described in the literature that isoprostanes mediate their biological activities, at least partially, via activation of the TBXA2R [190]. Otherwise it has been reported that 8-iso-$PGF_{2\alpha}$ induced neuromicrovascular endothelial cell death via a thromboxane A_2-dependent mechanism, which could be prevented by thromboxane A_2 synthase inhibitors [155]. In line with this theory others showed that 8-iso-$PGF_{2\alpha}$ evoked vasoconstriction in the pig retina and brain by stimulating thromboxane A_2 formation from endothelial and astroglial cells [107, 111].

However, in our experiments the synthase inhibitor ozagrel did not alter the inhibiting effect of 8-iso-$PGF_{2\alpha}$, 8-iso-PGE_2, and 8-iso-PGA_2 on VEGF-induced migration (Figure 3.12). These findings show that 8-iso-$PGF_{2\alpha}$ may activate cell-specific effects on distinct cell types. To clarify if the inhibitory effects of 8-iso-$PGF_{2\alpha}$ and U-46619 were attributable to cytotoxic effects in HDMECs, a cytotoxicity assay based on the measuring of LDH activity in supernatant of incubated cells were conducted. The Quantification of the LDH activity revealed that the inhibitory effects of 8-iso-$PGF_{2\alpha}$ and U-46119 were not due to cytotoxic effects in HDMECs, confirming that these effects were mediated via direct activation of the TBXA2R.

4.6 Investigation of 5-Series Isoprostanes

We also investigated the effect of the two 5-series isoprostanes (class VI) 5-F_{2t}-IsoP and 5-epi-5-F_{2t}-IsoP on VEGF-induced migration. Interestingly, only 5-epi-5-F_{2t}-IsoP but not 5-F_{2t}-IsoP inhibited the VEGF-induced migration although they solely differ in the orientation of the hydroxyl group on the side chain (Figure 3.19). This reveals that small differences in structure can have an extensive effect on the biological activity of isoprostanes.

4.7 Phytoprostanes

Whereas the physiological role of phytoprostanes in the life cycle of plants is just beginning to emerge, virtually nothing is known about their effects on human health and diseases. Because F_1-PhytoPs are structurally related to F_2-isoprostanes and their metabolites, which are known to exert potent biological activity, it is assumed that phytoprostanes could exert similar biological activity. We investigated the effect of several phytoprostanes on the VEGF-induced migration of HDMECs as surrogate mammalian cell line. Due to the fact that most of the tested substances inhibited the VEGF-induced migration, we conclude that phytoprostanes might have some bearing on human physiology. Phytoprostanes are formed by nonenzymatic oxidation of linolenate in plants. Notably, the highest phytoprostane levels found thus far were detected in birch pollen, where F_1-PhytoPs levels were found to be 2-fold higher compared to other fresh plant

parts [45]. F_1-PhytoPs are water soluble, therefore, it is feasible that these compounds are extracted from pollen or autoxidized plant dust by biological fluids. Thus it is not excluded that high levels of F_1-PhytoPs found in pollen and autoxidized plant cause tissue irritation in human. Given that F_2-isoprostanes play a role in a range of pulmonary clinical disorders, phytoprostanes might be possibly involved pulmonary pathophysiology, e.g. allergy and asthma. In addition, it has been reported that E_1-PhytoPs, which are also present in aqueous pollen extracts, causes T helper type 2 (Th2) cell polarization and therefore provide one of the initial signals driving the development and perpetuation of Th2-dominated immune response in pollen allergy [191]. Our data give just an idea that some kinds of phytoprostanes are able to exert biological activity in human cells. A possible association between phytoprostanes in pollen and pulmonary disorders remains to be investigated.

4.8 Isoprostanes as Critical Element in the Deregulation of Angiogenesis in Settings of Oxidative Stress

Oxidative stress is closely associated with the pathophysiological settings of CVD. The major source of ROS generation in ECs is the NADPH oxidase, which is activated by several stimuli like growth factors, cytokines, shear stress, and hypoxia. Beside their characteristic feature to oxidize and damage cellular structures, ROS function as signaling molecules that activate redox sensitive kinases, such as Akt and ERK-1/2, as well as transcription factors like HIF-1, which leads to an increased VEGF expression. Not only the VEGF expression but also VEGF signaling is positively regulated by ROS [192, 193]. Thus, these oxidant signaling events may contribute to various physiological responses including cell proliferation, migration, and angiogenesis. In this regard, pathophysiological conditions associated with oxidative stress should rather induce angiogenesis and therefore leading to revascularization and cardiovascular regeneration instead of exerting anti-angiogenic effects. The complex and divergent roles of ROS with regard to pro- and anti-angiogenic actions in cardiovascular injury are not completely understood but it is accepted that low levels of ROS produced in response to growth factors or transient ischemia/hypoxia may initiate angiogenesis, whereas high concentrations of ROS arising

during severe disease state of CVD cause oxidative stress, apoptosis, and cell death. Our results represent a possible signaling pathway which can explain the anti-angiogenic effects of ROS. Advanced CVD causes high ROS levels, which in turn initiate the formation of bioactive isoprostanes by peroxidation of arachidonic acid within the cell membranes. Isoprostanes exert anti-angiogenic effects via robust and persistent RhoA/Rho kinase activation mediated through the TBXA2R. In conclusion, in settings of oxidative stress, such as severe states of CVD, isoprostanes formation seems to be the critical component which deregulate angiogenesis (Figure 4.4).

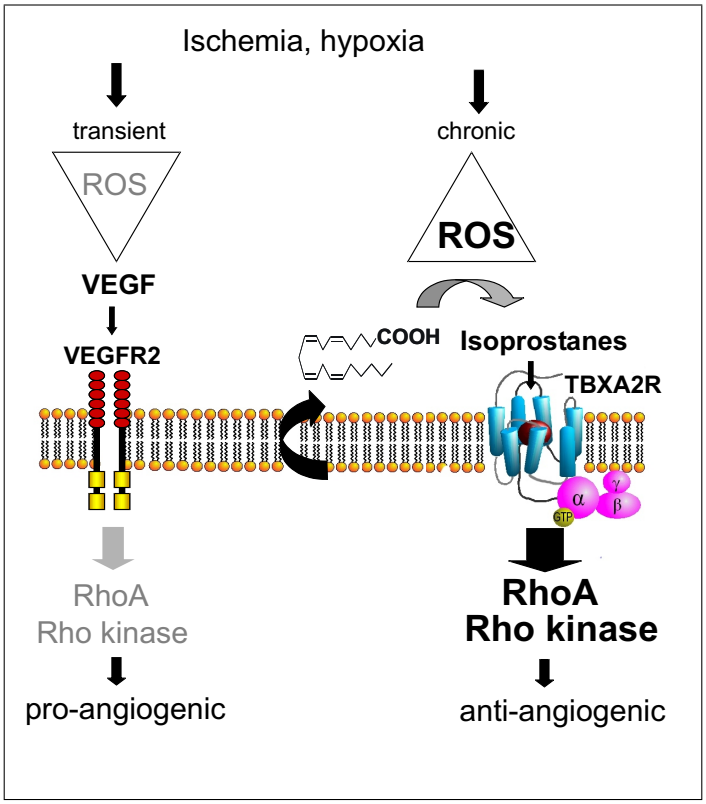

Figure 4.4: ROS-regulated pro- and anti-angiogenic signaling pathway during CVD. During initial stage of CVD transient low levels of ROS effect VEGF-induced angiogenesis via basal activation of RhoA/Rho kinase, which in turn increase endothelial migration and angiogenesis. However, during advanced stages of CVD, ROS levels increased, resulting in lipid oxidation and isoprostane formation. TBXA2R stimulation by isoprostanes leads to a persistent activation of RhoA and its downstream target Rho kinase resulting in decreased cell migration and angiogenesis. Taken from Sauer and Wartenberg, modified [194].

4.9 Conclusion

CVD, which includes myocardial infarction (MI), stroke, and peripheral vascular disease, remains far and away the leading cause of death in the United States and in most developed countries. This work gives insights for new therapeutic strategies for treatment of CVD. CVD comes along with hypoxic myocardium and is associated with oxidative stress, leading to the formation of isoprostanes. We clearly demonstrate that isoprostanes inhibited VEGF-induced angiogenesis *in vitro* and hypothesize therefore that isoprostanes counteract revascularization processes within CVD. Hence, treatment of CVD should support revascularization of the myocardium to improve the oxygen supply. We demonstrated the ability of the Rho kinase inhibitor Y-27623 to counteract the anti-angiogenic effects of isoprostanes. In this regard, the only commercially available Rho kinase inhibitor is fasudil. It is used intravenously for the treatment of cerebral vasospasm in Japan. Clinical studies with fasudil have suggested that the Rho kinase may be useful for the treatment of a wide range of CVD in addition to cerebral vasospasm, including angina pectoris, hypertension, pulmonary hypertension, stroke, and heart failure. These considerations are based on the observations that activated Rho kinase causes VSMC hypercontraction, accelerates VSMC proliferation and migration, and enhances accumulation of inflammatory cells in the adventitia. Those Rho-kinase-mediated cellular responses lead to the development of increased hypertension, pathological angiogenesis and vascular remodeling [195]. In contrast, our results showed that TBXA2-mediated Rho kinase activation causes anti-angiogenic effects in HDMECs, which are reversible by the Rho kinase inhibitor Y-27623, leading to the suggestion that Rho kinase inhibitors might improve revascularization processes in the hypoxic heart during CVD. These findings confirmed that the RhoA/Rho kinase activation can play contrary roles depending on the cell type and conditions. Therefore it is unlikely that a Rho kinase inhibitor can be appropriate to prevent isoprostanes-mediated anti-angiogenic effects during CVD without affecting serious adverse effects.

A further target for CVD treatment applies the prevention of TBXA2R activation by avoiding the formation of its physiological agonist thromboxane A_2. In this regard aspirin has shown to acetylate irreversibly the active site of the COX, which is required for the production of thromboxane A_2, a powerful promoter of aggregation. Although the principle underlying cause of CVD is atherosclerosis, in virtually all cases, the prox-

imate cause is thrombosis. Platelets play a significant role in the developments of all acute occlusive vascular events, which include MI and ischemic stroke. They adhere to damaged endothelial wall lining, promote aggregation of other platelets, and develop as a thrombus. Aspirin inhibits thrombus formation by inhibition of platelet aggregation. Drug therapies with aspirin has demonstrated clear net benefits in the treatment and prevention of CVD [196].

This work clearly demonstrates that TBXA2R activation induces anti-angiogenic effects *in vitro*. In line with this data TBXA2R activation might counteract revascularization processes during myocardial ischemic conditions. The observation that the TBXA2R antagonist SQ-29548 were able to abolish isoprostane-mediated anti-angiogenic effects, leads to the suggestion that a TBXA2R antagonist might be an appropriate tool to medicate CVD. A TBXA2R antagonist would offer advantages over aspirin regarding its specifity and efficiency. Directly inhibition of the TBXA2R by a specific antagonist would not affect COX-dependent processes. Therefore gastrointestinal side effects attributable to aspirin can be avoided. Furthermore a TBXA2R antagonist does not only abolish anti-angiogenic effects but also inhibits thrombus formation.

The TBXA2R express two isoforms in human ECs, the TBXA2R-α and TBXA2R-β [175, 128]. They display critical differences in their signaling and exhibit distinct patterns of expression in a variety of cell/tissue types. Whereas the TBXA2R-α is suggested to play a role in prostacyclin and NO-regulated vascular hemostasis, the physiological role of the TBXA2R-β is not clear yet [170]. Interestingly it has been shown that the TBXA2R-β, but not TBXA2R-α, expression is required for the inhibition of VEGF-induced HUVEC migration [167]. Therefore a specific TBXA2R-β antagonist could present a reconcilable tool to prevent isoprostanes-induced anti-angiogenic effects, without affecting undesirable side effects regarding the vascular hemostasis. On the other hand a specific TBXA2R-β antagonist will not have the ability to inhibit thrombus formation because platelets have shown to express solely the TBXA2R-α subtype. Due to the lack of commercial available specific TBXA2R-α- and TBXA2R-β antagonist, short hairpin RNA-mediated knockdown of the TBXA2R-α in HDMECs could be a possibility to find out which TBXA2R subtype is really required for isoprostanes-mediated anti-angiogenic effects.

5 Summary

Isoprostanes are generated via free radical-induced lipid peroxidation of AA. They are by-products of the formation of PGs from AA, catalysed by the prostaglandin H_2 synthase. Isoprostanes differ from their enzymatic analogues to their regio- and stereochemistry. Theoretically each isoprostane family consist of four regioisomers and 64 stereoisomers. Among the isoprostanes, 8-iso-$PGF_{2\alpha}$ and 8-iso-PGE_2 are prominent due to their TBXA2R-mediated biological activity. The present work reported that the isoprostanes 8-iso-$PGF_{2\alpha}$, 8-iso-PGE_2, and 8-iso-PGA_2 inhibit the VEGF-induced migration and tube formation of ECs *in vitro*, which represent essential steps in angiogenesis. Simultaneous addition of 8-iso-$PGF_{2\alpha}$, 8-iso-PGE_2, and 8-iso-PGA_2 exert a synergistic inhibitory effect on EC migration and tube formation. These data have important implications in settings where release of VEGF and increased isoprostanes formation coincide, such as myocardial ischemia in patients suffering from CHD. Concerning this matter isoprostanes might counteract VEGF-induced neovascularization processes and therefore prevent improved oxygen supply to the hypoxic tissue.

Experiments in the absence of VEGF showed that 8-iso-$PGF_{2\alpha}$ affects basal migration and tube formation of ECs in a biphasic fashion, with a stimulating effect at low concentrations and an inhibitory effect at high concentrations. However, the physiological relevance of these findings remains unclear due to the fact that VEGF is abundant presence *in vivo*.

It could be identified that isoprostanes exert their inhibiting effects on VEGF-induced EC migration and tube formation via activation of the TBXA2R. Further investigations indicate that TBXA2R-induced Rho kinase overactivation might play a key role in isoprostanes-mediated anti-angiogenic effects. This data contribute to an improved understanding of the molecular mechanisms of isoprostanes-mediated anti-angiogenic effects. TBXA2R antagonists or Rho kinase inhibitors may represent new therapeutic

strategies to combat capillary rarefication which has been observed in pathophysiological settings, such as oxidative stress-associated CVD.

Zusammenfassung

Isoprostane werden durch freie radikalische Oxidation der Arachidonsäure gebildet. Sie entstehen in Analogie zu der durch die Prostaglandin H_2-Synthase katalysierten Bildung von Prostaglandinen. Isoprostane unterscheiden sich von den Prostaglandinen hinsichtlich ihrer Regio- und Stereochemie. Theoretisch besteht jede Isoprostanfamilie aus jeweils vier Regio- und 64 Stereoisomeren. Eine besondere Bedeutung kommt den Isoprostanen 8-iso-$PGF_{2\alpha}$ and 8-iso-PGE_2 zu, von denen bekannt ist, dass sie über den Thromboxan-Rezeptor vermittelte, biologische Aktivitäten aufweisen. In dieser Arbeit konnte gezeigt werden, dass die Isoprostane 8-iso-$PGF_{2\alpha}$, 8-iso-PGE_2 and 8-iso-PGA_2 die VEGF-stimulierte Migration und Kapillarröhrchenbildung von Endothelzellen hemmen. Beide Vorgänge stellen physiologisch wichtige Schritte im Rahmen der Angiogenese dar. Zusätzlich konnte ein synergistischer Hemmeffekt bei simulataner Gabe aller drei Isoprostane auf die VEGF-stimulierte Migration und Kapillarröhrchenbildung von Endothelzellen festgestellt werden. Diese Erkenntnisse spielen bei klinischen Zuständen eine Rolle, wo es sowohl zu einer VEGF Freisetzung, als auch zur Bildung von Isoprostanen kommt, wie es beispielsweise im ischämischen Herzgewebe bei Patienten mit Herz-Kreislauferkrankungen der Fall sein kann. Hier könnten Isoprostane die VEGF-stimulierte Neubildung von kollateralen Blutgefäßen, die eine verbesserte Sauerstoffzufuhr des hypoxischen Gewebes gewährleisten würden, unterbinden.

Versuche in Abwesenheit von VEGF zeigten, dass 8-iso-$PGF_{2\alpha}$ sowohl die basale Migration als auch die Kapillarröhrchenbildung von Endothelzellen in einer biphasischen Weise beeinflusste. In niedrigen Konzentrationen zeigte es einen stimulierenden Effekt auf die Migration und Kapillarröhrchenbilung auf, während es in hohen Konzentrationen beide Vorgänge hemmte. Die physiologische Bedeutung dieser Ergebnisse sind schwer

zu deuten, da *in vivo* VEGF ubiquitär in Gefäßsystemen vorkommt.

Es konnte festgestellt werden, dass Isoprostane ihre hemmende Wirkung auf die VEGF-stimulierte Migration und Kapillarröhrchenbildung der Endothelzellen über eine Aktivierung des Thromboxan-Rezeptors ausübten. Außerdem lassen weitere Untersuchungen erkennen, dass eine über den Thromboxan-Rezeptor vermittelte Überaktivierung der Rho-Kinase für die antiangiogenischen Wirkungen der Isoprostane verantwortlich ist. Die Ergebnisse zeigen über welche molekularen Mechanismen Isoprostane ihre antiangiogenischen Effekte ausüben. Sowohl Thromboxan-Rezeptor-Antagonisten als auch Rho-Kinase-Inhibitoren könnten neue therapeutische Angriffspunkte darstellen, um einer kollaterale Rarefikation im ischämischen Herzgewebe entgegenzuwirken.

6 Materials

6.1 Chemicals

Substance Name	Risk and safety statements, when applicable	Company
8-iso-$PGF_{2\alpha}$		Cayman Chemical, Ann Arbor, USA
8-iso-PGA_2		Cayman Chemical, Ann Arbor, USA
8-iso-PGE_2		Cayman Chemical, Ann Arbor, USA
SQ-29548		Cayman Chemical, Ann Arbor, USA
U-46619		Cayman Chemical, Ann Arbor, USA
LY-294002		SIGMA GmbH Steinheim, Germany
Wortmannin		AXXORA DEUTSCHLAND GmbH Lörrach, Germany Steinheim, Germany
PD-98059		SIGMA GmbH Steinheim, Germany
Y-27623		SIGMA GmbH Steinheim, Germany
5-F_{2t}-IsoP		IBMM[1], Montpellier, France
5-epi-5-F_{2t}-IsoP		IBMM[1], Montpellier, France
B_1-PhytoP-I		IBMM[1], Montpellier, France
ent-B_1-PhytoPs-I		IBMM[1], Montpellier, France
B_1-PhytoP-II		IBMM[1], Montpellier, France
ent-B_1-PhytoP-II		IBMM[1], Montpellier, France
F_1-PhytoP-I		IBMM[1], Montpellier, France
ent-F_1-PhytoP-I		IBMM[1], Montpellier, France
ent-16-epi-F_1-PhytoP-I		IBMM[1], Montpellier, France
F_1-PhytoP-II		IBMM[1], Montpellier, France
9-epi-F_1-PhytoP-II		IBMM[1], Montpellier, France
ent-F_1-PhytoP-II		IBMM[1], Montpellier, France
ent-9-epi-F_1-PhytoP-II		IBMM[1], Montpellier, France

[1]In cooperation with Durant T., Institut des Biomolecules Max Mousseron

Substance Name	Risk and safety statements, when applicable	Company
2-Mercaptoethanol	R:22-24-34-51/53 S:26-36/37/39-45-61	SIGMA GmbH Steinheim, Germany
2-Propanol	R: 11-36-67 S: 7-16-24/25-26	Merck KgaA Darmstadt, Germany
40% bis-Acrylamide solution	R: 23/24/25-45-46-48 S: 36/37/39-45-60	Bio-Rad Laboratories Hercules, USA
Acetonitrile (CH_3CN)	R:11-20/21/22-36 S:16-36/37	Merck KgaA, Darmstadt, Germany
AH-6809		SIGMA GmbH Steinheim, Germany
Ammonium persulfate (APS)	R:8-22-36/37/38-42/43 S:22-24-26-37	Bio-Rad Laboratories Hercules, USA
Aqua ad injectabilia		Baxter Unterschleissheim, Germany
BCECF-AM		SIGMA GmbH Steinheim, Germany
Bio-Rad Precision Plus Protein Standards		Bio-Rad Laboratories Hercules, USA
Bio-Rad Protein Assay	R:10-22/34-39/23/24/25 S:7-26-34	Bio-Rad Laboratories Hercules, USA
Bovine serum albumin (BSA)		Sigma GmbH Steinheim, Germany
Bromphenol blue		
Developing solution G 150		AGFA-Geraert Leverkusen, Germany
Cytotoxicity Detection Kit		Roche Pharma AG Grenzach-Wyhlen, Germany
Dimethyl sulfoxide (DMSO)	R:36/37/38 S:23-26-36	SIGMA GmbH Steinheim, Germany
ECL Western Blotting Detection Reagents		Amersham Biosciences Little Chalfont, England
Ethanol 98%	R:11 S:16-7	Merck KgaA Darmstadt, Germany
Ethylenediaminetetraacetic- acid (EDTA)	R: 36-52/53 S: 26-61	SIGMA GmbH Steinheim, Germany

Substance Name	Risk and safety statements, when applicable	Company
Fixer G350		AGFA-Geraert Leverkusen, Germany
Glycerol		Merck KgaA Darmstadt, Germany
Glycin		Carl Roth GmbH Co Karlsruhe, Germany
Dipotassium phosphate ($K_2HPO_4 \cdot 3H_2O$)		Merck KgaA Darmstadt, Germany
Matrigel^{TM}		BD Biosciences Bedford, USA
Methanol	R:11-23/24/25-39 S:7-16-36/37-45	Merck KgaA Darmstadt, Germany
Monosodium phosphate (NaH_2PO_4)		Merck KgaA Darmstadt, Germany
Na_3VO_4		
Nonidet P-40 substitute	R:37-41 S:26-39	SIGMA GmbH Steinheim, Germany
O-Methylhydroxylamine-hydrochloride	R:21/22-34-43 S:26-36/37/39-45	SIGMA GmbH Steinheim, Germany
Ozagrel		Cayman Chemical, Ann Arbor, USA
PathScan Multiplex Western Cocktail		New England Biolabs GmbH Frankfurt am Main, Germany
Phosphate buffered saline (PBS) Dulbecco powder	S:22-24/25	Biochrom AG Berlin, Germany
Phospho-eNOS Antibody		New England Biolabs GmbH Frankfurt am Main, Germany
Pierce ECL substrate		Pierce, Rockford, USA
Ponceau S red staining solution	R:36/37/38-51/53 S:26-36	SIGMA GmbH Steinheim, Germany
VEGF		PromoCell Heidelberg, Germany
Potassium chloride (KCL)		Merck KgaA Darmstadt, Germany

Substance Name	Risk and safety statements, when applicable	Company
Potassium dihydrogen phosphate (KH_2PO_4)		Merck KgaA Darmstadt, Germany
Sodium dodecyl sulfate (SDS)	R:22-36/38 S:26-24/25	SIGMA GmbH Steinheim, Germany
Tetramethylethylendiamine (TEMED)	R:11-20/22-34 S:16-26-36/37/39-45-60	Merck KgaA Darmstadt, Germany
Tris salt		SIGMA Steinheim, Germany
TritonX-100	R:22-41-51/53 S:26-36/39-61	Merck KgaA Darmstadt, Germany
Trypsin		
Tween 20		SIGMA GmH Steinheim, Germany

6.2 Cells, Cell Culture Media and Consumable

Product	Company
Diff-Quick®	Medion Diagnostics GmbH Düdingen, Germany
EDTA 0.02%	SIGMA GmbH Steinheim, Germany
Endothelial Cell Basal Medium MV	PromoCell, Heidelberg, Germany
Endothelial Cell Growth Medium MV	PromoCell, Heidelberg, Germany
Fetal bovine serum (FBS) heat inactivated	Invitrogen Grand Island, USA
Gelatin 2% Solution f. Bovine Skin	SIGMA GmbH Steinheim, Germany
HCAECs	PromoCell, Heidelberg, Germany
HDMECs	PromoCell, Heidelberg, Germany
Vitrogen-100 type I collagen	Angiotech BioMaterials Palo Alto, USA

6.3 Consumables Supplies

Product	Company
1,5- and 2-mL Eppis	Eppendorf AG, Hamburg, Germany
10-, 100-, 1000- and 5000-µL pipettes	Eppendorf AG, Hamburg, Germany
10-, 100- and 1000-µL pipette tips	Sarstedt AG Co, Nümbrecht, Germany
15- and 50-mL Falcon tubes	Sarstedt AG Co, Nümbrecht, Germany
25- and 75-cm^2 cell culture flasks	Sarstedt AG Co, Nümbrecht, Germany
5000-µL pipette tips	Eppendorf AG, Hamburg, Germany
6- and 48-well plates	Nunc, Roskilde, Denmark
Blotting paper	Whatman, Dassel, Germany
Cell Scraper	Sarstedt AG Co, Nümbrecht, Germany
Curix X-ray film cassettes	Agfa, Köln, Germany
Cuvettes for photometry	Sarstedt AG Co, Nümbrecht, Germany
High performance chemiluminescence film	Amersham Biosciences, Little Chalfont, England
Latex Gloves	Kimberly-Clark, Zaventem, Belgium
Molecular sieve beads	Merck KGaA, Darmstadt, Germany
Nitrocellulose transfer membrane	Schleicher Schuell BioScience GmbH, Dassel Germany
Pasteur Pipettes	Brand, Wertheim, Germany
Sterile filer (0.22, 0.45 µM)	Qualilab, Bruchsal, Germany
Polycarbonate filters	NeuroProbe, Inc Gaithersburg, USA
100-5C18 Nucleosil column	Macherey Nagel GmbH& Co KG Düren, Germany

6.4 Equipment

Apparatus	Company
Boyden Chamber	Neuro Probe, Inc., Gaithersburg, USA
-20 °C Freezer	Liebherr, Rostock, Germany
-80 °C Freezer	Kryotec, Hamburg, Germany
96-well plate reader, Sunrise	Tecan, Crailsheim, Germany
Accu jet pipetting aid	Eppendorf AG, Hamburg, Germany
AxioCam PRc 5 camera	Zeiss, Göttingen, Germany
Benchtop centrifuge Rotina 35 R	Hettich, Tuttlingen, Germany
ChemGenius^2 Bio-imaging System	Syngene, Cambridge, UK
GC-MS	Varian, Darmstadt, Germany
Eppendorf tubes shaker Thermomixer Compact	Eppendorf AG, Hamburg, Germany
Hood with laminar vertical airflow, HPLC	Heraeus, Hanau, Switzerland Dionex, Idstein, Germany
LaminAir HB 2448	
Lambda 2S Photometer, for protein quantification	PerkinElmer, Jügesheim, Germany
LC-MS	Varian, Darmstadt, Germany
Micro centrifuge 5415 R	Eppendorf AG, Hamburg, Germany
Microscope, Axiovert 25	Zeiss, Oberkochen, Germany
pH-meter, digital	Knick, Berlin, Germany
Refrigerator	Liebherr, Rostock, Germany
Ultra-Pure Water System Milli-Q Plus	Millipore, Schwalbach, Germany
Vertical and Horizontal System for Electrophoresis with Power Supply Unit	Bio-Rad Laboratories, Hercules, USA
Vortexer, Reax top	Heidolph, Schwabach, Germany
CO_2 Incubator HERACell	Thermo Electron Corporation, Langenselbold, Germany

6.5 Softwares

Software
GraphPad Prism 4
LSM Image Browser v. 3.2.0, Zeiss
GeneSnap 6.02, Syngene
AxioVision 4.3.0, Zeiss

6.6 Buffer and Solutions Recipes

Lysis buffer

Nonidet P-40 Substitute	10 mL
Triton X-100	10 mL
Tris base	1.2 g
Potassium chloride KCL	186 mg
Sodium chloride NaCL	8.7 g
Glycerol phosphate	6.48 g
Sodium fluoride NaF	2.1 g
Sodium orthovanadate Na_3VO_4	183.9 g
Protease Inhibitor Cocktail	1 µL
Aqua ad injectabilia	q.s. 1.000 mL

Separating gel

bis-Acrylamide 40 % solution	2.53 mL
Aqua ad injectabilia	5.48 mL
Tris 2 M pH 8.8	2.0 mL
SDS 20 %	50 µL
TEMED	5 µL
APS 10 % (m/v) solution	50 µL

Collecting gel

bis-Acrylamide 40 % solution	0.6 mL
Aqua ad injectabiliba	3.8 mL
Tris 0.5 M, pH 8.8	1.6 mL
SDS 20 %	30 µL
TEMED	6 µL
APS 10% (m/v) solution	30 µL

1x Phosphate buffered saline (PBS)

according to manufacturer‘s instructions

3x Lämmli solution

1 M Tris	18.75 mL
Glycerol	30 mL
SDS %20	30 mL
2-Mercaptoethanol	15 mL
Bromphenol blue	2 mg

5x Running buffer

Tris base	15 g
Glycin	72 g
SDS 20 %	25 mL
Ultra-pure water	q.s. 1 L

10x Transfer puffer

Tris base	30.2 g
Glycin	144.2 g
SDS 20 %	10 mL
Ultra-pure water	q.s. 1 L

1x Transfer puffer

10x Transfer puffer	100 mL
Methanol	100 mL
Ultra-pure water	q.s. 1 L

10x Tris-buffered saline (TBS) buffer

Tris base	24.2 g
NaCl	80.0 g
Ultra-pure water	q.s. 1 L
Adjust pH to 7.6 with 1N hydrochloric acid HCL	

1x TBS-Tween (TBS-T) buffer

10x TBS buffer	100 mL
Tween 20	1 mL
Ultra-pure water	q.s. 1 L

Basal Medium

0.1% BSA in Endothelium Cell Basal Medium MV

Growth Medium

Growth factors supplement added in Endothelium Cell Growth Medium MV

7 Appendix

7.1 Abbreviations

8-iso-$PGF_{2\alpha}$	8-iso-Prostaglandin $F_{2\alpha}$
8-iso-PGE_2	8-iso-Prostaglandin E_2
8-iso-PGA_2	8-iso-Prostaglandin A_2
AA	arachidonic acid
AC	adenylyl cyclase
AHR	airway hyperresponsiveness
AP-1	activating protein-1
BSA	bovine serum albumin
cAMP	cyclic adenosine monophosphate
Cdc42	cell division cycle
CHD	coronary heart disease
COX	cyclooxygenase
CVD	cardiovascular disease
DAG	diacylglycerol
DHA	docosahexaenoic acid
DNA	deoxyribonucleic acid
EC	endothelial cell
ECL	enhanced chemoluminescent
ECM	extracellular matrix
EDTA	ethylendiaminetetraaceticacid
e.g.	*exempli gratia* (for example)
eNOS	endothelial nitric oxide synthase
ERK-1/2	extra-regulated protein kinase-1/2
FBS	fetal bovine serum
FAK	focal adhesion kinase
F-actin	filament-actin
GAPs	GTPase-activating proteins
GC-MS	gas chromatography-mass spectrometry
GC-MS/MS	gas chromatography-tandem mass spectrometry
GDI	guanine nucleotide dissociation inhibitors
GEF	guanine nucleotide exchange factors
g	gram
GPX	glutathionperoxidase

GRed	glutathione reductase
GSH	glutathione
GSSG	Glutathiondisulid
GDP	guanosinediphosphate
GTP	guanosinetriphosphate
h	hours
HCAEC	Human coronary artery endothelial cell
HDMEC	Human dermal microvascular endothelial cell
HIF	hypoxia inducible factor
HPETE	hydroperoxyeicosatetraenoic acid
HPLC	high-performance liquid chromatography
HUVEC	human umbilical vein endothelial cells
IBOP	[15-(1a,2b(5Z),3a-(1E,3S),4a)]-7-[3-hydroxy-4-(p-iodophenoxy)-1-butenyl-7-oxabicycloheptenoic acid
i.e.	*id est* (that is)
IsoP	isoprostane
IP3	inositol 1,4,5-triphosphate
IUPAC	International Union of Pure and Applied Chemistry
LC-MS	liquid chromatography-mass spectrometry
LC-MS/MS	liquid chromatography-tandem mass spectrometry
LDL	low-density lipoprotein
MAPK	mitogen-activated protein kinase
MCL	myosin light chain
MCLK	myosin light chain kinase
MDA	malondialdehyde
MEK-1/2	MAPK ERK Kinase-1/2
mg	milligram
mL	milliliter
min	minutes
µg	microgram
µL	microliter
µm	micrometer
µM	micromol
NADPH	Nicotinamide adenine dinucleotide phosphate
NF-kB	nuclear factor kB
°C	grad Celsius
NO	nitric oxide
ng	nanogram
p115-RhoGEF	p115 guanine nucleotide exchange factor for Rho

PBS	phosphate buffered saline
PhytoP	phytoprostane
PG	prostaglandin
PI3K	phosphatidylinositol 3-kinase
KDR	kinase insert domain-containing receptor
PKC	protein kinase C
PDGF	platelate derived growth factor
PLC	phospholipase C
PUFA	polyunsaturated fatty acids
q.s.	*quantum satis* (up to)
Rac1	ras-related C3 botulinum substrate
Raf-1	rat fibrosarcoma
Ras	rat sarcoma
RCF	relative centrifugal force
Rho	Ras homologues
RTKs	receptor tyrosine kinases
RNA, mRNA	ribonucleic acid, messengerRNA
ROCK	Rho-associated kinase
ROS	reactive oxygen species
SD	standard deviation
SDS	sodium dodecyl sulfate
sec	seconds
SOD	superoxide dismutase
SQ-29548	[1S-[1α,2α(Z),3α,4α]]-7-[3-[[2 [(Phenylamino) carbonal]hydrazino]methyl]-7-oxabicyclo[2.2.1] hept-2-yl-]-5-heptanoic acid
TBS, TBS-T	Tris-buffered saline, TBS-Tween
TEMED	Tetramethylethylenediamine
TBA	2-thiobarbituric acid
TBARS	thiobarbituric acid reactive substances
TBXA2R	thromboxane A_2 receptor
U-46619	9„11-dideoxy-9α,11α-methanoepoxy
UV	ultra violet
v	volume
VEGF	vascular endothelial growth factor
vs.	versus
VSMC	vascular smooth muscle cell

7.2 Risk and safety phrases

R-phrases

R1: Explosive when dry

R2: Risk of explosion by shock, friction fire or other sources of ignition

R3: Extreme risk of explosion by shock friction, fire or other sources of ignition

R4: Forms very sensitive explosive metallic compounds

R5: Heating may cause an explosion

R6: Explosive with or without contact with air

R7: May cause fire

R8: Contact with combustible material may cause fire

R9: Explosive when mixed with combustible material

R10: Flammable

R11: Highly flammable

R12: Extremely flammable

R13: Extremely flammable liquefied gas

R14: Reacts violently with water

R15: Contact with water liberates highly flammable gases

R16: Explosive when mixed with oxidizing substances

R17: Spontaneously flammable in air

R18: In use, may form flammable/explosive vapor-air mixture

R19: May form explosive peroxides

R20: Harmful by inhalation

R21: Harmful in contact with skin

R22: Harmful if swallowed

R23: Toxic by inhalation

R24: Toxic in contact with skin

R25: Toxic if swallowed

R26: Very toxic by inhalation

R27: Very toxic in contact with skin

R28: Very toxic if swallowed

R29: Contact with water liberates toxic gas

R30: Can become highly flammable in use

R31: Contact with acids liberates toxic gas

R32: Contact with acids liberates very toxic gas

R33: Danger of cumulative effects

R34: Causes burns

R35: Causes severe burns

R36: Irritating to eyes

R37: Irritating to respiratory system

R38: Irritating to skin

R39: Danger of very serious irreversible effects

R40: Possible risk of irreversible effects

R41: Risk of serious damage to eyes

R42: May cause sensitization by inhalation

R43: May cause sensitization by skin contact

R44: Risk of explosion if heated under confinement

R45: May cause cancer

R46: May cause heritable genetic damage

R47: May cause birth defect

R48: Danger of serious damage to health by prolonged exposure

R49: May cause cancer by inhalation

R50: Very toxic to aquatic organisms

R51: Toxic to aquatic organisms

R52: Harmful to aquatic organisms

R53: May cause long-term adverse effects in the aquatic environment

R54: Toxic to flora

R55: Toxic to fauna

R56: Toxic to soil organisms

R57: Toxic to bees

R58: May cause long-term adverse effects in the environment

R59: Dangerous to the ozone layer

R60: May impair fertility

R61: May cause harm to the unborn child

R62: Possible risk of impaired fertility

R63: Possible risk of harm to the unborn child

R64: May cause harm to breastfed babies

R65: Harmful: may cause lung damage if swallowed

R66: Repeated exposure may cause skin dryness or cracking

R67: Vapors may cause drowsiness and dizziness

R68: Possible risk of irreversible effects

S-phrases

S1: Keep locked up

S2: Keep out of reach of children

S3: Keep in a cool place

S4: Keep away from living quarters

S5: Keep contents under ... (appropriate liquid to be specified by the manufacturer)

S6: Keep under ... (inert gas to be specified by the manufacturer)

S7: Keep container tightly closed

S8: Keep container dry

S9: Keep container in a well ventilated place

S12: Do not keep the container sealed

S13: Keep away from food, drink and animal feeding stuffs

S14: Keep away from ... (incompatible materials to be indicated by the manufacturer)

S15: Keep away from heat

S16: Keep away from sources of ignition-No Smoking

S17: Keep away from combustible material

S18: Handle and open container with care

S20: When using do not eat or drink

S21: When using, do not smoke

S22: Do not breathe dust

S23: Do not breathe gas/fumes/vapor/spray (appropriate wording to be specified by manufacturer)

S24: Avoid contact with skin

S25: Avoid contact with eyes

S26: In case of contact with eyes, rinse immediately with plenty of water and see medical advice S27: Take off immediately all contaminated clothing

S28: After contact with skin, wash immediately with plenty of ... (to be specified by The manufacturer) S29: Do not empty into drains

S30: Never add water to this product

S33: Take precautionary measures against static discharges

S34: Avoid shock and friction

S35: This material and its container must be disposed of in a safe way

S36: Wear suitable protective clothing

S37: Wear suitable gloves

S38: In case of insufficient ventilation, wear suitable respiratory equipment

S39: Wear eye/face protection

S40: To clean the floor and all objects contaminated by this material use (to be specified by the manufacturer)

S41: In case of fire and/or explosion do not breathe fumes

S42: During fumigation/spraying wear suitable respiratory equipment (appropriate wording to be specified by the manufacturer)

S43: In case of fire, use ... (indicate in the space the precise type of fire fighting equipment. If water increases the risk, add "never use water")

S44: If you feel unwell, seek medical advice (show the label where possible)

S45: In case of accident or if you feel unwell, seek medical advice immediately (show the label where possible)

S46: If swallowed, seek medical advice immediately and show the container or label

S47: Keep at temperature not exceeding ... °C (to be specified by the manufacturer)

S48: Keep wetted with ... (appropriate material to be specified by the manufacturer)

S49: Keep only in the original container

S50: Do not mix with ... (to be specified by the manufacturer)

S51: Use only in well-ventilated areas

S52: Not recommended for interior use on large surface areas

S53: Avoid exposure - obtain special instructions before use

S54: Obtain the consent of pollution control authorities before discharging to waste water treatment plants

S55: Treat using the best available techniques before discharge into drains or the Aquatic environment

S56: Do not discharge into drains or the environment; dispose to an authorized waste collection point

S57: Use appropriate containment to avoid environmental contamination

S58: To be disposed of as hazardous waste

S59: Refer to manufacturer/supplier for information on recovery/recycling

S60: This material and/or its container must be disposed of as hazardous waste

S61: Avoid release to the environment. Refer to special instructions / safety data sheet

S62: If swallowed, do not induce vomiting: seek medical advice immediately and Show the container label

S63: In case of accident by inhalation: remove casualty to fresh air and keep at rest

S64: If swallowed, rinse mouth with water(only if the person is conscious)

7.3 Curriculum Vitae

Personal data:

First name:	Anke
Last name:	Gnann
Date of birth:	21.07.1978
City of birth:	Marburg

Education:

09 / 1988 - 06 / 1997	Gymnasium Oedeme, Lüneburg
06 / 1997	Abitur
10 / 1998 - 09 / 2002	Study of pharmacy at the Philipps University of Marburg
08 / 2000	1. state examination
09 / 2002	2. state examination
12 / 2003	3. state examination
06 / 2003 - 11 / 2003	Internship at the Viereck Apotheke, Berlin
11 / 2002 - 05 / 2003	Internship at the Arcaden Apotheke, Berlin
Since 02.05	PhD student at the Institute of Experimental and Clinical Pharmacology and Toxicology, University Medical Center Hamburg-Eppendorf

Work experience:

01 / 2007 - 07 / 2008	St. Johannis Apotheke, Hamburg
09 / 2004 - 12 / 2007	Michel Apotheke, Hamburg
04 / 2004 - 08 / 2004	Förster Apotheke, Hamburg

7.4 Publications and congress participations

7.4.1 Publications

Benndorf RA, Schwedhelm E, **Gnann A**, Taheri R, Kom G, Didié M, Steenpass A, Ergün S, Böger RH. Isoprostanes inhibit vascular endothelial growth factor-induced endothelial cell migration, tube formation, and cardiac vessel sprouting in vitro, as well as angiogenesis in vivo via activation of the thromboxane A(2) receptor: a potential link between oxidative stress and impaired angiogenesis. Circ Res. 2008 Oct 24;103(9):1037-46.

7.4.2 Congress participations

Gnann A, Benndorf RA, Schwedhelm E, Kom GD, Böger RH. Isoprostanes inhibit in vitro migration and tube formation of endothelial cells via the thromboxane receptor. Journal of Vascular Research, 2005; 42 (S2): II/6. 3rd European Meeting of Vascular Biology and Medicine, Hamburg, September 28-30, 2005.

Benndorf R, Schwedhelm E, **Gnann A**, Kom GD, Ergün S, Böger RH. Isoprostane inhibieren die Migration und in vitro-Kapillarröhrenbildung von humanen Endothelzellen über den Thromboxan A2-Rezeptor. Z Kardiol 2005; 94 (S1), V582. 71st Spring Meeting of the German Society for Cardiology and Cardiovascular Research, Mannheim, March 31-April 02, 2005

Gnann A, Benndorf RA, Schwedhelm E, Kom GD, Ergün S, Böger RH. Isoprostanes inhibit migration and in vitro tube formation of endothelial cells via the thromboxane A2 receptor. Naunyn Schmiedeberg's Archives of pharmacology 2005; 371 (S1): R24. 46th Spring Meeting of the German society for experimental and clinical pharmacology and toxicology, Mainz, March 15-17, 2005.

Gnann A, Benndorf RA, Schwedhelm E, Kom GD, Steenpaß A, Ergün S, Didie M, Böger RH. Isoprostane hemmen in vitro die die VEGF-induzierte Migration und Gefäßbildung von Endothelzellen über eine Aktivierung des Thromboxanrezeptors. Z Kardiol 2008; V1603. 74st Spring Meeting of the German Society for Cardiology and Cardiovascular Research, Mannheim, March 27-March 29, 2008

7.5 Annexes

Statement

I herewith declare on oath that the work reported in the thesis submitted at the University of Hamburg and entitled

The influence of isoprostanes on Angiogenesis

was realized in person in the Clinical Pharmacology of the Institute of Experimental and Clinical Pharmacology and Toxicology under the supervision of Prof. Rainer H. Böger and that no other resources than those therein listed were used in the writing process of the mentioned thesis.

I furthermore certify that neither the present nor another thesis was submitted as doctoral thesis in another national or in a foreign university.

Hamburg, March 06, 2009

Anke Gnann

7.6 Acknowledgement

I thank Prof. Dr. Böger who gave me the opportunity to perform my Ph.D. research in the Institute of Experimental and Clinical Pharmacology and Toxicology of the University Medical Center Hamburg-Eppendorf. I thank him for supervising and supporting me during my thesis.

I thank Prof. Dr. Duchstein for accepting the supervision of my Ph.D. thesis vis-à-vis the Department of Chemistry of the University of Hamburg.

Thanks to Dr. Edzard Schwedhelm, Dr. Ralf Benndorf, Dr. Thomas Rau, Anna Steenpaß, Mariola Kastner, Cornelia Woermann, my fellow students and all the staff at the Institute for the permanent willingness to exchange ideas and practical tips. I particularly thank Dr. Edzard Schwedhelm for his knowledgeability and his availability.

Thanks to Dr. Ghainsom Kom for proofreading my thesis.

Last but not least, I thank my family, my parents Monika and Wilfried, my brother Volker, my sister Heike, and Stephan and Ines for their unconditional and constant support.

Bibliography

[1] W. A. Pryor. Oxy-radicals and related species: their formation, lifetimes, and reactions. *Annu Rev Physiol*, 48:657–67, 1986.

[2] I. Fridovich. Superoxide radical: an endogenous toxicant. *Annu Rev Pharmacol Toxicol*, 23:239–57, 1983.

[3] B. Halliwell and J. M. Gutteridge. The importance of free radicals and catalytic metal ions in human diseases. *Mol Aspects Med*, 8(2):89–193, 1985.

[4] C. Rice-Evans and R. Burdon. Free radical-lipid interactions and their pathological consequences. *Prog Lipid Res*, 32(1):71–110, 1993.

[5] S. Grimm and P. A. Baeuerle. The inducible transcription factor NF-kappa B: structure-function relationship of its protein subunits. *Biochem J*, 290 (Pt 2):297–308, 1993.

[6] B. Halliwell. How to characterize a biological antioxidant. *Free Radic Res Commun*, 9(1):1–32, 1990.

[7] H. Sies. Strategies of antioxidant defense. *Eur J Biochem*, 215(2):213–9, 1993.

[8] G. W. Burton, A. Joyce, and K. U. Ingold. Is vitamin E the only lipid-soluble, chain-breaking antioxidant in human blood plasma and erythrocyte membranes? *Arch Biochem Biophys*, 221(1):281–90, 1983.

[9] L. J. Martin. DNA damage and repair: relevance to mechanisms of neurodegeneration. *J Neuropathol Exp Neurol*, 67(5):377–87, 2008.

[10] M. K. Shigenaga, C. J. Gimeno, and B. N. Ames. Urinary 8-hydroxy-2'-deoxyguanosine as a biological marker of in vivo oxidative DNA damage. *Proc Natl Acad Sci U S A*, 86(24):9697–701, 1989.

[11] M. F. Beal. Oxidatively modified proteins in aging and disease. *Free Radic Biol Med*, 32(9):797–803, 2002.

[12] C. D. Smith, J. M. Carney, P. E. Starke-Reed, C. N. Oliver, E. R. Stadtman, R. A. Floyd, and W. R. Markesbery. Excess brain protein oxidation and enzyme dysfunction in normal aging and in Alzheimer disease. *Proc Natl Acad Sci U S A*, 88(23):10540–3, 1991.

[13] A. Yoritaka, N. Hattori, K. Uchida, M. Tanaka, E. R. Stadtman, and Y. Mizuno. Immunohistochemical detection of 4-hydroxynonenal protein adducts in Parkinson disease. *Proc Natl Acad Sci U S A*, 93(7):2696–701, 1996.

[14] B. Halliwell and S. Chirico. Lipid peroxidation: its mechanism, measurement, and significance. *Am J Clin Nutr*, 57(5 Suppl):715S–724S; discussion 724S–725S, 1993.

[15] C. A. Riely, G. Cohen, and M. Lieberman. Ethane evolution: a new index of lipid peroxidation. *Science*, 183(121):208–10, 1974.

[16] L. L. de Zwart, J. H. Meerman, J. N. Commandeur, and N. P. Vermeulen. Biomarkers of free radical damage applications in experimental animals and in humans. *Free Radic Biol Med*, 26(1-2):202–26, 1999.

[17] D. H. Nugteren, D. A. Van Dorp, S. Bergstrom, M. Hamberg, and B. Samuelsson. Absolute configuration of the prostaglandins. *Nature*, 212(5057):38–9, 1966.

[18] W. A. Pryor, J. P. Stanley, and E. Blair. Autoxidation of polyunsaturated fatty acids: II. A suggested mechanism for the formation of TBA-reactive materials from prostaglandin-like endoperoxides. *Lipids*, 11(5):370–9, 1976.

[19] N. A. Porter and M. O. Funk. Letter: Peroxy radical cyclization as a model for prostaglandin biosynthesis. *J Org Chem*, 40(24):3614–5, 1975.

[20] J. D. Morrow, K. E. Hill, R. F. Burk, T. M. Nammour, K. F. Badr, and 2nd Roberts, L. J. A series of prostaglandin F2-like compounds are produced in vivo in humans by a non-cyclooxygenase, free radical-catalyzed mechanism. *Proc Natl Acad Sci U S A*, 87(23):9383–7, 1990.

[21] J. D. Morrow, T. A. Minton, K. F. Badr, and 2nd Roberts, L. J. Evidence that the F2-isoprostane, 8-epi-prostaglandin F2 alpha, is formed in vivo. *Biochim Biophys Acta*, 1210(2):244–8, 1994.

[22] J. D. Morrow and L. J. Roberts. The isoprostanes: unique bioactive products of lipid peroxidation. *Prog Lipid Res*, 36(1):1–21, 1997.

[23] T. J. Montine, K. S. Montine, E. E. Reich, E. S. Terry, N. A. Porter, and J. D. Morrow. Antioxidants significantly affect the formation of different classes of isoprostanes and neuroprostanes in rat cerebral synaptosomes. *Biochem Pharmacol*, 65(4):611–7, 2003.

[24] Y. Chen, J. D. Morrow, and 2nd Roberts, L. J. Formation of reactive cyclopentenone compounds in vivo as products of the isoprostane pathway. *J Biol Chem*, 274(16):10863–8, 1999.

[25] J. Rokach, S. P. Khanapure, S. W. Hwang, M. Adiyaman, J. A. Lawson, and G. A. FitzGerald. Nomenclature of isoprostanes: a proposal. *Prostaglandins*, 54(6):853–73, 1997.

[26] D. F. Taber, J. D. Morrow, and 2nd Roberts, L. J. A nomenclature system for the isoprostanes. *Prostaglandins*, 53(2):63–7, 1997.

[27] 2nd Roberts, L. J., T. J. Montine, W. R. Markesbery, A. R. Tapper, P. Hardy, S. Chemtob, W. D. Dettbarn, and J. D. Morrow. Formation of isoprostane-like compounds (neuroprostanes) in vivo from docosahexaenoic acid. *J Biol Chem*, 273(22):13605–12, 1998.

[28] R. J. Waugh, J. D. Morrow, 2nd Roberts, L. J., and R. C. Murphy. Identification and relative quantitation of F2-isoprostane regioisomers formed in vivo in the rat. *Free Radic Biol Med*, 23(6):943–54, 1997.

[29] 2nd Roberts, L. J. and J. D. Morrow. Products of the isoprostane pathway: unique bioactive compounds and markers of lipid peroxidation. *Cell Mol Life Sci*, 59(5):808–20, 2002.

[30] H. Yin, J. D. Morrow, and N. A. Porter. Identification of a novel class of endoperoxides from arachidonate autoxidation. *J Biol Chem*, 279(5):3766–76, 2004.

[31] H. Yin, C. M. Havrilla, J. D. Morrow, and N. A. Porter. Formation of isoprostane bicyclic endoperoxides from the autoxidation of cholesteryl arachidonate. *J Am Chem Soc*, 124(26):7745–54, 2002.

[32] D. Pratico, J. A. Lawson, and G. A. FitzGerald. Cyclooxygenase-dependent forma-

tion of the isoprostane, 8-epi prostaglandin F2 alpha. *J Biol Chem*, 270(17):9800–8, 1995.

[33] D. Pratico, O. P. Barry, J. A. Lawson, M. Adiyaman, S. W. Hwang, S. P. Khanapure, L. Iuliano, J. Rokach, and G. A. FitzGerald. IPF2alpha-I: an index of lipid peroxidation in humans. *Proc Natl Acad Sci U S A*, 95(7):3449–54, 1998.

[34] M. Adiyaman, J. A. Lawson, S. P. Khanapure, G. A. FitzGerald, and J. Rokach. Total synthesis of 17,17,18,18-d4-iPF2alpha-VI and quantification of iPF2alpha-VI in human urine by gas chromatography/mass spectrometry. *Anal Biochem*, 262(1):45–56, 1998.

[35] J. A. Lawson, H. Li, J. Rokach, M. Adiyaman, S. W. Hwang, S. P. Khanapure, and G. A. FitzGerald. Identification of two major F2 isoprostanes, 8,12-iso- and 5-epi-8, 12-iso-isoprostane F2alpha-VI, in human urine. *J Biol Chem*, 273(45):29295–301, 1998.

[36] J. D. Morrow, J. A. Awad, H. J. Boss, I. A. Blair, and 2nd Roberts, L. J. Non-cyclooxygenase-derived prostanoids (F2-isoprostanes) are formed in situ on phospholipids. *Proc Natl Acad Sci U S A*, 89(22):10721–5, 1992.

[37] 2nd Roberts, L. J., K. P. Moore, W. E. Zackert, J. A. Oates, and J. D. Morrow. Identification of the major urinary metabolite of the F2-isoprostane 8-iso-prostaglandin F2alpha in humans. *J Biol Chem*, 271(34):20617–20, 1996.

[38] C. Chiabrando, A. Valagussa, C. Rivalta, T. Durand, A. Guy, E. Zuccato, P. Villa, J. C. Rossi, and R. Fanelli. Identification and measurement of endogenous beta-oxidation metabolites of 8-epi-Prostaglandin F2alpha. *J Biol Chem*, 274(3):1313–9, 1999.

[39] S. Basu. Metabolism of 8-iso-prostaglandin F2alpha. *FEBS Lett*, 428(1-2):32–6, 1998.

[40] G. L. Milne, L. Gao, A. Porta, G. Zanoni, G. Vidari, and J. D. Morrow. Identification of the major urinary metabolite of the highly reactive cyclopentenone isoprostane 15-A(2t)-isoprostane in vivo. *J Biol Chem*, 280(26):25178–84, 2005.

[41] S. Parchmann and M. J. Mueller. Evidence for the formation of dinor isoprostanes E1 from alpha-linolenic acid in plants. *J Biol Chem*, 273(49):32650–5, 1998.

[42] R. Imbusch and M. J. Mueller. Analysis of oxidative stress and wound-inducible dinor isoprostanes F(1) (phytoprostanes F(1)) in plants. *Plant Physiol*, 124(3):1293–304, 2000.

[43] I. Thoma, M. Krischke, C. Loeffler, and M. J. Mueller. The isoprostanoid pathway in plants. *Chem Phys Lipids*, 128(1-2):135–48, 2004.

[44] A. Okazawa, I. Kawikova, Z. H. Cui, B. E. Skoogh, and J. Lotvall. 8-Epi-PGF2alpha induces airflow obstruction and airway plasma exudation in vivo. *Am J Respir Crit Care Med*, 155(2):436–41, 1997.

[45] R. Imbusch and M. J. Mueller. Formation of isoprostane F(2)-like compounds (phytoprostanes F(1)) from alpha-linolenic acid in plants. *Free Radic Biol Med*, 28(5):720–6, 2000.

[46] J. D. Morrow, Y. Chen, C. J. Brame, J. Yang, S. C. Sanchez, J. Xu, W. E. Zackert, J. A. Awad, and L. J. Roberts. The isoprostanes: unique prostaglandin-like products of free-radical-initiated lipid peroxidation. *Drug Metab Rev*, 31(1):117–39, 1999.

[47] I. Thoma, C. Loeffler, A. K. Sinha, M. Gupta, M. Krischke, B. Steffan, T. Roitsch, and M. J. Mueller. Cyclopentenone isoprostanes induced by reactive oxygen species trigger defense gene activation and phytoalexin accumulation in plants. *Plant J*, 34(3):363–75, 2003.

[48] B. Halliwell. Lipid peroxidation, antioxidants and cardiovascular disease: how should we move forward? *Cardiovasc Res*, 47(3):410–8, 2000.

[49] M. B. Kadiiska, B. C. Gladen, D. D. Baird, D. Germolec, L. B. Graham, C. E. Parker, A. Nyska, J. T. Wachsman, B. N. Ames, S. Basu, N. Brot, G. A. Fitzgerald, R. A. Floyd, M. George, J. W. Heinecke, G. E. Hatch, K. Hensley, J. A. Lawson, L. J. Marnett, J. D. Morrow, D. M. Murray, J. Plastaras, 2nd Roberts, L. J., J. Rokach, M. K. Shigenaga, R. S. Sohal, J. Sun, R. R. Tice, D. H. Van Thiel, D. Wellner, P. B. Walter, K. B. Tomer, R. P. Mason, and J. C. Barrett. Biomarkers of oxidative stress study II: are oxidation products of lipids, proteins, and DNA markers of CCl4 poisoning? *Free Radic Biol Med*, 38(6):698–710, 2005.

[50] L. J. Roberts and J. D. Morrow. Measurement of F(2)-isoprostanes as an index of oxidative stress in vivo. *Free Radic Biol Med*, 28(4):505–13, 2000.

[51] G. Davi, G. Ciabattoni, A. Consoli, A. Mezzetti, A. Falco, S. Santarone, E. Pennese, E. Vitacolonna, T. Bucciarelli, F. Costantini, F. Capani, and C. Patrono. In vivo formation of 8-iso-prostaglandin F2alpha and platelet activation in diabetes mellitus: effects of improved metabolic control and vitamin E supplementation. *Circulation*, 99(2):224–9, 1999.

[52] S. Devaraj, S. V. Hirany, R. F. Burk, and I. Jialal. Divergence between LDL oxidative susceptibility and urinary F(2)-isoprostanes as measures of oxidative stress in type 2 diabetes. *Clin Chem*, 47(11):1974–9, 2001.

[53] Jr. Keaney, J. F., M. G. Larson, R. S. Vasan, P. W. Wilson, I. Lipinska, D. Corey, J. M. Massaro, P. Sutherland, J. A. Vita, and E. J. Benjamin. Obesity and systemic oxidative stress: clinical correlates of oxidative stress in the Framingham Study. *Arterioscler Thromb Vasc Biol*, 23(3):434–9, 2003.

[54] J. D. Morrow, B. Frei, A. W. Longmire, J. M. Gaziano, S. M. Lynch, Y. Shyr, W. E. Strauss, J. A. Oates, and 2nd Roberts, L. J. Increase in circulating products of lipid peroxidation (F2-isoprostanes) in smokers. Smoking as a cause of oxidative damage. *N Engl J Med*, 332(18):1198–203, 1995.

[55] M. Reilly, N. Delanty, J. A. Lawson, and G. A. FitzGerald. Modulation of oxidant stress in vivo in chronic cigarette smokers. *Circulation*, 94(1):19–25, 1996.

[56] Z. Wang, G. Ciabattoni, C. Creminon, J. Lawson, G. A. Fitzgerald, C. Patrono, and J. Maclouf. Immunological characterization of urinary 8-epi-prostaglandin F2 alpha excretion in man. *J Pharmacol Exp Ther*, 275(1):94–100, 1995.

[57] G. Davi, P. Alessandrini, A. Mezzetti, G. Minotti, T. Bucciarelli, F. Costantini, F. Cipollone, G. B. Bon, G. Ciabattoni, and C. Patrono. In vivo formation of 8-Epi-prostaglandin F2 alpha is increased in hypercholesterolemia. *Arterioscler Thromb Vasc Biol*, 17(11):3230–5, 1997.

[58] M. R. Mehrabi, C. Ekmekcioglu, F. Tatzber, A. Oguogho, R. Ullrich, A. Morgan, F. Tamaddon, M. Grimm, H. D. Glogar, and H. Sinzinger. The isoprostane, 8-epi-PGF2 alpha, is accumulated in coronary arteries isolated from patients with coronary heart disease. *Cardiovasc Res*, 43(2):492–9, 1999.

[59] E. Schwedhelm, A. Bartling, H. Lenzen, D. Tsikas, R. Maas, J. Brummer, F. M. Gutzki, J. Berger, J. C. Frolich, and R. H. Böger. Urinary 8-iso-prostaglandin

F2alpha as a risk marker in patients with coronary heart disease: a matched case-control study. *Circulation*, 109(7):843–8, 2004.

[60] K. Fukuda, S. S. Davies, T. Nakajima, B. H. Ong, S. Kupershmidt, J. Fessel, V. Amarnath, M. E. Anderson, P. A. Boyden, P. C. Viswanathan, 2nd Roberts, L. J., and J. R. Balser. Oxidative mediated lipid peroxidation recapitulates proarrhythmic effects on cardiac sodium channels. *Circ Res*, 97(12):1262–9, 2005.

[61] N. Delanty, M. P. Reilly, D. Pratico, J. A. Lawson, J. F. McCarthy, A. E. Wood, S. T. Ohnishi, D. J. Fitzgerald, and G. A. FitzGerald. 8-epi PGF2 alpha generation during coronary reperfusion. A potential quantitative marker of oxidant stress in vivo. *Circulation*, 95(11):2492–9, 1997.

[62] M. P. Reilly, N. Delanty, L. Roy, J. Rokach, P. O. Callaghan, P. Crean, J. A. Lawson, and G. A. FitzGerald. Increased formation of the isoprostanes IPF2alpha-I and 8-epi-prostaglandin F2alpha in acute coronary angioplasty: evidence for oxidant stress during coronary reperfusion in humans. *Circulation*, 96(10):3314–20, 1997.

[63] D. Pratico, L. Iuliano, A. Mauriello, L. Spagnoli, J. A. Lawson, J. Rokach, J. Maclouf, F. Violi, and G. A. FitzGerald. Localization of distinct F2-isoprostanes in human atherosclerotic lesions. *J Clin Invest*, 100(8):2028–34, 1997.

[64] C. Gniwotta, J. D. Morrow, 2nd Roberts, L. J., and H. Kuhn. Prostaglandin F2-like compounds, F2-isoprostanes, are present in increased amounts in human atherosclerotic lesions. *Arterioscler Thromb Vasc Biol*, 17(11):3236–41, 1997.

[65] C. Vassalle, N. Botto, M. G. Andreassi, S. Berti, and A. Biagini. Evidence for enhanced 8-isoprostane plasma levels, as index of oxidative stress in vivo, in patients with coronary artery disease. *Coron Artery Dis*, 14(3):213–8, 2003.

[66] M. H. Shishehbor, R. Zhang, H. Medina, M. L. Brennan, D. M. Brennan, S. G. Ellis, E. J. Topol, and S. L. Hazen. Systemic elevations of free radical oxidation products of arachidonic acid are associated with angiographic evidence of coronary artery disease. *Free Radic Biol Med*, 41(11):1678–83, 2006.

[67] Z. Mallat, I. Philip, M. Lebret, D. Chatel, J. Maclouf, and A. Tedgui. Elevated levels of 8-iso-prostaglandin F2alpha in pericardial fluid of patients with heart failure: a potential role for in vivo oxidant stress in ventricular dilatation and progression to heart failure. *Circulation*, 97(16):1536–9, 1998.

[68] J. L. Cracowski, F. Tremel, C. Marpeau, J. P. Baguet, F. Stanke-Labesque, J. M. Mallion, and G. Bessard. Increased formation of F(2)-isoprostanes in patients with severe heart failure. *Heart*, 84(4):439–40, 2000.

[69] P. Minuz, P. Patrignani, S. Gaino, M. Degan, L. Menapace, R. Tommasoli, F. Seta, M. L. Capone, S. Tacconelli, S. Palatresi, C. Bencini, C. Del Vecchio, G. Mansueto, E. Arosio, C. L. Santonastaso, A. Lechi, A. Morganti, and C. Patrono. Increased oxidative stress and platelet activation in patients with hypertension and renovascular disease. *Circulation*, 106(22):2800–5, 2002.

[70] P. Montuschi, M. Corradi, G. Ciabattoni, J. Nightingale, S. A. Kharitonov, and P. J. Barnes. Increased 8-isoprostane, a marker of oxidative stress, in exhaled condensate of asthma patients. *Am J Respir Crit Care Med*, 160(1):216–20, 1999.

[71] R. Dworski, J. J. Murray, 2nd Roberts, L. J., J. A. Oates, J. D. Morrow, L. Fisher, and J. R. Sheller. Allergen-induced synthesis of F(2)-isoprostanes in atopic asthmatics. Evidence for oxidant stress. *Am J Respir Crit Care Med*, 160(6):1947–51, 1999.

[72] P. Montuschi, J. V. Collins, G. Ciabattoni, N. Lazzeri, M. Corradi, S. A. Kharitonov, and P. J. Barnes. Exhaled 8-isoprostane as an in vivo biomarker of lung oxidative stress in patients with COPD and healthy smokers. *Am J Respir Crit Care Med*, 162(3 Pt 1):1175–7, 2000.

[73] D. Pratico, S. Basili, M. Vieri, C. Cordova, F. Violi, and G. A. Fitzgerald. Chronic obstructive pulmonary disease is associated with an increase in urinary levels of isoprostane F2alpha-III, an index of oxidant stress. *Am J Respir Crit Care Med*, 158(6):1709–14, 1998.

[74] P. Montuschi, S. A. Kharitonov, G. Ciabattoni, M. Corradi, L. van Rensen, D. M. Geddes, M. E. Hodson, and P. J. Barnes. Exhaled 8-isoprostane as a new non-invasive biomarker of oxidative stress in cystic fibrosis. *Thorax*, 55(3):205–9, 2000.

[75] G. Ciabattoni, G. Davi, M. Collura, L. Iapichino, F. Pardo, A. Ganci, R. Romagnoli, J. Maclouf, and C. Patrono. In vivo lipid peroxidation and platelet activation in cystic fibrosis. *Am J Respir Crit Care Med*, 162(4 Pt 1):1195–201, 2000.

[76] P. Montuschi, G. Ciabattoni, P. Paredi, P. Pantelidis, R. M. du Bois, S. A. Kharitonov, and P. J. Barnes. 8-Isoprostane as a biomarker of oxidative stress

in interstitial lung diseases. *Am J Respir Crit Care Med*, 158(5 Pt 1):1524–7, 1998.

[77] C. T. Carpenter, P. V. Price, and B. W. Christman. Exhaled breath condensate isoprostanes are elevated in patients with acute lung injury or ARDS. *Chest*, 114(6):1653–9, 1998.

[78] M. P. Reilly, D. Pratico, N. Delanty, G. DiMinno, E. Tremoli, D. Rader, S. Kapoor, J. Rokach, J. Lawson, and G. A. FitzGerald. Increased formation of distinct F2 isoprostanes in hypercholesterolemia. *Circulation*, 98(25):2822–8, 1998.

[79] G. Davi, G. Di Minno, A. Coppola, G. Andria, A. M. Cerbone, P. Madonna, A. Tufano, A. Falco, P. Marchesani, G. Ciabattoni, and C. Patrono. Oxidative stress and platelet activation in homozygous homocystinuria. *Circulation*, 104(10):1124–8, 2001.

[80] T. Ide, H. Tsutsui, N. Ohashi, S. Hayashidani, N. Suematsu, M. Tsuchihashi, H. Tamai, and A. Takeshita. Greater oxidative stress in healthy young men compared with premenopausal women. *Arterioscler Thromb Vasc Biol*, 22(3):438–42, 2002.

[81] T. A. Ikizler, J. D. Morrow, L. J. Roberts, J. A. Evanson, B. Becker, R. M. Hakim, Y. Shyr, and J. Himmelfarb. Plasma F2-isoprostane levels are elevated in chronic hemodialysis patients. *Clin Nephrol*, 58(3):190–7, 2002.

[82] S. Holt, B. Reeder, M. Wilson, S. Harvey, J. D. Morrow, 2nd Roberts, L. J., and K. Moore. Increased lipid peroxidation in patients with rhabdomyolysis. *Lancet*, 353(9160):1241, 1999.

[83] T. J. Montine, M. F. Beal, M. E. Cudkowicz, H. O'Donnell, R. A. Margolin, L. McFarland, A. F. Bachrach, W. E. Zackert, L. J. Roberts, and J. D. Morrow. Increased CSF F2-isoprostane concentration in probable AD. *Neurology*, 52(3):562–5, 1999.

[84] D. Pratico, C. M. Clark, V. M. Lee, J. Q. Trojanowski, J. Rokach, and G. A. FitzGerald. Increased 8,12-iso-iPF2alpha-VI in Alzheimer's disease: correlation of a noninvasive index of lipid peroxidation with disease severity. *Ann Neurol*, 48(5):809–12, 2000.

[85] T. J. Montine, M. D. Neely, J. F. Quinn, M. F. Beal, W. R. Markesbery, L. J. Roberts, and J. D. Morrow. Lipid peroxidation in aging brain and Alzheimer's disease. *Free Radic Biol Med*, 33(5):620–6, 2002.

[86] T. J. Montine, M. F. Beal, D. Robertson, M. E. Cudkowicz, I. Biaggioni, H. O'Donnell, W. E. Zackert, L. J. Roberts, and J. D. Morrow. Cerebrospinal fluid F2-isoprostanes are elevated in Huntington's disease. *Neurology*, 52(5):1104–5, 1999.

[87] N. Mattsson, S. Haghighi, O. Andersen, Y. Yao, L. Rosengren, K. Blennow, D. Pratico, and H. Zetterberg. Elevated cerebrospinal fluid F2-isoprostane levels indicating oxidative stress in healthy siblings of multiple sclerosis patients. *Neurosci Lett*, 414(3):233–6, 2007.

[88] A. Greco, L. Minghetti, and G. Levi. Isoprostanes, novel markers of oxidative injury, help understanding the pathogenesis of neurodegenerative diseases. *Neurochem Res*, 25(9-10):1357–64, 2000.

[89] E. A. Meagher, O. P. Barry, A. Burke, M. R. Lucey, J. A. Lawson, J. Rokach, and G. A. FitzGerald. Alcohol-induced generation of lipid peroxidation products in humans. *J Clin Invest*, 104(6):805–13, 1999.

[90] D. Pratico, L. Iuliano, S. Basili, D. Ferro, C. Camastra, C. Cordova, G. A. FitzGerald, and F. Violi. Enhanced lipid peroxidation in hepatic cirrhosis. *J Investig Med*, 46(2):51–7, 1998.

[91] J. D. Morrow, K. P. Moore, J. A. Awad, M. D. Ravenscraft, G. Marini, K. F. Badr, R. Williams, and 2nd Roberts, L. J. Marked overproduction of non-cyclooxygenase derived prostanoids (F2-isoprostanes) in the hepatorenal syndrome. *J Lipid Mediat*, 6(1-3):417–20, 1993.

[92] A. Aboutwerat, P. W. Pemberton, A. Smith, P. C. Burrows, R. F. McMahon, S. K. Jain, and T. W. Warnes. Oxidant stress is a significant feature of primary biliary cirrhosis. *Biochim Biophys Acta*, 1637(2):142–50, 2003.

[93] A. Burke, G. A. FitzGerald, and M. R. Lucey. A prospective analysis of oxidative stress and liver transplantation. *Transplantation*, 74(2):217–21, 2002.

[94] S. Basu, M. Whiteman, D. L. Mattey, and B. Halliwell. Raised levels of F(2)-isoprostanes and prostaglandin F(2alpha) in different rheumatic diseases. *Ann Rheum Dis*, 60(6):627–31, 2001.

[95] J. L. Cracowski, C. Marpeau, P. H. Carpentier, B. Imbert, M. Hunt, F. Stanke-Labesque, and G. Bessard. Enhanced in vivo lipid peroxidation in scleroderma spectrum disorders. *Arthritis Rheum*, 44(5):1143–8, 2001.

[96] S. Basu, K. Michaelsson, H. Olofsson, S. Johansson, and H. Melhus. Association between oxidative stress and bone mineral density. *Biochem Biophys Res Commun*, 288(1):275–9, 2001.

[97] J. L. Cracowski, B. Bonaz, G. Bessard, J. Bessard, C. Anglade, and J. Fournet. Increased urinary F2-isoprostanes in patients with Crohn's disease. *Am J Gastroenterol*, 97(1):99–103, 2002.

[98] X. Hou, 2nd Roberts, L. J., D. F. Taber, J. D. Morrow, K. Kanai, Jr. Gobeil, F., M. H. Beauchamp, S. G. Bernier, G. Lepage, D. R. Varma, and S. Chemtob. 2,3-Dinor-5,6-dihydro-15-F(2t)-isoprostane: a bioactive prostanoid metabolite. *Am J Physiol Regul Integr Comp Physiol*, 281(2):R391–400, 2001.

[99] P. Montuschi, P. Barnes, and 2nd Roberts, L. J. Insights into oxidative stress: the isoprostanes. *Curr Med Chem*, 14(6):703–17, 2007.

[100] N. Leitinger, J. Huber, C. Rizza, D. Mechtcheriakova, V. Bochkov, Y. Koshelnick, J. A. Berliner, and B. R. Binder. The isoprostane 8-iso-PGF(2alpha) stimulates endothelial cells to bind monocytes: differences from thromboxane-mediated endothelial activation. *Faseb J*, 15(7):1254–6, 2001.

[101] M. Tang, T. Cyrus, Y. Yao, L. Vocun, and D. Pratico. Involvement of thromboxane receptor in the proatherogenic effect of isoprostane F2alpha-III: evidence from apolipoprotein E- and LDL receptor-deficient mice. *Circulation*, 112(18):2867–74, 2005.

[102] T. Yura, M. Fukunaga, R. Khan, G. N. Nassar, K. F. Badr, and A. Montero. Free-radical-generated F2-isoprostane stimulates cell proliferation and endothelin-1 expression on endothelial cells. *Kidney Int*, 56(2):471–8, 1999.

[103] K. H. Kang, J. D. Morrow, 2nd Roberts, L. J., J. H. Newman, and M. Banerjee. Airway and vascular effects of 8-epi-prostaglandin F2 alpha in isolated perfused rat lung. *J Appl Physiol*, 74(1):460–5, 1993.

[104] L. J. Janssen, M. Premji, S. Netherton, A. Catalli, G. Cox, S. Keshavjee, and D. J. Crankshaw. Excitatory and inhibitory actions of isoprostanes in human and canine airway smooth muscle. *J Pharmacol Exp Ther*, 295(2):506–11, 2000.

[105] R. S. Wagner, C. Weare, N. Jin, E. R. Mohler, and R. A. Rhoades. Characterization of signal transduction events stimulated by 8-epi-prostaglandin(PG)F2 alpha in rat aortic rings. *Prostaglandins*, 54(2):581–99, 1997.

[106] S. W. Hoffman, S. Moore, and E. F. Ellis. Isoprostanes: free radical-generated prostaglandins with constrictor effects on cerebral arterioles. *Stroke*, 28(4):844–9, 1997.

[107] X. Hou, Jr. Gobeil, F., K. Peri, G. Speranza, A. M. Marrache, P. Lachapelle, 2nd Roberts, J., D. R. Varma, S. Chemtob, and E. F. Ellis. Augmented vasoconstriction and thromboxane formation by 15-F(2t)-isoprostane (8-iso-prostaglandin F(2alpha)) in immature pig periventricular brain microvessels. *Stroke*, 31(2):516–24; discussion 525, 2000.

[108] K. Takahashi, T. M. Nammour, M. Fukunaga, J. Ebert, J. D. Morrow, 2nd Roberts, L. J., R. L. Hoover, and K. F. Badr. Glomerular actions of a free radical-generated novel prostaglandin, 8-epi-prostaglandin F2 alpha, in the rat. Evidence for interaction with thromboxane A2 receptors. *J Clin Invest*, 90(1):136–41, 1992.

[109] M. Banerjee, K. H. Kang, J. D. Morrow, L. J. Roberts, and J. H. Newman. Effects of a novel prostaglandin, 8-epi-PGF2 alpha, in rabbit lung in situ. *Am J Physiol*, 263(3 Pt 2):H660–3, 1992.

[110] M. Bernareggi, G. Rossoni, and F. Berti. Bronchopulmonary effects of 8-epi-PGF2A in anaesthetised guinea pigs. *Pharmacol Res*, 37(1):75–80, 1998.

[111] I. Lahaie, P. Hardy, X. Hou, H. Hassessian, P. Asselin, P. Lachapelle, G. Almazan, D. R. Varma, J. D. Morrow, 2nd Roberts, L. J., and S. Chemtob. A novel mechanism for vasoconstrictor action of 8-isoprostaglandin F2 alpha on retinal vessels. *Am J Physiol*, 274(5 Pt 2):R1406–16, 1998.

[112] B. M. Kromer and J. R. Tippins. Coronary artery constriction by the isoprostane 8-epi prostaglandin F2 alpha. *Br J Pharmacol*, 119(6):1276–80, 1996.

[113] R. Marley, D. Harry, R. Anand, B. Fernando, S. Davies, and K. Moore. 8-Isoprostaglandin F2 alpha, a product of lipid peroxidation, increases portal pressure in normal and cirrhotic rats. *Gastroenterology*, 112(1):208–13, 1997.

[114] J. L. Cracowski, F. Stanke-Labesque, P. Devillier, O. Chavanon, M. Hunt, C. Souvignet, and G. Bessard. Human internal mammary artery contraction by isoprostaglandin F(2alpha) type-III [8-iso-prostaglandin F(2alpha). *Eur J Pharmacol*, 397(1):161–8, 2000.

[115] E. Schwedhelm and R. H. Böger. Application of gas chromatography-mass spec-

trometry for analysis of isoprostanes: their role in cardiovascular disease. *Clin Chem Lab Med*, 41(12):1552–61, 2003.

[116] Y. Liang, P. Wei, R. W. Duke, P. D. Reaven, S. M. Harman, R. G. Cutler, and C. B. Heward. Quantification of 8-iso-prostaglandin-F(2alpha) and 2,3-dinor-8-iso-prostaglandin-F(2alpha) in human urine using liquid chromatography-tandem mass spectrometry. *Free Radic Biol Med*, 34(4):409–18, 2003.

[117] A. W. Taylor, R. S. Bruno, and M. G. Traber. Women and smokers have elevated urinary F(2)-isoprostane metabolites: a novel extraction and LC-MS methodology. *Lipids*, 43(10):925–36, 2008.

[118] L. P. Audoly, B. Rocca, J. E. Fabre, B. H. Koller, D. Thomas, A. L. Loeb, T. M. Coffman, and G. A. FitzGerald. Cardiovascular responses to the isoprostanes iPF(2alpha)-III and iPE(2)-III are mediated via the thromboxane A(2) receptor in vivo. *Circulation*, 101(24):2833–40, 2000.

[119] R. A. Benndorf, E. Schwedhelm, A. Gnann, R. Taheri, G. Kom, M. Didie, A. Steenpass, S. Ergun, and R. H. Böger. Isoprostanes inhibit vascular endothelial growth factor-induced endothelial cell migration, tube formation, and cardiac vessel sprouting in vitro, as well as angiogenesis in vivo via activation of the thromboxane A2 receptor. A potential link between oxidative stress and impaired angiogenesis. *Circ Res*, 2008.

[120] R. A. Armstrong. Platelet prostanoid receptors. *Pharmacol Ther*, 72(3):171–91, 1996.

[121] S. Narumiya, Y. Sugimoto, and F. Ushikubi. Prostanoid receptors: structures, properties, and functions. *Physiol Rev*, 79(4):1193–226, 1999.

[122] J. A. Oates, G. A. FitzGerald, R. A. Branch, E. K. Jackson, H. R. Knapp, and 2nd Roberts, L. J. Clinical implications of prostaglandin and thromboxane A2 formation (1). *N Engl J Med*, 319(11):689–98, 1988.

[123] G. G. Neri Serneri, P. A. Modesti, A. Fortini, R. Abbate, A. Lombardi, and G. F. Gensini. Reduction in prostacyclin platelet receptors in active spontaneous angina. *Lancet*, 2(8407):838–41, 1984.

[124] D. J. Fitzgerald, W. Rocki, R. Murray, G. Mayo, and G. A. FitzGerald. Thromboxane A2 synthesis in pregnancy-induced hypertension. *Lancet*, 335(8692):751–4, 1990.

[125] M. Hirata, Y. Hayashi, F. Ushikubi, Y. Yokota, R. Kageyama, S. Nakanishi, and S. Narumiya. Cloning and expression of cDNA for a human thromboxane A2 receptor. *Nature*, 349(6310):617–20, 1991.

[126] R. M. Nusing, M. Hirata, A. Kakizuka, T. Eki, K. Ozawa, and S. Narumiya. Characterization and chromosomal mapping of the human thromboxane A2 receptor gene. *J Biol Chem*, 268(33):25253–9, 1993.

[127] M. K. Raychowdhury, M. Yukawa, L. J. Collins, S. H. McGrail, K. C. Kent, and J. A. Ware. Alternative splicing produces a divergent cytoplasmic tail in the human endothelial thromboxane A2 receptor. *J Biol Chem*, 269(30):19256–61, 1994.

[128] S. M. Miggin and B. T. Kinsella. Expression and tissue distribution of the mRNAs encoding the human thromboxane A2 receptor (TP) alpha and beta isoforms. *Biochim Biophys Acta*, 1425(3):543–59, 1998.

[129] K. Yin, P. V. Halushka, Y. T. Yan, and P. Y. Wong. Antiaggregatory activity of 8-epi-prostaglandin F2 alpha and other F-series prostanoids and their binding to thromboxane A2/prostaglandin H2 receptors in human platelets. *J Pharmacol Exp Ther*, 270(3):1192–6, 1994.

[130] M. Fukunaga, T. Yura, R. Grygorczyk, and K. F. Badr. Evidence for the distinct nature of F2-isoprostane receptors from those of thromboxane A2. *Am J Physiol*, 272(4 Pt 2):F477–83, 1997.

[131] M. Fukunaga, N. Makita, 2nd Roberts, L. J., J. D. Morrow, K. Takahashi, and K. F. Badr. Evidence for the existence of F2-isoprostane receptors on rat vascular smooth muscle cells. *Am J Physiol*, 264(6 Pt 1):C1619–24, 1993.

[132] N. Nakahata. Thromboxane A2: physiology/pathophysiology, cellular signal transduction and pharmacology. *Pharmacol Ther*, 118(1):18–35, 2008.

[133] P. Carmeliet. Angiogenesis in health and disease. *Nat Med*, 9(6):653–60, 2003.

[134] B. A. Bryan and P. A. D'Amore. What tangled webs they weave: Rho-GTPase control of angiogenesis. *Cell Mol Life Sci*, 64(16):2053–65, 2007.

[135] P. Carmeliet. Mechanisms of angiogenesis and arteriogenesis. *Nat Med*, 6(4):389–95, 2000.

[136] N. Ferrara, H. P. Gerber, and J. LeCouter. The biology of VEGF and its receptors. *Nat Med*, 9(6):669–76, 2003.

[137] H. Kimura and H. Esumi. Reciprocal regulation between nitric oxide and vascular endothelial growth factor in angiogenesis. *Acta Biochim Pol*, 50(1):49–59, 2003.

[138] J. Dai and A. B. Rabie. VEGF: an essential mediator of both angiogenesis and endochondral ossification. *J Dent Res*, 86(10):937–50, 2007.

[139] I. Shiojima and K. Walsh. Role of Akt signaling in vascular homeostasis and angiogenesis. *Circ Res*, 90(12):1243–50, 2002.

[140] B. D. Manning and L. C. Cantley. AKT/PKB signaling: navigating downstream. *Cell*, 129(7):1261–74, 2007.

[141] M. Morales-Ruiz, D. Fulton, G. Sowa, L. R. Languino, Y. Fujio, K. Walsh, and W. C. Sessa. Vascular endothelial growth factor-stimulated actin reorganization and migration of endothelial cells is regulated via the serine/threonine kinase Akt. *Circ Res*, 86(8):892–6, 2000.

[142] T. Murohara, B. Witzenbichler, I. Spyridopoulos, T. Asahara, B. Ding, A. Sullivan, D. W. Losordo, and J. M. Isner. Role of endothelial nitric oxide synthase in endothelial cell migration. *Arterioscler Thromb Vasc Biol*, 19(5):1156–61, 1999.

[143] L. Morbidelli, S. Donnini, and M. Ziche. Role of nitric oxide in the modulation of angiogenesis. *Curr Pharm Des*, 9(7):521–30, 2003.

[144] E. Ackah, J. Yu, S. Zoellner, Y. Iwakiri, C. Skurk, R. Shibata, N. Ouchi, R. M. Easton, G. Galasso, M. J. Birnbaum, K. Walsh, and W. C. Sessa. Akt1/protein kinase Balpha is critical for ischemic and VEGF-mediated angiogenesis. *J Clin Invest*, 115(8):2119–27, 2005.

[145] A. K. Pullikuth and A. D. Catling. Scaffold mediated regulation of MAPK signaling and cytoskeletal dynamics: a perspective. *Cell Signal*, 19(8):1621–32, 2007.

[146] R. Seger and E. G. Krebs. The MAPK signaling cascade. *Faseb J*, 9(9):726–35, 1995.

[147] C. Huang, K. Jacobson, and M. D. Schaller. MAP kinases and cell migration. *J Cell Sci*, 117(Pt 20):4619–28, 2004.

[148] I. Cascone, E. Giraudo, F. Caccavari, L. Napione, E. Bertotti, J. G. Collard, G. Serini, and F. Bussolino. Temporal and spatial modulation of Rho GTPases during in vitro formation of capillary vascular network. Adherens junctions and

myosin light chain as targets of Rac1 and RhoA. *J Biol Chem*, 278(50):50702–13, 2003.

[149] M. V. Hoang, M. C. Whelan, and D. R. Senger. Rho activity critically and selectively regulates endothelial cell organization during angiogenesis. *Proc Natl Acad Sci U S A*, 101(7):1874–9, 2004.

[150] G. P. van Nieuw Amerongen and V. W. van Hinsbergh. Cytoskeletal effects of rho-like small guanine nucleotide-binding proteins in the vascular system. *Arterioscler Thromb Vasc Biol*, 21(3):300–11, 2001.

[151] L. Lamalice, F. Le Boeuf, and J. Huot. Endothelial cell migration during angiogenesis. *Circ Res*, 100(6):782–94, 2007.

[152] A. J. Ridley. Rho family proteins: coordinating cell responses. *Trends Cell Biol*, 11(12):471–7, 2001.

[153] M. Amano, Y. Fukata, and K. Kaibuchi. Regulation and functions of Rho-associated kinase. *Exp Cell Res*, 261(1):44–51, 2000.

[154] L. J. Janssen and T. Tazzeo. Involvement of TP and EP3 receptors in vasoconstrictor responses to isoprostanes in pulmonary vasculature. *J Pharmacol Exp Ther*, 301(3):1060–6, 2002.

[155] S. Brault, A. K. Martinez-Bermudez, A. M. Marrache, Jr. Gobeil, F., X. Hou, M. Beauchamp, C. Quiniou, G. Almazan, C. Lachance, 2nd Roberts, J., D. R. Varma, and S. Chemtob. Selective neuromicrovascular endothelial cell death by 8-Iso-prostaglandin F2alpha: possible role in ischemic brain injury. *Stroke*, 34(3):776–82, 2003.

[156] J. L. Elmhurst, P. A. Betti, and P. K. Rangachari. Intestinal effects of isoprostanes: evidence for the involvement of prostanoid EP and TP receptors. *J Pharmacol Exp Ther*, 282(3):1198–205, 1997.

[157] D. L. Clarke, M. G. Belvisi, E. Hardaker, R. Newton, and M. A. Giembycz. E-ring 8-isoprostanes are agonists at EP2- and EP4-prostanoid receptors on human airway smooth muscle cells and regulate the release of colony-stimulating factors by activating cAMP-dependent protein kinase. *Mol Pharmacol*, 67(2):383–93, 2005.

[158] S. R. Datta, A. Brunet, and M. E. Greenberg. Cellular survival: a play in three Akts. *Genes Dev*, 13(22):2905–27, 1999.

[159] R. Anjum and J. Blenis. The RSK family of kinases: emerging roles in cellular signalling. *Nat Rev Mol Cell Biol*, 9(10):747–58, 2008.

[160] H. Scholz, A. Yndestad, J. K. Damas, T. Waehre, S. Tonstad, P. Aukrust, and B. Halvorsen. 8-isoprostane increases expression of interleukin-8 in human macrophages through activation of mitogen-activated protein kinases. *Cardiovasc Res*, 59(4):945–54, 2003.

[161] S. M. Miggin and B. T. Kinsella. Thromboxane A(2) receptor mediated activation of the mitogen activated protein kinase cascades in human uterine smooth muscle cells. *Biochim Biophys Acta*, 1539(1-2):147–62, 2001.

[162] M. Katz, I. Amit, and Y. Yarden. Regulation of MAPKs by growth factors and receptor tyrosine kinases. *Biochim Biophys Acta*, 1773(8):1161–76, 2007.

[163] T. M. Seasholtz and J. H. Brown. RHO SIGNALING in vascular diseases. *Mol Interv*, 4(6):348–57, 2004.

[164] M. W. Renshaw, D. Toksoz, and M. A. Schwartz. Involvement of the small GTPase rho in integrin-mediated activation of mitogen-activated protein kinase. *J Biol Chem*, 271(36):21691–4, 1996.

[165] I. Mueed, T. Tazzeo, C. Liu, E. Pertens, Y. Zhang, I. Cybulski, L. Semelhago, J. Noora, A. Lamy, K. Teoh, V. Chu, and L. J. Janssen. Isoprostanes constrict human radial artery by stimulation of thromboxane receptors, Ca2+ release, and RhoA activation. *J Thorac Cardiovasc Surg*, 135(1):131–8, 2008.

[166] Y. Gao, R. Yokota, S. Tang, A. W. Ashton, and J. A. Ware. Reversal of angiogenesis in vitro, induction of apoptosis, and inhibition of AKT phosphorylation in endothelial cells by thromboxane A(2). *Circ Res*, 87(9):739–45, 2000.

[167] A. W. Ashton and J. A. Ware. Thromboxane A2 receptor signaling inhibits vascular endothelial growth factor-induced endothelial cell differentiation and migration. *Circ Res*, 95(4):372–9, 2004.

[168] S. Pal, J. Wu, J. K. Murray, S. H. Gellman, M. A. Wozniak, P. J. Keely, M. E. Boyer, T. M. Gomez, S. M. Hasso, J. F. Fallon, and E. H. Bresnick. An antiangiogenic neurokinin-B/thromboxane A2 regulatory axis. *J Cell Biol*, 174(7):1047–58, 2006.

[169] D. Nie, Y. Guo, D. Yang, Y. Tang, Y. Chen, M. T. Wang, A. Zacharek, Y. Qiao, M. Che, and K. V. Honn. Thromboxane A2 receptors in prostate carcinoma: expression and its role in regulating cell motility via small GTPase Rho. *Cancer Res*, 68(1):115–21, 2008.

[170] L. P. Kelley-Hickie, M. B. O'Keeffe, H. M. Reid, and B. T. Kinsella. Homologous desensitization of signalling by the alpha (alpha) isoform of the human thromboxane A2 receptor: a specific role for nitric oxide signalling. *Biochim Biophys Acta*, 1773(6):970–89, 2007.

[171] L. P. Kelley-Hickie and B. T. Kinsella. Homologous desensitization of signalling by the beta (beta) isoform of the human thromboxane A2 receptor. *Biochim Biophys Acta*, 1761(9):1114–31, 2006.

[172] B. P. Eliceiri, R. Klemke, S. Stromblad, and D. A. Cheresh. Integrin alphavbeta3 requirement for sustained mitogen-activated protein kinase activity during angiogenesis. *J Cell Biol*, 140(5):1255–63, 1998.

[173] K. Nagasawa, N. Kitada, C. Tsuji, M. Ogawa, T. Yokoyama, N. Ohnishi, S. Iwakawa, and K. Okumura. Distribution of pirarubicin in human blood. *Chem Pharm Bull (Tokyo)*, 40(10):2866–9, 1992.

[174] G. P. van Nieuw Amerongen, P. Koolwijk, A. Versteilen, and V. W. van Hinsbergh. Involvement of RhoA/Rho kinase signaling in VEGF-induced endothelial cell migration and angiogenesis in vitro. *Arterioscler Thromb Vasc Biol*, 23(2):211–7, 2003.

[175] T. Hirata, F. Ushikubi, A. Kakizuka, M. Okuma, and S. Narumiya. Two thromboxane A2 receptor isoforms in human platelets. Opposite coupling to adenylyl cyclase with different sensitivity to Arg60 to Leu mutation. *J Clin Invest*, 97(4):949–56, 1996.

[176] K. Wikström, D. J. Kavanagh, H. M. Reid, and B. T. Kinsella. Differential regulation of RhoA-mediated signaling by the TPalpha and TPbeta isoforms of the human thromboxane A2 receptor: independent modulation of TPalpha signaling by prostacyclin and nitric oxide. *Cell Signal*, 20(8):1497–512, 2008.

[177] H. Zhou and R. H. Kramer. Integrin engagement differentially modulates epithelial cell motility by RhoA/ROCK and PAK1. *J Biol Chem*, 280(11):10624–35, 2005.

[178] D. J. Webb, C. M. Brown, and A. F. Horwitz. Illuminating adhesion complexes in migrating cells: moving toward a bright future. *Curr Opin Cell Biol*, 15(5):614–20, 2003.

[179] H. Yin, L. Gao, H. H. Tai, L. J. Murphey, N. A. Porter, and J. D. Morrow. Urinary prostaglandin F2alpha is generated from the isoprostane pathway and not the cyclooxygenase in humans. *J Biol Chem*, 282(1):329–36, 2007.

[180] E. A. Cox and A. Huttenlocher. Regulation of integrin-mediated adhesion during cell migration. *Microsc Res Tech*, 43(5):412–9, 1998.

[181] M. Takemoto, J. Sun, J. Hiroki, H. Shimokawa, and J. K. Liao. Rho-kinase mediates hypoxia-induced downregulation of endothelial nitric oxide synthase. *Circulation*, 106(1):57–62, 2002.

[182] J. A. Nagy and D. R. Senger. VEGF-A, cytoskeletal dynamics, and the pathological vascular phenotype. *Exp Cell Res*, 312(5):538–48, 2006.

[183] S. Banai, M. T. Jaklitsch, M. Shou, D. F. Lazarous, M. Scheinowitz, S. Biro, S. E. Epstein, and E. F. Unger. Angiogenic-induced enhancement of collateral blood flow to ischemic myocardium by vascular endothelial growth factor in dogs. *Circulation*, 89(5):2183–9, 1994.

[184] N. Ferrara and S. Bunting. Vascular endothelial growth factor, a specific regulator of angiogenesis. *Curr Opin Nephrol Hypertens*, 5(1):35–44, 1996.

[185] S. H. Lee, P. L. Wolf, R. Escudero, R. Deutsch, S. W. Jamieson, and P. A. Thistlethwaite. Early expression of angiogenesis factors in acute myocardial ischemia and infarction. *N Engl J Med*, 342(9):626–33, 2000.

[186] K. Tamura, H. Nakajima, H. Rakue, A. Sasame, Y. Naito, Y. Nagai, and C. Ibukiyama. Elevated circulating levels of basic fibroblast growth factor and vascular endothelial growth factor in patients with acute myocardial infarction. *Jpn Circ J*, 63(5):357–61, 1999.

[187] E. Schwedhelm, R. A. Benndorf, R. H. Böger, and D. Tsikas. Mass spectrometric analysis of F2-Isoprostanes: markers and mediators of oxidative stress. *Current Pharmaceutical Analysis*, 3(1):39–51, 2007.

[188] E. S. Musiek, L. Gao, G. L. Milne, W. Han, M. B. Everhart, D. Wang, M. G. Backlund, R. N. DuBois, G. Zanoni, G. Vidari, T. S. Blackwell, and J. D. Morrow.